REVIEWS OF GEOPHYSICS, VOL. 24, NO. 3, PAGES 579–624, AUGUST 1986

Strainmeters and Tiltmeters

DUNCAN CARR AGNEW

Institute of Geophysics and Planetary Physics, University of California, San Diego, La Jolla

Despite steady effort over the last century, continuously recording tiltmeters and strainmeters have not yet been successful except for earth tide measurements. This article reviews the techniques and instrument designs that have been developed in this field. The continuous measurement of true tectonic motions, which have rates of 10^{-14} s^{-1}, requires extremely high instrument stability, but more rapid motions (tides and seismic waves apart) are even smaller and not much more easily detectable. Much past effort has been spent improving the transducers used in these instruments, which usually measure small displacements; the commonest choices are optical (the most accurate), capacitive (the most sensitive), and inductive (the most rugged). Nowadays building a transducer is the easiest part; a much harder task, equally important to a good design, is attaching the instrument to the ground so that it can detect the signal wanted. This part of the design includes choosing a location. A large underground opening is thermally stable but distorting; a surface installation is easy to build but noisy because of soil weathering; and a borehole is inaccessible to weather but also to the operator. All such installations (and indeed the whole field of strain and tilt measurement) of course rely on the assumption that the deformations of interest can be measured over baselengths of a few hundred meters or less; this is true for tides and seismic waves, but unproven for tectonic motions. Appropriate attachment techniques differ for each location, and many mundane details (such as cementing techniques for borehole instruments) remain to be worked out. The goal of measuring tectonic and tidal tilt has created many tiltmeter designs. Most are relatively small instruments that use some form of pendulum or bubble level; a few use a liquid surface to measure tilts over a long baseline. Repeated experience has shown the latter type, when well built, to be superior to the former, proving end-monument motions to be a dominant source of noise. The same appears to hold true for strainmeters, the best results coming from long-base laser instruments, though strainmeters using rigid or flexible material length standards are useful for special purposes, and borehole instruments show promise. Because achieving a good design has been so difficult, it is important to select the goals an instrument must meet and be prepared to compromise on others. The difficulty of validating results from this type of instrument makes comparison tests essential; such tests as have been made so far show that good results cannot be gotten at low cost or without careful attention to details.

CONTENTS

1. INTRODUCTION

> We are compelled to regard, at least provisionally, these enormous changes of level either as a local phenomenon, or as due to some systematic error in [the] mode of observation.

Paper number 6R0083
8755-1209/86/006R-0083$15.00

This evaluation of certain tilt observations was written by G. H. Darwin over a century ago. His reports [*Darwin*, 1881, 1882] show that the observation of tilt of the ground was then a new subject, of clear importance but lacking reliable data. Observed tilts formed no consistent pattern, and it was unclear how much they were caused by instrumental defects, how much by imperfect attachment to the ground, and how much by real tilting of the earth.

Darwin's first report mentions that in 1877 oscillations in the level of the transit instrument at Pulkova, Russia, were seen following an earthquake in Ecuador. In the ensuing century, measurements of seismic waves have improved greatly, but continuous tilt and strain measurements, the subject of this review, have advanced very little. Darwin's opinion would be apt for many recent observations. It is now possible to observe earth tides (Darwin's own goal), but otherwise the field has few trustworthy data. This is not for lack of trying, but because it is hard to build adequate instruments; in particular, the earth has turned out to be such a stable body that to measure its deformation requires optical and electronic methods that have only recently become available.

Designs for tiltmeters and strainmeters are extremely diverse, mostly because we do not know the right way to measure tilt and strain (though we have learnt that some ways are wrong). Since there is no agreed body of techniques, I have spent more space on basic principles than is usual in discussing instrumentation. The next section discusses what tilt and strain are, the size of signals to be measured, and how instrument quality is described; peri-

pheral though these matters may seem to instrument design, confusion over them has often caused difficulties in comparing results from different instruments. The reader more interested in design details may turn to section 3, which reviews techniques used in both tiltmeters and strainmeters. I have paid special attention to methods of attaching the instrument to the earth, for it is this, rather than making a sensitive enough detector, that now limits these measurements. Sections 4 and 5 discuss particular instruments. I have tried to include all that have either seen substantial use or shown promise for further development, with particularly full descriptions of those designs not well discussed in the journal literature. While this article is not a review of the results of strain and tilt measurements, I have mentioned some observations, if only to provide a basis for comparing different instruments. *Goulty* [1976] has given a good short review of the aims of tiltmeter and strainmeter measurements and of the success attained; *Hanna* [1985] describes related techniques used for the much larger deformations that occur in geotechnical engineering.

2. Fundamental Principles

2.1. *Defining Tilt and Strain*

Though there are good instrumental reasons for measuring them separately, tilt and strain are very similar quantities: both are measures of deformation, though tilt includes other effects as well. It is useful to begin with a purely kinematic description to show how each is related to the usual measures of deformation. This is best done in tensor notation [*Malvern*, 1969]; it is then relatively easy to write the expressions for specific coordinate systems.

We adopt a fixed coordinate system and a Lagrangian description in which $\mathbf{x}(\mathbf{X},t)$ is the position of the particle whose position was $\mathbf{X}$ at $t = 0$. Choosing a particular particle $\mathbf{X}_1$, we define several quantities, all functions of some other particle $\mathbf{X}_2$. These include the baseline

$$\mathbf{d}(\mathbf{X}_2,t) = \mathbf{x}(\mathbf{X}_2,t) - \mathbf{x}(\mathbf{X}_1,t)$$

the relative displacement vector

$$\mathbf{s}(\mathbf{X}_2,t) = \mathbf{d}(\mathbf{X}_2,t) - \mathbf{d}(\mathbf{X}_2,0) \equiv \mathbf{d}(\mathbf{X}_2,t) - \mathbf{d}_0(\mathbf{X}_2)$$

and the baselength and direction

$$l(\mathbf{X}_2) = |\mathbf{d}_0(\mathbf{X}_2)| \qquad \hat{\mathbf{d}}(\mathbf{X}_2) = \mathbf{d}_0(\mathbf{X}_2)/l(\mathbf{X}_2)$$

From this point on we assume that the endpoints $\mathbf{X}_1$ and $\mathbf{X}_2$ have been selected, and omit dependence on them.

We now assume, as is almost always valid for the solid earth, that the baseline $\mathbf{d}$ does not move very much, so that $|\mathbf{s}|/l \ll 1$. We may then define the infinitesimal rotation of $\mathbf{d}$ as

$$(\mathbf{d} \times \mathbf{d}_0)/l^2 = (\mathbf{s} \times \hat{\mathbf{d}}_0)/l$$

and the associated *deformational tilt* relative to a reference direction $\hat{\mathbf{z}}$ as

$$\boldsymbol{\Omega}_D = \hat{\mathbf{z}} \times (\mathbf{s} \times \hat{\mathbf{d}}_0)/l$$

This tilt describes part of any change in the orientation of $\mathbf{d}$; the change in its length is given by the *extension*

$$\epsilon = \frac{|\mathbf{d}| - |\mathbf{d}_0|}{l} \simeq (\mathbf{s} \cdot \mathbf{d}_0)/l$$

We next impose the condition that to a good approximation

$$\mathbf{s} = \mathbf{d} \cdot \nabla\mathbf{s}$$

where the gradient is evaluated at $\mathbf{X}_1$. For this to be valid for any direction of $\mathbf{d}$, $\nabla\mathbf{s}$ must be sensibly constant for a distance l around $\mathbf{X}_1$. This condition is that of uniform strain and is not always satisfied in practice (section 2.2). Together with our earlier requirement that $|\mathbf{s}| \ll l$ it implies that the strains are infinitesimal.

We next write

$$\begin{aligned}\mathbf{s} &= \mathbf{d} \cdot [\tfrac{1}{2}(\nabla\mathbf{s}+\mathbf{s}\nabla)+\tfrac{1}{2}(\nabla\mathbf{s}-\mathbf{s}\nabla)] \\ &= \mathbf{d} \cdot \mathbf{E} + \mathbf{r} \times \mathbf{d}\end{aligned}$$

where we have defined the strain tensor

$$\mathbf{E} \equiv \tfrac{1}{2}(\nabla\mathbf{s}+\mathbf{s}\nabla)$$

and rotation vector

$$\mathbf{r} = \tfrac{1}{2}(\nabla \times \mathbf{s})$$

The extension then becomes

$$\epsilon = \hat{\mathbf{d}}_0 \cdot \mathbf{E} \cdot \hat{\mathbf{d}}_0 \tag{1}$$

so that if $\mathbf{E}$ is zero, there are no changes in length; the material moves as if it were rigid. The deformational tilt is

$$\boldsymbol{\Omega}_D = \hat{\mathbf{z}} \times ((\hat{\mathbf{d}}_0 \cdot \mathbf{E}) \times \hat{\mathbf{d}}_0 - (\mathbf{r} \times \hat{\mathbf{d}}_0) \times \hat{\mathbf{d}}_0) \tag{2}$$

The tilt thus depends on the direction of the element we choose, the deformations $\mathbf{E}$ and $\mathbf{r}$, and the reference direction $\hat{\mathbf{z}}$. While we could imagine establishing such a direction using a gyroscope, this at present would not give adequate stability [*Farrell*, 1969]; a suspended bar [*Robertson et al.*, 1982] could also be used, but this is not practical at the periods of interest. In practice, we use a pendulum that in the undisturbed state defines the reference direction as the local vertical:

$$\hat{\mathbf{z}}_0 = \nabla U_0 / |\nabla U_0| \equiv \nabla U_0 / g$$

where U_0 is the local gravitational potential, and $\hat{\mathbf{z}}_0$ points up. The use of such a sensor means that the measured tilt will contain terms arising from changes in the potential (U_1) and local accelerations, as well as from local deformation. If both these new terms are small compared to the gravitational acceleration g, the full expression for the tilt vector $\boldsymbol{\Omega}$ is

$$\begin{aligned}\boldsymbol{\Omega} = {} & (\hat{\mathbf{z}}_0 \cdot \hat{\mathbf{d}}_0)(\hat{\mathbf{d}}_0 \cdot \mathbf{E}) - \hat{\mathbf{d}}_0(\hat{\mathbf{z}}_0 \cdot \hat{\mathbf{d}}_0 \cdot \mathbf{E}) \\ & + \hat{\mathbf{z}}_0 \times (\hat{\mathbf{d}}_0(\mathbf{r} \cdot \hat{\mathbf{d}}_0) - \mathbf{r}) \\ & - g^{-1}[\nabla U_1 - \hat{\mathbf{z}}_0(\hat{\mathbf{z}}_0 \cdot \nabla U_1) + \ddot{\mathbf{x}} - \hat{\mathbf{z}}_0(\hat{\mathbf{z}}_0 \cdot \ddot{\mathbf{x}})]\end{aligned} \tag{3}$$

This expression breaks the measured tilt into five terms. Three are deformational (two involving $\mathbf{E}$ and one $\mathbf{r}$) and two inertial (one involving the change in potential U_1 and one the acceleration $\ddot{\mathbf{x}}$). Under special circumstances the deformational terms can be greatly simplified. If $\mathbf{T}$ is the stress tensor, then at a free surface of a body, $\hat{\mathbf{n}} \cdot \mathbf{T} = 0$, where $\hat{\mathbf{n}}$ is the normal to the sur-

face. For an isotropic elastic material this implies that $\hat{\mathbf{n}} \cdot \mathbf{E} = 0$; if we make the baseline normal to the free surface ($\hat{\mathbf{d}}_0 = \hat{\mathbf{n}}$), the deformational tilt becomes

$$\boldsymbol{\Omega}_D = \hat{\mathbf{z}}_0 \times (\hat{\mathbf{d}}_0(\mathbf{r} \cdot \hat{\mathbf{d}}_0) - \mathbf{r})$$

independent of the strain $\mathbf{E}$. Such independence also occurs when both the free surface and the baseline are horizontal ($\hat{\mathbf{n}} = \hat{\mathbf{z}}_0$ and $\hat{\mathbf{n}} \cdot \hat{\mathbf{d}}_0 = 0$). At a horizontal free surface, therefore, the tilt of a vertical element (normal to the surface) is the same as that of a horizontal element, and neither depends on the strain. Another definition of tilt sometimes used is the slope of an uplift, defined by $\nabla(\hat{\mathbf{z}} \cdot \mathbf{s})$; this is equivalent to the sum of (2) evaluated for any two perpendicular and horizontal vectors. In general the tilt depends on the local strain and the direction of the baseline; such tilt-strain coupling can be very important in actual measurements (section 3.4.2).

That $\hat{\mathbf{n}} \cdot \mathbf{E} = 0$ at a free surface also means that the strain tensor there has three independent components rather than the usual six. Measurements along three different $\hat{\mathbf{d}}_0$ are therefore sufficient to define the surface strains; from these we can deduce others, such as the vertical strain. While this is strictly true only at the free surface, it remains a good approximation when the depth is much less than the vertical wavelength of the strain field. (For certain types of problems, such as deformation by atmospheric pressure, the surface of the earth is not a free surface.)

While most tiltmeters and strainmeters are designed to measure the change in orientation or length of a linear element, other designs are possible. One example is the volumetric strainmeter, or dilatometer. This is, of necessity, embedded in the medium being deformed. If we define a closed surface S which moves with the medium, and let its volume be $v(t)$, the dilatometer measures

$$D(t) = \frac{v(t) - v(0)}{v(0)}$$

If we now define the dilatation by

$$\Delta = \mathrm{tr}(\mathbf{E}) = \nabla \cdot \mathbf{s}$$

then by Green's theorem, for infinitesimal strain

$$D(t) = \frac{1}{v(0)} \int_{v(0)} \Delta \, dv$$

which for uniform strain, with Δ constant, implies

$$D = \Delta \tag{4}$$

irrespective of the shape of S. This type of strainmeter will be discussed in section 5.4.

There is no universal convention for the sign of tilt and strain. The definition of extension used here is the commonest one, which makes extensional strain positive. Because compressional stress is then negative, the opposite convention is common in the rock mechanics literature. Another source of confusion is the use of engineering strain, for which the off-diagonal components of the strain tensor are twice as large as the tensor ones used here (for example, the engineering shear strain γ_{12} is $\partial_1 s_2 + \partial_2 s_1$; the corresponding tensor component is $0.5(\partial_1 s_2 + \partial_2 s_1)$). The tilt sign convention adopted here is that a positive tilt in some direction means that a plumb bob would move in that direction. Both strain and tilt are dimensionless, and strain is always just a number; it is often convenient to use ϵ for strain in dimensional expressions, such as $\epsilon\ s^{-1}$ for strain rate. Two systems of units are used for tilt. One is radians, which has the advantage that a numerically equal tilt and strain correspond to deformations of the same size. The other is an inconsistent extension of the Babylonian sexagesimal division of the circle, using decimal arcseconds (1 arcsecond = 4.848 μrad); for very small angles it has no advantage over radians.

2.2. *The Assumption of Uniform Deformation.*

Most analyses of strain discuss the motion of elements of infinitesimal length. I have instead let the baselength l be finite and required that $\nabla\mathbf{s}$ be constant over that length. In practice, of course, we have no choice but to measure over some finite baseline and then compute $\nabla\mathbf{s}$ assuming it to be constant; what we find is the average of the actual $\nabla\mathbf{s}$ (or some part of it) measured over $\mathbf{d}$. The length of the instrument thus imposes a fundamental limit on what we can detect; if the wavelength of a deformational signal is λ, the measured response will be proportional to $\sin(2\pi l/\lambda)/(2\pi l/\lambda)$, which is 1 for λ large, but goes to zero for $\lambda \ll l$. Using a baselength l thus forces us to presume that deformations with wavelengths less than l do not occur; if they do they are filtered out.

Real strains and tilts are nonuniform, of course; the causes of this may be put into five classes:

1. The stress field of the phenomenon being measured will always be spatially varying, and thus will cause nonuniform deformation even in a homogeneous medium.

2. Rocks are in fact not homogeneous on any scale, and the associated spatial variation in elastic moduli will cause nonuniform strains even for a uniform stress.

3. The irregular topography of the earth will also cause the strain to be nonuniform.

4. The instrument itself may cause an especially large variation in modulus; if embedded in the medium, it is an inhomogeneity which will distort the strains from what they would have been otherwise. Alternatively, the instrument may require that such an inhomogeneity be present, in the form of an underground cavity.

5. Finally, there may be local displacements unrelated to 'true' strain and tilt. We suppose that the relative displacement of the end of the instrument is given by

$$\mathbf{s} = \mathbf{s}_T + \mathbf{s}_N$$

where $\nabla\mathbf{s}_T$ is the true deformation gradient and $\mathbf{s}_N$ is an additional displacement which varies randomly in space. (Since we can measure only $\mathbf{s}$, this separation can be made on conceptual, but not operational, grounds). If $\nabla\mathbf{s}_T$ varies over lengths much greater than the baselength l, $|\mathbf{s}_N|/|\mathbf{s}_T| \propto l^{-1}$. Unless we are interested in short-wavelength phenomena, or believe that we can reduce $\mathbf{s}_N$, we thus want to make l as large as possible.

These five classes have been listed in an order which progresses roughly from 'signal' to 'noise'. From the standpoint of instrument design, the first class is part of what we want to measure, and the second and third may

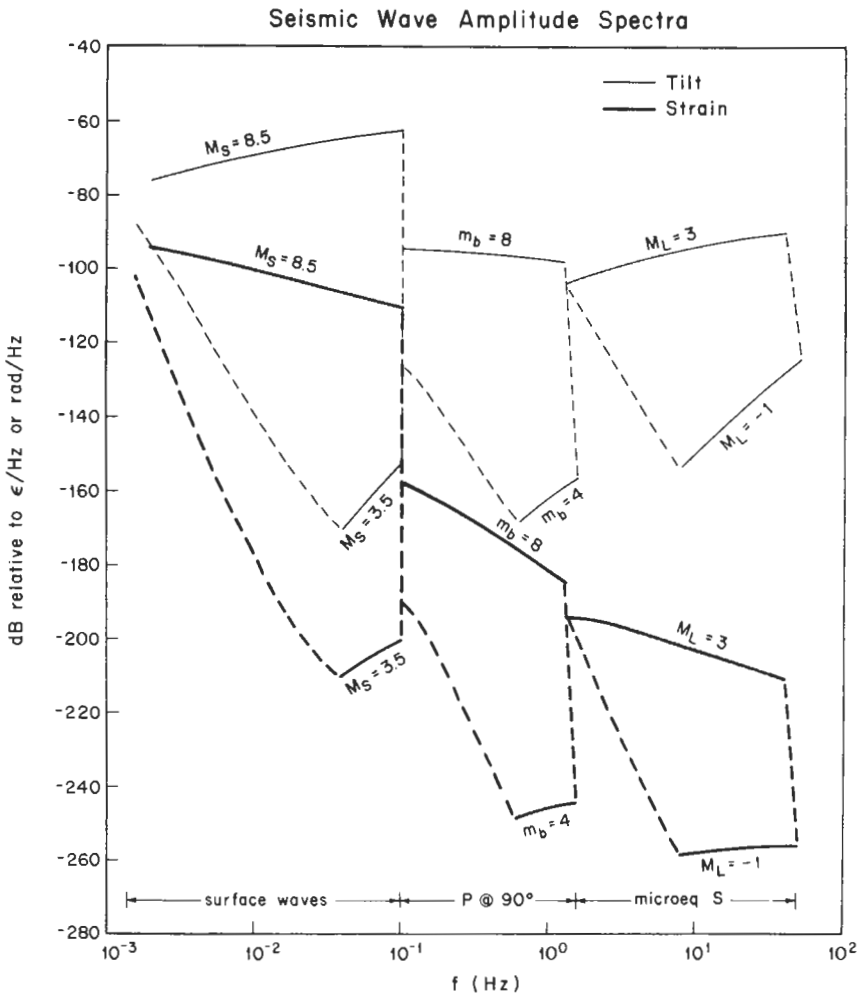

Fig. 1. Amplitude spectra of tilt and strain for three classes of seismic waves over a range of earthquake magnitudes. The original values were given by *Aki and Richards* [1980, Figure 10.10] in terms of displacement. The scaling to tilt was ω^2/g and to strain ω/c.

or may not be, but in any case all three are beyond our control. The fourth is a source of distortion rather than noise in the usual sense, and will be discussed in sections 3.4.2 and 3.4.3. The fifth class causes the greatest difficulties in tiltmeter and strainmeter design; some of the problems and possible solutions will be discussed in sections 3.4.1 and 3.4.4.

2.3. *The Phenomena to be Measured*

The expressions (1), (3), and (4) contain all that is needed to find the strain or tilt that will be measured by a particular instrument in a known deformation field. This section describes the strains and tilts usually seen, as a rough guide to what an instrument must be designed to measure.

Many geophysical phenomena are propagating waves, and it is useful to have approximate rules for the resulting tilts and strains. In the one-dimensional case the displacement s as a function of position x and time t is

$$s(x,t) = se^{i(\omega t - kx)}$$

where ω is the frequency and k the wavenumber. As equation (3) shows, tiltmeters respond to both deformation and acceleration. From elementary considerations the ratio of the first to the second is of order

$$(\partial_x s)/(\partial_t^2 s/g) \propto g/\omega c \tag{5}$$

where c is the phase velocity. Horizontal seismometers measure exactly the same quantity as tiltmeters (scaled by g to put it in terms of acceleration), but are called seismometers because they measure phenomena for which this ratio is small (accelerations dominate), whereas for tiltmeters it is large. Another rough argument gives the relative size of displacements to be measured in strainmeters and conventional seismometers. In a strainmeter the displacement we measure is slk; in a seismometer with natural frequency ω_0 it is $s\omega^2/\omega_0^2$ (for $\omega < \omega_0$). For these quantities to be equal we must have have $l = \omega c/\omega_0^2$. Even if we assume a seismometer period of 20 seconds, we find that except for waves with very long periods, l is much too large to be practical. At short periods ($\omega > \omega_0$) the seismometer response is s, so we would need $l = k^{-1}$, which is impractically long except at very high frequencies and would also cause spatial aliasing. The displacements to be detected in a seismometer are thus almost always larger than those in a strainmeter, making the latter more difficult to design.

Figure 1 shows the range of amplitude spectra for tilt

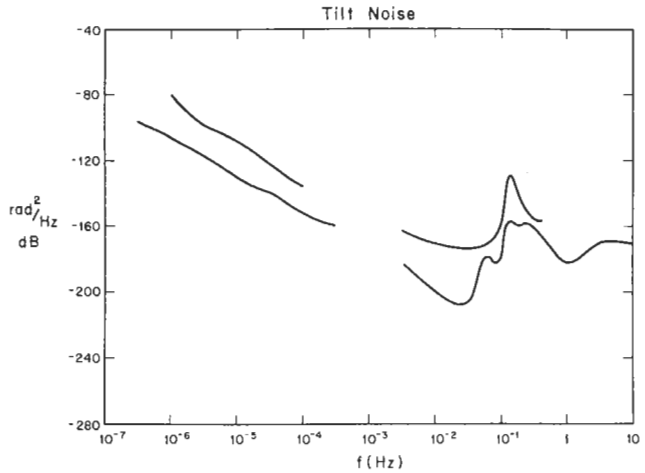

Fig. 2. Range of tilt noise power spectra: the lower curve is the quietest recorded, and the upper the expected level at a noisier but still observationally reasonable site. The lower curve from 3×10^{-6} to 3×10^{-4} Hz is from the long fluid tiltmeter at Piñon Flat Observatory (F. Wyatt, personal communication, 1984) and above 3×10^{-3} Hz is from horizontal seismic noise at Queen Creek [*Fix*, 1972]. The upper curve from 10^{-6} to 10^{-4} Hz is from a Kinemetrics tiltmeter at Piñon Flat Observatory [*Wyatt and Berger*, 1980] and above 3×10^{-2} Hz is based on horizontal seismic noise recorded near the Pacific coast [*Block and Dratler*, 1972; *Haubrich and Iyer*, 1962].

and strain from teleseismic surface waves, *P* waves, and local *S* waves. The tilt spectra include acceleration; the differences between the values for strain and those for tilt show how much acceleration dominates at higher frequencies. At very low frequencies it does not; calculations of response to low-order normal modes must include the terms involving deformation and changes in the potential (equation (3)) as well as the acceleration term [*Gilbert*, 1980]. As equation (5) shows, the ratio of deformation to acceleration depends not only on the period but also on the phase velocity c. Strain measurements are therefore less sensitive than inertial measurements to waves with a high phase velocity, such as many teleseismic body waves.

The lower limit of what we can detect, for any signal, is set by background noise. Figures 2 and 3 show power spectra for tilt and strain noise over a wide range of frequency. In practice, noise in the seismic band (10^{-3} Hz and larger) is extremely variable both in space and time; the limits shown roughly encompass the range most usually seen. The source of noise varies with frequency. For frequencies of 0.5 Hz and greater, the main sources are body wave energy [*Haubrich and McCamy*, 1969] with $c = 10$ km s^{-1} or more, and local sources such as machinery or wind-blown vegetation. Between 0.05 and 0.5 Hz the largest source is microseisms: surface waves ($c \simeq 3$ km s^{-1}) generated at sea, and therefore extremely variable with time. For frequencies of 10^{-3} to 0.05 Hz the noise appears to be caused by atmospheric pressure changes deforming the ground. The largest fluctuations are those caused by wind turbulence [*Kimball and Lemon*, 1970; *McDonald and Herrin*, 1974], which propagate at roughly the wind velocity ($c = 5$—30 m s^{-1}) and vary in strength with the wind. During calms the main source of pressure fluctuations is infrasound ($c = 300$ m s^{-1}) [*Sorrells and Douze*, 1974]. The low velocity of both sorts of pressure changes means that the ratio (5) is much larger than for seismic waves of the same period. When the wind is high this makes horizontal seismometers much noisier than vertical ones. However, this low velocity also means that the deformation is quasi-static, and dies away with depth [*Murphy and Savino*, 1975; *Peterson et al.*, 1976] so that burial reduces noise.

At frequencies below 10^{-3} Hz, deformation must be quasi-static. The sources of noise in this frequency range, or indeed whether the curve shown reflects ground or instrument noise, are not known. Some possible sources of noise are thermoelastic deformation [*Berger*, 1975; *Harrison and Herbst*, 1977], pore pressure changes and joint deformation related to groundwater motion [*Herbst*, 1976; *Takemoto*, 1983; *Evans and Wyatt*, 1984; *Kümpel and Lohr*, 1985], and air pressure changes [*Suyehiro*, 1982].

If frequencies above 0.1 Hz are filtered out, the largest signal on a tilt or strain record is the earth tides (and occasionally a large earthquake). Figure 4 shows how the average tidal amplitude would vary with latitude on an elastic, oceanless earth (this is called the body tide). Tilt tides are about four times larger than strain tides because they involve the direct attractions of the sun and moon (the U_1 terms in (3)) as well as the deformation caused by them. (The deformational tilt tide ($\boldsymbol{\Omega}_D$) is about the same size as the strain tide.) In addition to the body tide, the mass shifts of ocean tides produce loading effects [*Farrell*, 1972], again involving both potential changes and deformations. The size of these load tides depends on the tidal constituent and the location of the instrument. Figure 5, showing the relative size of M_2 load tides on an east-west line across the United States, illustrates what is generally true, that near the coast the tilt and strain loads can equal or exceed the body tide, whereas well inland they are only small perturbations to it.

A final class of tilts and strains are those caused by tec-

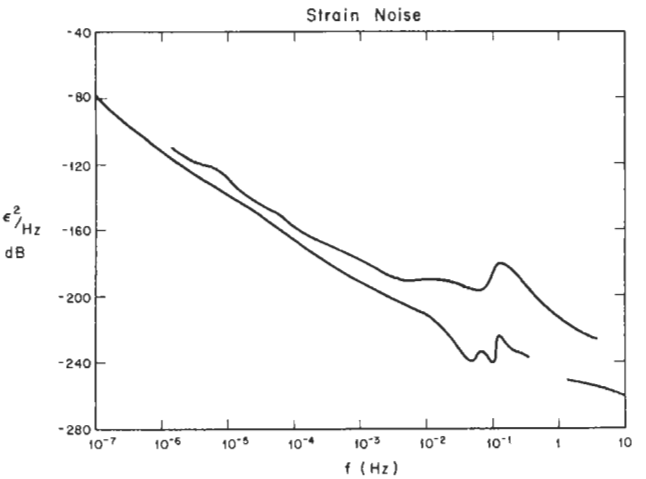

Fig. 3. Range of strain noise power spectra, as in Figure 2. The lower curve up to 10^{-2} Hz is from the NW laser strainmeter at Piñon Flat Observatory [*Agnew*, 1979]; from this frequency to 0.3 Hz it is from measurements with a rod strainmeter at Queen Creek [*Fix and Sherwin*, 1972], and from 1 to 10 Hz from laser strainmeter data in the Poorman Mine [*Berger and Levine*, 1974]. The upper curve is from the laser strainmeter in Queensbury tunnel [*Beavan and Goulty*, 1977].

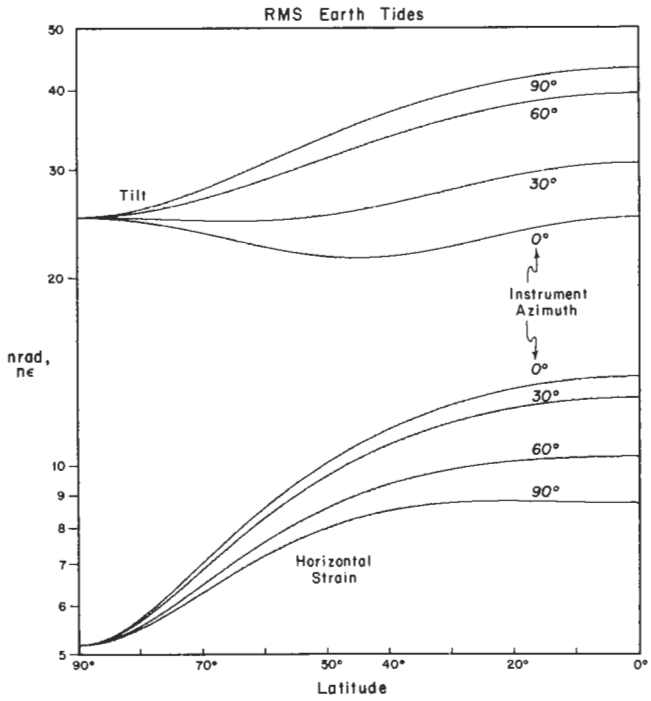

Fig. 4. Root-mean-square amplitude of the combined diurnal and semidiurnal body tides in tilt and strain, as a function of latitude and for different instrument azimuths, on an elastic oceanless earth.

tonic movement. These fall into two groups, widely separated in frequency. One is coseismic steps caused by elastic rebound at the times of earthquakes. Reliable observations of these [*McGarr et al.*, 1982*a*; *Wyatt and Agnew*, 1982] show that they vary in accordance with the values found from dislocation theory; while complete formulae [*Okada*, 1985] are complicated, a simple rule is that for a point source the deformation at a distance r will be of the order of $M_0/\mu r^3$, where M_0 is the seismic moment and μ is the shear modulus of the material. While many coseismic steps seem to occur rapidly, some [*Sacks et al.*, 1981] may last over periods of minutes; the strain rates involved are $10^{-10}\epsilon$ s^{-1} or more.

The second group, at much longer periods, is the strains and tilts associated with nonseismic tectonic motion. The spatial distribution, temporal variation, and even size of these deformations are poorly understood. Most information on them has come from geodetic measurements, which are relatively infrequent and imprecise. Strain rates in the western United States [*Savage*, 1983] seem to range between 3×10^{-15} and $3\times10^{-14}\epsilon$ s^{-1} (1 year $= 10^{7.5}$ seconds). Rates of tilting are clouded by uncertainties over leveling methods [*Mark et al.*, 1981; *Strange*, 1981] but seem to be of the same order [*Reilinger et al.*, 1984]. Measurements in Japan suggest similar rates [*Thatcher and Matsuda*, 1981]. Deformation rates are higher following large earthquakes [*Mavko*, 1981]. In restricted regions, rates can be much higher: for example, 3×10^{-12} rad s^{-1} around some volcanoes [*Duffield et al.*, 1982] and 10^{-12} rad s^{-1} in regions undergoing subsidence because of groundwater withdrawal [*Poland and Davis*, 1969].

2.4. *Defining Instrument Quality*

As noted in section 1, there is no agreed 'best design' for tiltmeters and strainmeters; the result is that there often seem to be as many designs as there are instruments. It is useful to set out what goals an ideal instrument would attain; even if reaching them all is impracticable, an awareness of them will suggest what trade-offs can be made. It is important to have common standards for describing instrumental quality, so that improvements in design can be quantified and recognized (for an example of progress in design encouraged by adoption of a common standard, see *Barton* [1966, chapters 1 and 2]). Lacking such standards, comparisons can too easily turn polemical [*Sydenham*, 1974*a*; *Levine*, 1975; *King et al.*, 1975; *Sydenham*, 1975].

Table 1 lists some desirable features that a design could aim for, and for each feature the areas of enquiry for which it is especially important. To take one example, the geophysically interesting effects associated with earth tides are often only a few percent of the total tide [*Baker*, 1978], so that a very accurate calibration is necessary if the measurements are to be of any value. On the other hand, so little is known about tectonic deformation that a measurement of it to within 20% would be valuable; the difficulty in such measurements comes from instrument noise. If stability and accurate calibration cannot be combined, it is necessary to decide what the primary purpose of an instrument will be, and design accordingly. The economic aspects, especially capital cost, are sometimes overemphasized. The exigencies of research funding make it seem overly desirable to keep the capital cost low, even though over the life of the system the operating cost will exceed the initial cost of even expensive instruments. (The one exception would be measurements at active volcanoes, where instrument life may be short.)

To examine instrument quality quantitatively, we suppose that the instrument output $w(t)$ for an input $y(t)$ is

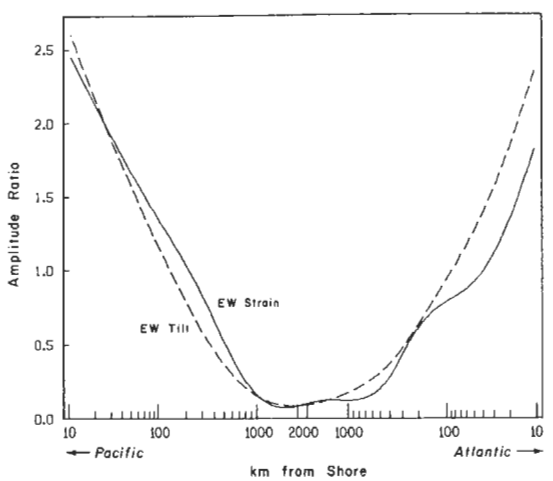

Fig. 5. Amplitude of the M_2 load tide contribution to east-west tilt and strain along a line across the United States at 40°N; the scale has logarithmic singularities at both coastlines for clarity. The loads were computed from the ocean tide model of *Schwiderski* [1979] and were normalized by the amplitudes of the corresponding body tide at this latitude (40.6 nrad for tilt, 4.06 nε for strain).

TABLE 1. Goals for Strainmeter and Tiltmeter Designs

Property	Applicable Field
Low Noise	
High frequency (periods < 1 hour)	Seismic waves, coseismic offsets
Low frequency (periods 1 hour to 1 week)	Earth tides, rapid tectonic deformation
Very low frequency (periods > 1 week) (also called 'stability')	Gradual tectonic motion
Instrument Response	
Accurate and stable calibration	Earth tides
High dynamic range	Seismic waves
Immunity to high acceleration	Coseismic offsets
Linear response	Seismic waves, earth tides
No hysteresis	Coseismic offsets
Broadband response	Seismic waves
Economic	
Low operating cost	All
Ease of installation	All
Low capital cost	Volcano monitoring

$$w(t) = h(t) * y(t) + n(t) \tag{6}$$

where $h(t)$ is the impulse response, the asterisk denotes convolution, and $n(t)$ is noise. 'Noise' here is whatever we are not interested in, and 'signal' whatever we are. It is not necessarily true that one is of geophysical interest and the other not: the long-period seismologist and earth tidalist each regard the other's signal as noise.

The counterpart of (6) often seen in elementary discussions of measurement is

$$w_i = hy + n_i \tag{7}$$

where y is the quantity to be measured, h the scale factor of the instrument, and n_i the error of the ith measurement w_i. The accuracy of the measurement is dependent on h being correct and on the mean of n, E[n], being zero; the precision depends on the variance of the error, Var[n], being small. If our purpose is to detect changes in y with time, we do not care about E[n] but cannot resolve changes much smaller than $(\mathrm{Var}[n]/Nh^2)^{1/2}$, where N is the number of measurements, and the errors are assumed to be Gaussian and independent.

Despite their apparent similarity, equation (7) cannot be generalized into equation (6) without the addition of a wide range of new concepts. These are needed because the variables in (6) are functions of time. Fairly simple statistical concepts are adequate for an understanding of (7), but to be able to work with the quantities in equation (6) requires the techniques of time series analysis. There are a great many references available on this subject [*Bracewell*, 1965; *Priestley*, 1981], and it is neither appropriate nor possible to give a full discussion here. I shall instead give a brief summary of some useful descriptive techniques, and simple rules which may be used to make rough estimates from them.

Just what technique is appropriate depends on the nature of $y(t)$ and $n(t)$ or, more precisely, what idealized properties we choose to assign to them. The signal y may be approximated by a simple step (coseismic offsets), a more complicated transient (seismic waves), a sum of sine waves (earth tides), a stochastic process (microseisms, strain fluctuations), or a secular change (strain accumulation). The noise n is usually taken to be a stochastic process, often with a slowly varying mean value ('drift'), but otherwise stationary. Such a model for noise is often sufficient and always necessary. An immediate consequence of (6) is that w is then also, in part, a stationary stochastic process.

How may such processes be described? Statistical measures *must* be used: we can define the mean, variance, and higher moments of a random variable, but not its amplitude. A stationary process is not most usefully described in the time domain; just because it is stationary, one part will look like another. However, such processes commonly show considerable variation with frequency; such variation is quantitatively described by the *power spectrum* of the process. The most intuitively appealing approach to the power spectrum is to imagine putting the signal into a narrowband filter that passes only frequencies between $f_0 - \Delta f/2$ and $f_0 + \Delta f/2$. The output of such a filter will be another stochastic process with a variance σ^2. The power spectrum $P(f_0)$ may then be calculated using

$$P(f_0) = \sigma^2/\Delta f \tag{8}$$

In practice, (8) is not used to define the power spectrum, which is more formally the Fourier transform of the autocovariance function. It provides, however, a good working rule. When P varies with frequency, the equivalent expression is

$$\sigma^2 = \int_{f_0-\Delta f/2}^{f_0+\Delta f/2} P(f)\, df \tag{9}$$

When y, n, and hence w are all stationary stochastic processes we may rewrite (7) in the frequency domain as

$$W(f) = |H(f)|^2 Y(f) + N(f)$$

where $H(f)$ is the Fourier transform of $h(t)$, the other capital letters indicating power spectra.

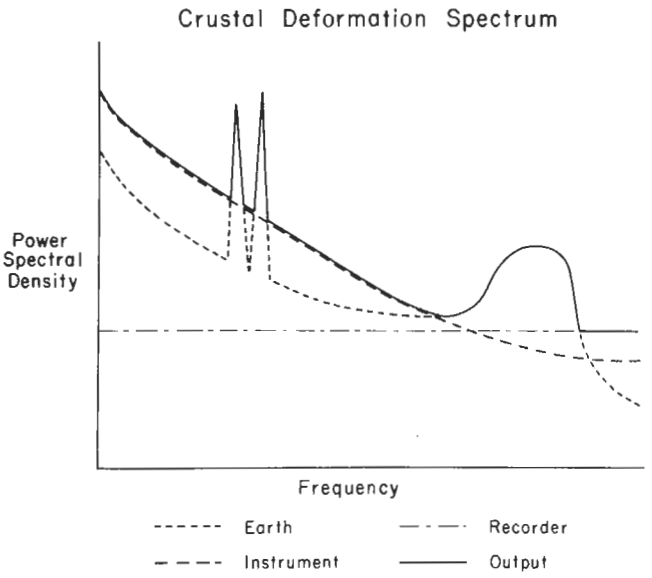

Fig. 6. Generalized version of a power spectrum of the output of a tiltmeter or strainmeter, showing the different parts of the total spectrum as they might appear on a log-log scale. See text for explanation.

Equations (8) and (9) are very useful in understanding power spectra and their relationship to a time series. The correct units for a power spectrum are variance (amplitude squared) divided by frequency, so that the units for tilt spectra are $\text{rad}^2\ \text{Hz}^{-1}$. The square root of this is often used in engineering; such spectra can be converted to conventional power spectra by squaring. Another engineering practice is to use decibels (dB) as a convenient way of handling quantities which vary by such large factors that logarithmic scales are appropriate (and rare is the spectrum for which this is not true). If two quantities have variances σ_1^2 and σ_2^2, the ratio between them is $10\log_{10}(\sigma_1^2/\sigma_2^2)$ dB; for amplitudes a_1 and a_2 the expression is therefore $20\log_{10}(a_1/a_2)$ dB. To be useful, spectra must be plotted on an absolute scale, in which 0 dB ($P = 1$) is a known physical value; for example, the tilt noise spectra in Figure 2 are in decibels relative to a power level of $1\ \text{rad}^2\ \text{Hz}^{-1}$; this reference level, or the strain equivalent $1\ \epsilon^2\ \text{Hz}^{-1}$, will be used in this paper unless another is specified.

As an example of the use of power spectra, consider the statement made above that the earth tides dominate any low-passed strain record. For frequencies less than 10^{-2} Hz, the noise spectrum is roughly $5\times10^{-24}/f^2\ \epsilon^2\ \text{Hz}^{-1}$ for f in hertz. When looking at a record for tides the eye classifies everything at much lower frequencies as 'drift'; we may take 2×10^{-6} Hz (6 days) as our lower limit and 10^{-2} Hz as our upper limit. Application of (8) then gives a standard deviation, or rms amplitude, of 2×10^{-9}, only 10% of the average tidal amplitude at most latitudes. (The peak-to-peak amplitude of a random process is about five times the rms value.) Tides are not stochastic processes; as a consequence they have well-defined amplitudes but not a power spectral level. We may, however, use (8) to get an approximate rule for finding one: the rms amplitude of a sine wave of amplitude a is $\frac{1}{2}a^2$, and for a record length τ the smallest resolvable frequency is τ^{-1}, making the apparent spectral level $\frac{1}{2}a^2\tau$. At tidal periods the strain noise level is about $10^{-14}\ \epsilon^2\ \text{Hz}^{-1}$, and so in a 1-year record a sine wave of amplitude 1.5×10^{-10} would have a 20 dB signal-to-noise ratio.

If $y(t)$ is a transient, rather than a sinusoid, the signal-to-noise ratio is the square root of

$$\int_0^\infty \frac{|S(f)|^2}{P(f)}\,df$$

where $S(f)$ is the amplitude spectrum of the signal. The value of this ratio determines whether or not a transient signal can be detected against background noise [*Helstrom*, 1968]. If we use the same units for both signal and noise, and plot them in decibels (effectively squaring the amplitude), then the plots are directly comparable. This has been done in Figures 1, 2, and 3, so that we can see (for example) that the cutoff in observed body waves for frequencies less than 0.5 Hz is a direct consequence of the microseism peak in the noise spectrum.

One specification often given for deformation instruments is their 'resolution.' It may seem perverse to recast such an obvious notion in the recondite form of a power spectrum, but as the discussion above has tried to show, the very simplicity of such a concept makes it an inadequate description of instrumental performance. Returning to equation (7) and the definition of resolution immediately following it, we see that for this simple model the resolution may be made as small as we wish by enough averaging. For a time series record this may not be so, because the noise level may rise at low frequency. In this context, what resolution usually means is the smallest step that could be seen without much averaging; in practice, it is taken to be the rms variation visible on a short section of the record, filtering out the long-period changes 'by eye.' If we approximate this variation as band-limited white noise of variance σ^2, the equivalent power spectrum is then $\sigma^2/f_{\max}$, where $f_{\max}$ is the upper limit of frequencies recorded.

The very low frequency components are usually called drift and are described by polynomial functions of time. Sometimes they really are secular trends, but more often we cannot tell whether they are this or merely random fluctuations with periods longer than the available record. This problem is common to all studies of phenomena with very red spectra [*Press*, 1978]; the only cure is to wait for more data and to be cautious in extrapolating.

Figure 6 is a schematic log-log power spectrum drawn to emphasize some of these points for strain and tilt measurements. The instrument noise is the heavy dashed line, which over most of the frequency range is the main source of energy. Earth noise lies below this except at tidal frequencies (the two peaks on the left) and microseisms (the hump on the right). Just because there is so much energy in the earth at these frequencies, detecting them does not show that instrument noise is low; good tidal records, for instance, are necessary but not sufficient for an instrument to be able to detect slow tectonic motions. An absolute lower limit is set by the quantization noise in the recorder [*Widrow*, 1961; *Zürn*, 1974], which for a step size Δw and sampling internal Δt has a flat power spectrum with the value $(\Delta w)^2\Delta t/6$. For a properly designed system this will dominate only at the highest frequencies.

TABLE 2. Properties of Construction Materials

Material	α K^{-1} (10^{-6})	ρ kg m^{-3} (10^3)	E N m^{-2} (10^{10})	Ξ K^{-1} (10^{-4})	c_p J kg^{-1} K^{-1} (10^3)	K W m^{-1} K^{-1} (10^2)
PVC	80.	1.5	0.3		1.	0.0015
Aluminum	24.	2.8	7.	−5.8	0.96	1.6
Brass	20.	8.5	9.7	−3.9	0.38	1.2
Stainless steel	16.	8.0	20.	−2.6	0.51	0.15
Concrete	10.	2.4	3.		0.9	0.01
Ni-Span C	8.	8.1	18	<0.1	0.51	0.13
Dimension stone	6.	2.9	7.	−3.	0.8	0.02
Carbon fiber	−0.78	1.7	24		0.72	
Invar	0.6	8.0	15.	−5.	0.52	0.13
Fused silica	0.55	2.2	7.	1.2	0.72	0.013
Zerodur	−0.02	2.5	9.			

Quantities are coefficient of linear thermal expansion (α), density (ρ), Young's modulus (E) and its variation with temperature ($\Xi = E^{-1}\partial_T E$), specific heat (c_p), and thermal conductivity (K). Numbers should be multiplied by the scaling factor at the head of each column.

3. Basic Design Techniques

3.1. *Introduction*

The definition adopted in section 2.1 for an ideal instrument was either a line joining two points in the deforming medium, or a closed surface in it. A tiltmeter measured the orientation of the line relative to the local vertical, an extensometer changes in the length of the line, and a dilatometer changes in the volume defined by the surface. To build instruments that approach these ideals we need three things: (1) a stable reference, of length or volume for strainmeters, and of direction (the local vertical) for tiltmeters, (2) a method of comparing this reference with the motions of the instrument frame, and (3) a procedure for attaching the instrument frame to the ground so that it only responds to 'true' ground deformation.

This section describes solutions of these problems which are useful for more than one kind of instrument. Section 3.2 discusses some aspects of instrument design related to the stability of materials. Comparing the reference with the instrument frame requires measuring small displacements; section 3.3 discusses optical, capacitive, and electromagnetic displacement sensors. The last problem, attachment to the earth (section 3.4), is by far the most complex and is not yet completely solved. The environment the instrument is installed in often determines the attachment procedure, and so that section discusses the advantages and disadvantages of some common environments.

3.2. *Mechanical Design*

A good design requires the appropriate arrangement of parts, which cannot be found by following set procedures [*Ferguson*, 1977]. Some guidelines are suggested by the properties of materials, some of which are given in Table 2 for materials often used in tiltmeters and strainmeters.

Temperature effects are a major problem in this field. Figure 7 shows a spectrum of air temperature at a desert site; comparison of it with Figures 2 and 3 shows that for thermal effects to be less than strain or tilt noise at daily periods ($f \approx 10^{-5}$ Hz), the instrument would need a temperature coefficient of 10^{-10} K^{-1}. In regions with a less harsh climate the daily peak would be smaller but the continuum near the same level, so that a temperature coefficient of 10^{-9} K^{-1} would suffice. As no material approaches these values, thermal control is always needed. Operation in the field often limits the amount of thermal isolation that is practical, and an instrument must almost always be designed to be insensitive to temperature.

A common method of thermal isolation is burial in the

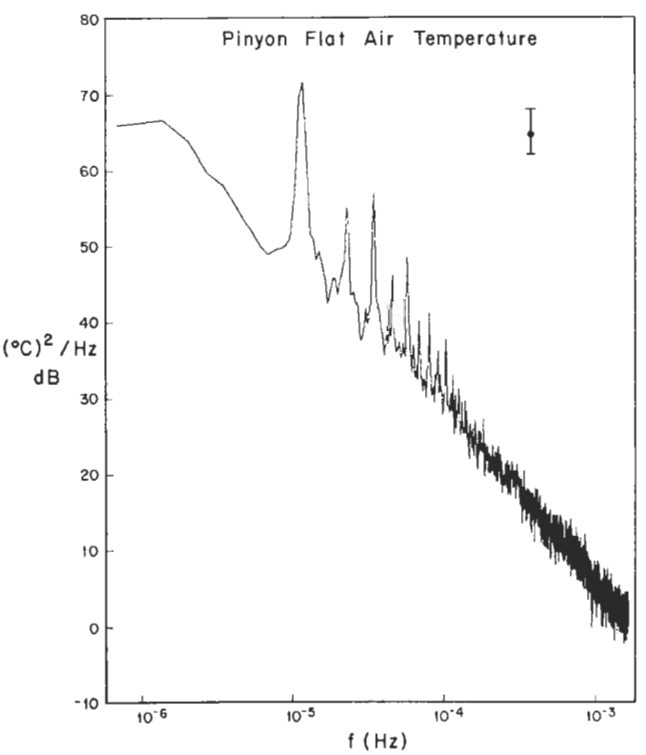

Fig. 7. Power spectrum of air temperature measured inside a standard meteorological shelter at Pinyon Flat, a high desert location in southern California (33.61°N, 116.46°W, 1280 m elevation), for March 23 through July 4, 1983. The error bars are 95% confidence limits. This shows the continuum of the temperature spectrum, which decreases rapidly at high frequencies, and also the lines from the diurnal cycle in temperature, the largest being at 1.16×10^{-5} Hz. At this location this cycle is roughly a square wave, so that the odd harmonics are larger than the even ones.

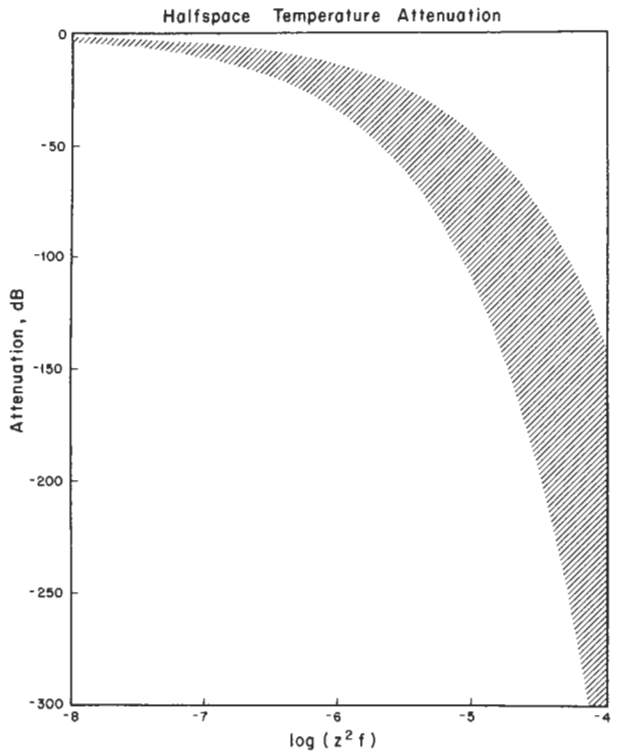

Fig. 8. Temperature attenuation in a halfspace of a uniform surface temperature varying sinusoidally with time. The abcissa is $\log(z^2 f)$, where z is the depth in meters and f the frequency in hertz. The shaded band shows the range of attenuation for rocks and soils.

ground. Figure 8 shows the attenuation for conduction of heat from a surface disturbance into a halfspace, for typical rocks and soils. The low thermal diffusivities of these materials makes them excellent passive insulators. For example, at daily periods burial 1 m deep gives 50 to 100 dB attenuation, compared with 30 dB for a well-insulated and air-conditioned surface building. (Active thermostats [*Sporton*, 1972] can give higher thermal stability.) At annual periods ($f \approx 3\times10^{-8}$ Hz) the attenuation is only 2 to 6 dB at 1 m but 70 to 170 dB at 30 m. In tunnels or caves the thermal stability may be worse because of exchange of inside and outside air, but despite the difficulties of these buried locations (such as high humidity in many tunnels and total immersion in most boreholes) their temperature stability eliminates many design problems and has made them a popular location for deformation measurements. They are discussed further in sections 3.4.2 and 3.4.3.

The biggest source of temperature sensitivity is usually dimensional changes. For example, if we mount a 10-cm-wide base on brass leveling screws, the length of these must differ by less than 5 μm for the temperature sensitivity of tilt to be less than 1 nrad K^{-1}. Temperature sensitivity can sometimes be reduced by using symmetrical arrangements of parts, as in the three-plate capacitor displacement sensor (section 3.3.2) or the linear variable differential transformer (section 3.3.3). Another useful technique is to arrange components so that expansion of one set is compensated by contraction of another. For example, since the α of some steels is only 1.2×10^{-5} K^{-1}, half that of aluminum, two steel tubes may be combined with one aluminum tube to make a length standard little affected by temperature, on the same principle as Harrison's 1720 'gridiron' clock pendulum [*Rawlings*, 1944]. For this type of compensation to work well the parts must be dynamically as well as statically balanced: not only must the expansion coefficients be matched, but also the compensating parts must change temperature at the same rate. The design must balance the effects of different thermal diffusivities (the diffusivity being $K/\rho c_p$), heat capacities, and radiational effects [*Jones and Forbes*, 1962]. This becomes difficult when large temperature gradients can exist between different parts of an instrument. In a small instrument such gradients can be kept low by providing so much insulation that the temperature varies more slowly than the time needed for the interior to equilibrate; compensation can then be very useful. In larger instruments thermal gradients are harder to suppress, the problem being greatest for long-base tiltmeters and strainmeters: not only are these large, but because of their size they must be installed near the surface.

Another way to reduce thermal sensitivity is to use materials with a low expansion coefficient. Invar and related alloys are extensively used because of their machineability. Fused silica has also been popular, especially for strainmeters, though other glasses (such as Schott 'Zerodur') now available have even smaller expansion coefficients [*Berthold and Jacobs*, 1976]. Another possible material is carbon fiber [*Gill*, 1972], which has so far been used only in wire strainmeters (section 5.2). Even with such materials, care is needed in design; for example, an Invar positioning screw must be fed through an Invar nut rather than a regular tapped hole [*Westphal et al.*, 1983].

Next to thermal expansion, imperfections in elasticity are the biggest problem with materials. In an ideal world we could build our instruments from materials that were perfectly rigid, flexible, or springy; in reality we have only approximations to these. Nonrigid members are commonly used in two different ways. One way is as elastic supports for parts that have to be moved smoothly through small distances [*Jones*, 1962]. A common example is the cross-strip flexure hinge for small angular motions; these are commercially available, and there are design methods [*Eastman*, 1933; *Weinstein*, 1967*a*, *b*] for building ones with special properties such as low stiffness. When used as a support, an elastic member is commonly acting against a stiff constraint, such as a micrometer head, and changes in its elasticity have little effect.

The other application is typified by the suspension of a simple pendulum, whose purpose is merely to keep the suspended mass from falling. As the pendulum swings, the elasticity of the suspension acts against the soft constraints of the inertia of the bob and the gravitational force on it. In this use we would like the material to behave perfectly flexibly or, barring that, elastically. If q is the displacement of the pendulum bob away from the position at which the suspension is fully relaxed, and $F(q)$ is the other forces acting on it, with k being the spring rate of the suspension, equilibrium requires $kq = -F(q)$. For small changes in k, q will vary in pro-

TABLE 3. Creep Rates

Material	Test Duration	Creep Rate s^{-1}	Creep Rate yr^{-1}	Source
Pt-Ir (standard meter)	65 yr	$<10^{-16}$	$<3\times10^{-9}$	*Hart and Baird* [1961]
Invar wire, 100 N tension	2 yr	3×10^{-14}	10^{-6}	*Gervaise* [1974]
Fused silica	~70 days	-6×10^{-15}	-2×10^{-7}	*Berthold et al.* [1977]
Zerodur	~70 days	$<3\times10^{-16}$	$<10^{-8}$	*Berthold et al.* [1977]
Super Invar	~70 days	$<3\times10^{-16}$	$<10^{-8}$	*Berthold et al.* [1977]
Cer-vit	~70 days	6×10^{-15}	2×10^{-7}	*Berthold et al.* [1977]
Invar*	~70 days	7×10^{-14}	2×10^{-6}	*Berthold et al.* [1977]
Bronze	35 yr	1.5×10^{-15}	4.4×10^{-8}	*Bomford* [1962]

*May not have been properly annealed.

portion to

$$\frac{dq}{dk} = \frac{-q}{k+F'(q)}$$

and hence when F' is small (a 'soft' constraint) the elasticity of the suspension must be low for variations in it to be unimportant.

Here too temperature changes cause trouble. Most springy materials weaken with temperature, and if an elastic member provides much of the restoring force, temperature variations of the elastic constant can cause larger effects than dimensional changes. Compensation can correct for a weakening spring by an increase in length, or the spring can be made from a constant-modulus alloy such as 'Ni-Span C.'

More subtle and less easily quantified problems arise from time-dependent departures from elastic behavior. One such is elastic afterworking, in which the strain produced in response to an applied stress takes some time to reach its final value, but the body eventually returns to its undeformed state after the stress is removed. This effect is distinct from creep, in which the additional strain produced by continued application of stress is not recovered. Both of these are forms of hysteresis, in which the present shape of the deforming body depends not only on the present stresses but also on their history; the form of the dependence is often nonlinear and itself highly dependent on the composition of the body and how it is fabricated. Hysteresis becomes proportionately greater with larger strains, and for that reason is worst in astatized suspensions (section 4.1.1), which are designed to produce large deflections in response to small forces. The effect is well known in metal gravimeter springs [*Harrison and LaCoste*, 1978] and has also been seen in some tiltmeters with metal suspensions. Because fused quartz has little hysteresis [*Strong*, 1938], it is a good material for such applications, though the high thermal coefficient of its Young's modulus can create problems.

While creep may occur in the absence of stress, it is usually faster for larger stresses. The instrument assembly should therefore be as stress-free as possible; *Jones and Richards* [1973] describe useful design techniques. There should be as few interfaces between different components as possible, because stresses often concentrate there. One problem with the thermal compensation schemes discussed above is that they necessarily involve many contacts between different materials. Creep can often be reduced by appropriate heat treatment, which both eliminates residual stresses from machining and stabilizes the material [*Wilding*, 1970; *Wenschof*, 1980]. At room temperature and low stress, creep is so slow that measuring it is difficult. Table 3 lists some available values; the most precise measurements are those made by *Berthold et al.* [1977] using a stabilized optical system as a reference. Their specimens were kept in a tightly controlled environment; values obtained in a field instrument are likely to be worse. As the rates in this table are comparable to those of tectonic deformation, there is little hope of a strainmeter with a material length standard being able to measure such deformation.

3.3. *Displacement-Measuring Techniques*

Virtually all tiltmeters and strainmeters require that the displacement of some part be measured, and because the deformations are small, these displacements are also. In the early stages of instrument development much ingenuity was expended on clever techniques for amplifying these displacements to an easily measured level. Improved electronic and optical sensors have made this work obsolete. There are many different types of displacement transducer available [*Neubert*, 1975; *Roughton and Jones*, 1979; *Garratt*, 1979]. This section discusses those that have seen the widest use in deformation instruments: optical methods (optical levers and interferometers), capacitance bridges, and electromagnetic transducers, especially linear variable differential transformers.

3.3.1. *Optical methods.* A measurement technique applied in some of the earliest crustal deformation measurements, and still in use today, is the optical lever, sometimes called Poggendorf's method. The basic principle is to use a reflected light beam to magnify the rotation of a mirror; if this rotation is θ, the beam will be displaced by $2r\theta$ at a distance r. The simplest arrangement is to focus the reflected beam on moving photographic paper, but this gives only an analog record. To get an electrical output the beam may instead be directed on a pair of photocells whose outputs cancel when the beam is centered, with any deflection producing a voltage. Such systems can be made very sensitive and compact, especially when suitably arranged Ronchi grids are placed in the light path [*Jones*, 1961; *Filloux*, 1967, 1970], though care must be taken to limit distortions caused by diffraction [*Palmer and Hollmann*, 1972] and to keep the intensity of the light source constant. Jones has reported a high-frequency noise level of -210 dB (rad^2 Hz^{-1}), and Filloux a long-term stability of 10 nrad.

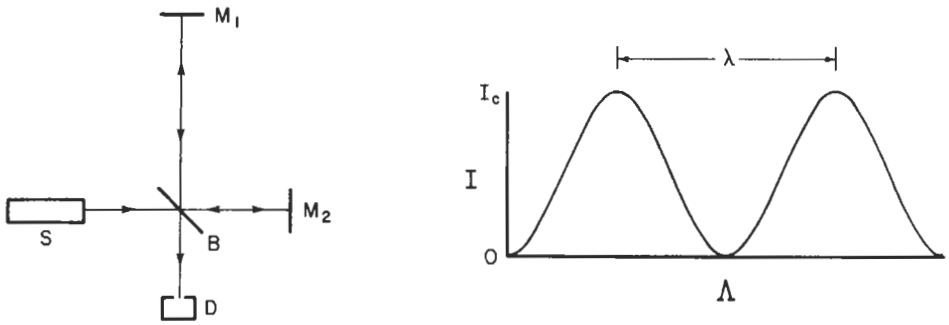

Fig. 9. (Left) A schematic view of a Michelson interferometer. (Right) Plot of the intensity I_c measured by the detector D as a function of the difference in optical path length between the two arms (Λ). See text for discussion.

The optical lever exploits the low mass of a light beam; the other optical system in wide use, the interferometer, depends on the wave nature of light. Figure 9 shows a schematic version [*Born and Wolf*, 1980] of a Michelson interferometer (the type most widely used). A parallel beam of light from a source S is sent to a beamsplitter B, where it is divided equally and goes to two reflectors M_1 and M_2. The returned beams meet and interfere at B, the interfered energy going (in part) to a detector D. If the source is monochromatic with intensity I, the electric field of the beam incident at B from S will be the real part of $\Sigma = ae^{i\omega t}$ with $I = \frac{1}{2}\Sigma\Sigma^*$. If the optical path lengths BM_1B and BM_2B are Λ_1 and Λ_2 respectively, then the electric field of the interfering beams will be

$$\Sigma_c = \tfrac{1}{2}a\left(e^{i(\omega t+k\Lambda_1)} + e^{i(\omega t+k\Lambda_2+\Theta)}\right)$$

where Θ is a phase shift introduced by the multiple reflections and transmissions and $k = 2\pi/\lambda$ is the wavenumber of the light. The intensity seen by D is $\frac{1}{2}\Sigma_c\Sigma_c^*$ or

$$I_c = \tfrac{1}{2}I[1 + \cos(k(\Lambda_2-\Lambda_1) + \Theta)] \qquad (10)$$

which will vary with the path length difference $\Lambda = \Lambda_2 - \Lambda_1$ as shown in Figure 9. Counting the light to dark transitions (fringes) thus allows us to detect movements of either arm of the interferometer.

The design most commonly used to make interferometric measurements fixes one arm and lets the other move. Counting fringes gives an inherently digital output and, since the value of λ is usually known to 4 or 5 figures, one which is very accurately calibrated. On the other hand, this gives rather low resolution, since λ is $\approx 6\times10^{-7}$ m, though fringe subdivision is possible. Another problem is that Λ_1 and Λ_2 are the optical path lengths; if light travels through a medium of refractive index n, then $\Lambda_1 = n\,l_1$, where l_1 is the physical length. With $\lambda = 6.33\times10^{-7}$ m (a common laser wavelength), dry air has a refractive index of $n = 1 + 7.86\times10^{-7}\,p/T$, where p is the pressure and T the absolute temperature [*Owens*, 1967]. The temperature and pressure coefficients of n (and hence Λ) for $T = 288$ K are then $9.5\times10^{-12}p$ K^{-1} and 2.7×10^{-9} Pa^{-1}. The temperature sensitivity is not severe (at atmospheric pressure not much worse than for Invar), but the sensitivity to pressure changes (which are harder to shield against) means that an open-air system will give large spurious signals unless both arms vary together. While in theory the observations could be corrected using temperature and pressure measurements, in practice the limited accuracy of these keeps the uncertainty near 10^{-8} [*Estler*, 1985], too large for most geophysical studies. The simplest solution is to regulate the pressure by holding it near zero; this also reduces the temperature sensitivity and nearly eliminates bending and distortion of the light beam by temperature gradients. Mechanical vacuum pumps can easily reach 1 Pa.

The discussion above assumed perfectly monochromatic light; in practice the light will be a mix of frequencies. It is easy to see that for the fringes to be visible the maximum intensity for light at one frequency should not coincide with the minimum for another frequency; this means that the cosine argument in (10) should be nearly constant. If the range of wavenumbers in the light source is Δk, this implies $\Delta k\Lambda << \pi$. The coherence length L is $2\pi/\Delta k$; in terms of this quantity we get $\Lambda << L/2$. A more exact analysis of fringe visibility [*Born and Wolf*, 1980] shows that for a source with a Gaussian line shape the fringe visibility will be 80% of its maximum value for $\Lambda < 0.25L$. One special but useful case is when $\Lambda = 0$; if $\Theta = \pi$ the intensity is zero no matter what the value of k. This is the *white-light interferometer*, so called from the nature of the source. In such a system there is only one fringe, so that to detect changes in the length of one path we must alter the other to agree. This interferometer, while not itself a measuring system, is a convenient method of unambiguous noncontact position location (unless the mirror phase shift Θ changes). If instead one arm of the interferometer is fixed and length changes in the other are detected by counting fringes, the source must have a narrow bandwidth (or long coherence length). To meet this requirement the source now almost always used is a laser.

A complete discussion of lasers would be out of place, especially since there are many good treatments available [*Sinclair and Bell*, 1969; *Verdeyan*, 1981], but some background is necessary to make clear what is needed in a laser used for crustal deformation interferometry. The goal in such an application is high spectral purity. We need a laser which produces light that is as monochromatic as possible (Δk small, or L large) and whose frequency does not change with time. The second requirement comes from the appearance of the product $k\Lambda$ in equation (10); a change in k cannot be distinguished from a change in Λ. If we use a Michelson interferometer with one fixed arm, strain in the other arm

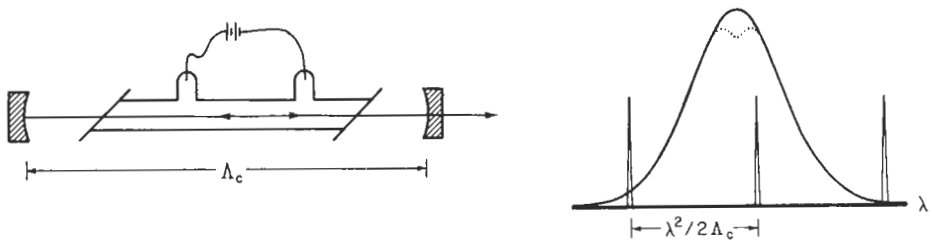

Fig. 10. (Left) A schematic view of a laser, the plasma tube being inside an optical cavity of length Λ_c. (Right) The gain curves of different parts of the system: the heavy solid line is the gain curve of the plasma tube, the dotted line the effect on this of saturated absorption (Lamb dip), and the light line (spikes) the cavity response.

and fractional changes in wavelength (or frequency) of the light used are numerically equivalent, so that wavelength stability must be 3×10^{-15} s^{-1} or better. (The same relation holds for other types of interferometer.)

The laser universally used for the best frequency stability is a HeNe gas laser, shown schematically in Figure 10. This comprises a tube (the gain cell) filled with an excited plasma and set between two highly reflective mirrors, which form an optical cavity resonator. The excitation causes the Ne atoms to be in an inverted population distribution, with more in a high-energy than in a lower-energy state. Stimulated emission can then take place: a light wave of frequency corresponding to the transition energy can cause an atom to lose energy by radiating exactly in phase with the incident wave. Thus, a light wave with the correct frequency will be coherently amplified as it passes through the tube. The mirrors reflect the light back and forth, with some amplification on each pass until a steady state is reached. One mirror transmits a small fraction of the incident light, and it is this light that emerges from the laser.

The wavelength range over which stimulated emission takes place is very narrow: $\Delta k/k$ can be 10^{-13} or less, which for the visible Ne line with $\lambda = 632.8$ nm gives a coherence length of 6000 km. However, the light produced by the laser is not so narrowband. The atoms in the tube are not at rest but have a range of velocities relative to it. A light wave with frequency slightly different from the transition frequency will interact with those atoms whose motion causes a Doppler shift that makes the light appear to have the transition frequency. Because the velocity distribution is Maxwell-Boltzmann, waves with increasingly different frequencies will see fewer atoms with the correct velocity and will be less amplified as they pass through the tube. The right-hand sketch of Figure 10 shows the gain curve, or amount of amplification versus wavelength. Doppler broadening means that lasing can take place over a wavelength range of about 2 pm, or $\delta k/k = 3\times10^{-6}$. Outside this range there are too few atoms (and hence too little amplification) to overcome losses: the laser is below the gain threshold and will not lase.

At a given moment the wavelength of light emitted by the laser is determined by the distance between the end mirrors. The wavelength must correspond to a resonant mode of the optical cavity formed by these mirrors. If it does not, the multiply reflected waves will not interfere constructively and there will not be sustained amplification. The approximate condition for resonance is $\lambda = 2\Lambda_c/N$, where Λ_c is the optical cavity length and N an integer, each value of N corresponding to a different longitudinal mode. While the cavity has losses, giving each of its resonances a finite bandwidth, this bandwidth is much less than the Doppler width, making the laser output spectrum approximately the product of the gain curve and a series of unit spikes at the resonant wavelengths (also shown schematically in Figure 10). In most lasers there are several modes whose wavelengths fall inside the gain curve; the output of these devices is a mix of frequencies, with a coherence length of 0.1 to 1 m. To get a long coherence length the laser must be made to be *single frequency*, with only one mode excited. (In the laser literature 'multimode' often refers to the transverse structure of the light beam; the modes considered here are longitudinal.) The spacing between modes is $\lambda^2/2\Lambda_c$ so that for Λ_c sufficiently small (less than about 15 cm) there will only be one mode excited; the others will fall too far from the center of the gain curve.

A single-frequency laser is sufficiently monochromatic to be used in long-base interferometry, but the wavelength of the emitted light depends directly on Λ_c and thus will shift with changes in the physical separation between the mirrors or the refractive index of the path between them. These can both vary a lot (10^{-6} or more), the only restriction being provided by the width of the gain curve; once the mode wavelength moves too far from the center of the gain curve, the laser will stop lasing in that mode. The wavelength must therefore be stabilized in some way; how best to do this has been much studied since lasers were developed [*Baird and Hanes*, 1974], and it remains an active field. Almost all techniques let λ depend on Λ_c, but add a feedback loop that varies the physical length of the cavity to keep the emitted wavelength 'locked' to some particular behavior. One method, described more fully in section 5.3, is to require the wavelength to be at a transmission peak of a second, passive, optical cavity. Since this cavity need not contain a lasing medium, it can be environmentally controlled more precisely and made more stable than the laser cavity.

Most stabilization schemes lock the output wavelength to an atomic feature. A wide range of methods set the lock point using the shape of the gain curve. One, Lamb-dip stabilization, depends on the phenomenon of saturated absorption. Any particular resonant mode is formed by the sum of oppositely traveling waves. When the mode wavelength differs from the center of the gain profile, the oppositely traveling waves interact with two sets of atoms: those with the appropriate speed going to the left, and those going at the same speed to the right.

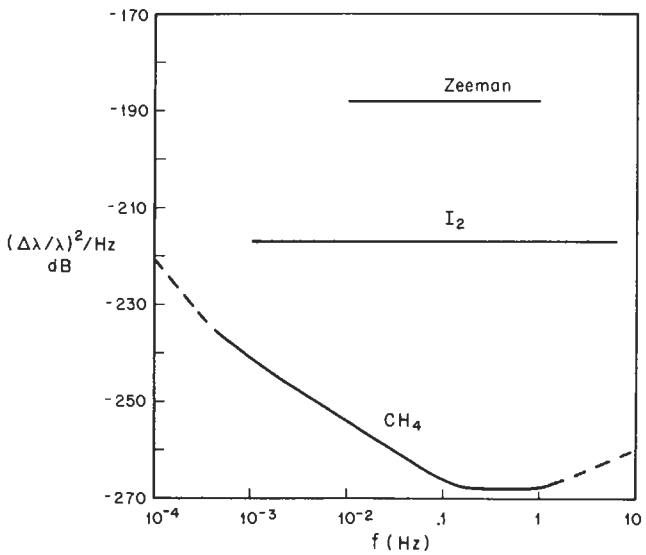

Fig. 11. Power spectra of frequency stability of different stabilized lasers. The Zeeman system is that of *Baer et al.* [1980], the iodine that of *Layer* [1980], and the methane that of *Hall* [1973]. In the original literature the frequency stability is given in terms of the Allan variance, which is an integral over the power spectrum that takes simple forms for power-law spectra [*Rutman*, 1978].

For a wavelength at the peak of the gain curve the same atoms (those at rest) interact with both waves, so that the number of atoms available is only about half as many as for wavelengths nearby. If we assume that as much amplification as possible is taking place (saturation), then, because fewer atoms are available to amplify this wavelength, the intensity of the laser will dip as the wavelength varies across the peak (the dotted line in Figure 10). Locking to this *Lamb dip* is one way of stabilizing the wavelength to the center of the gain curve. Other methods include adjusting two modes on either side of the curve to have equal strength [*Brown*, 1981] or utilizing the Zeeman effect to produce two closely spaced modes which are kept in a fixed intensity or beat frequency relationship [*Baer et al.*, 1980]. Some of these techniques are now available commercially, though at present they are so new that manufacturers' claims are sometimes not met. Their stability, while much better than that of a 'free-running' laser, is nonetheless affected by shifts in the gain curve, which alters as the tube ages and as changes in the pressure and gas composition occur.

The most stable lasers use a passive saturated absorption cell placed within the optical cavity, in series with the gain cell. The absorption cell is filled with a gas chosen to have an absorption line at a wavelength within the gain curve; this absorption line, like the laser gain, will be Doppler broadened but, by a process exactly parallel to the Lamb dip, the absorption will be less at the peak of the absorption curve, giving an enhanced laser output at this frequency. The gas used in the absorption cell, being purely passive, can be chosen for the insensitivity of its spectral peak to pressure or magnetic fields, rather than its lasing efficiency; and, because the cell does not contain a hot plasma, its properties will be more stable with time. The two systems that have seen the most use are one using an HeNe laser radiating at 3.39 μm and a methane absorption cell [*Levine and Hall*, 1972], and one using the 632.8-nm line with an iodine absorption cell [*Layer*, 1980]. Both of these have been used in laser strainmeters. The iodine system has become the more popular (not least because it emits in the visible), and a compact version of it is commercially available.

Figure 11 shows the power spectrum of wavelength fluctuations for three types of stabilized lasers. The power spectral levels in Figure 11 are directly comparable to those in Figure 3 if the laser is used as the light source for a strainmeter. In the seismic band the Zeeman stabilized system would be noisier than ground strain, the iodine system comparable, and the methane quieter. At longer periods, ground noise rises as f^{-2}, while the stability of most oscillators goes like f^{-1}, so all three laser systems would probably be acceptable. The stability of this particular Zeeman system has been measured at 5×10^{-9} over 5 months, more than adequate for most strain measurements. The long-term stability of the iodine and methane systems is harder to assess because there is no more stable system to compare them with; comparisons between lasers [*Chartier*, 1983] show stabilities of 3×10^{-19} s^{-1} over 6 years.

A question of some interest when using a laser in a field instrument is how long it will last. For tubes of the type shown in Figure 10, with end windows epoxied on to the plasma tube, the mean time between failure is about 16 months for continuous operation (F. Wyatt, personal communication, 1983). This design is now little used, having been replaced by 'hard seal' construction in which the end mirrors are inside the tube and the end seals are glass-to-metal joints. Tubes of this type have a mean life of about 48 months [*Malk and Ramsay*, 1982], with the manufacturers' warranty usually being 18 months. Unfortunately, with presently available laser tubes the older design must often be used for absorption stabilized systems.

3.3.2. *Capacitance transducers.* The most sensitive displacement transducers used in geophysical instruments measure changes in capacitance caused by the displacement of one part of the transducer. Figure 12*a* shows the commonest physical arrangement: a three-plate differential capacitor, with the center plate moveable and the outer ones fixed. If all three plates have area A, and γ_p is the permittivity of the material between them, the capacitances are (ignoring fringing fields)

$$C_1 = \gamma_p \frac{A}{d} \frac{1}{1-q/d} \qquad C_2 = \gamma_p \frac{A}{d} \frac{1}{1+q/d}$$

where d is the distance between plate surfaces when the middle plate is centered and q is its displacement from the center. The earliest capacitive displacement transducers, such as those developed by Benioff [*Gile*, 1974], used C_1 and C_2 in matched L-C resonators driven at a fixed frequency. Variations in q would alter C_1 and C_2 and make one resonator frequency closer to that of the driver and the other farther away. Summing and rectifying the outputs of the resonators gave an output which varied with q. This technique, though sensitive, is nonlinear at large displacements and has been replaced by designs in which the transducer forms part of a bridge. A recent

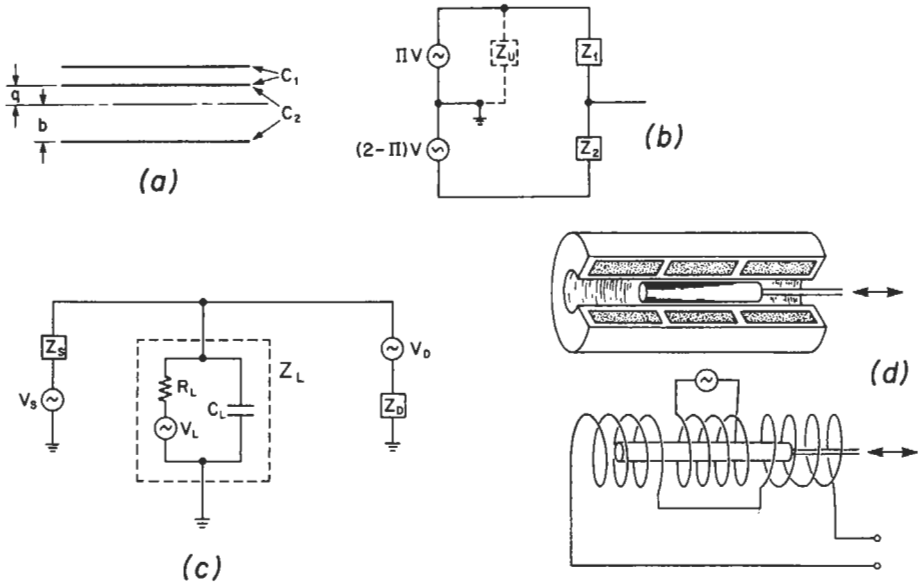

Fig. 12. (*a*) Simplified drawing of a three-plate capacitor displacement sensor. (*b*) Equivalent circuit of a capacitor sensor. The input voltages may be produced by a divider with $0 \leqslant \Pi \leqslant 2$; Z_U is stray impedance to ground between this and the sensor. (*c*) Equivalent circuit of a sensor S connected though a cable to a detector D. V_S is sensor output, V_D detector noise. (*d*) A cutaway view (above) and schematic drawing (below) of an LVDT.

review by *Hugill* [1982] covers the different possible designs in some detail; I concentrate here on those most often used.

The basic principle can be understood using only electrostatics. If we apply a voltage V to the top plate in Figure 12*a*, and an opposite voltage to the bottom plate, the electric field between the plates is constant, and the voltage level is a linear function of position. A system using constant voltage sources would not in fact work very well, since measuring the voltage on the center plate would cause charge transfer and distort the field. More importantly, the output voltage on the center plate would vary only at the frequencies of interest (a few hertz and below), and at such low frequencies all electronic devices become more noisy than their thermal limits. These 'excess noises' generally have a spectrum that rises as f^{-1} for frequencies below 1 Hz (below 10 kHz for some devices), and so to get the best performance measurements should be made at high frequencies, the signal being the amplitude of the high-frequency output. If V varies rapidly, we have a field that while varying in time is spatially constant at any moment, so the induced voltage on the center plate remains a linear function of position.

To describe this quantitatively we need AC circuit theory. Figure 12*b* shows the circuit for this transducer, with Z_1 and Z_2 being the impedances corresponding to the two parts of the capacitor; $Z_j = (i\omega C_j)^{-1}$. They are driven at a frequency ω by two AC voltage sources that have amplitudes ΠV and $(2-\Pi)V$ and zero output impedance. (The source voltages are written in this way because they are usually generated by a voltage divider which can be set over the range $0 \leqslant \Pi \leqslant 2$.) Elementary circuit theory shows that this arrangement is equivalent to an ideal voltage source with output level

$$V_S = \frac{\Pi Z_2 - (2-\Pi)Z_1}{Z_1+Z_2} V = (\Pi - 1 + q/d)V \qquad (11)$$

and source impedance

$$Z_S = \frac{Z_1 Z_2}{Z_1+Z_2} = \frac{1-(q/d)^2}{2i\omega C_0} \qquad (12)$$

where $C_0 = \gamma_p A/d$ is the capacitance when the middle plate is centered. For dry air at STP γ_p is 8.859×10^{-12} F/m, and so for transducers of average size C_0 is on the order of 10 pF. The source impedance can thus be quite large and cannot be neglected in computing the transducer response. Figure 12*c* shows the equivalent circuit including the detector, with impedance Z_D, and leakage along the cable between the center plate and detector, represented by a single shunt impedance to ground Z_L. In practice, Z_L must be partly resistive to bleed off charge on the center plate, and will also have a substantial capacitive part, the capacitance to ground of this cable ($\approx$ 40 pF per meter of cable length) almost always exceeding that of the actual transducer. The voltage across the detector, which for our purposes may be regarded as the output, is then

$$\frac{V_S}{1+Z_S(Z_L^{-1}+Z_D^{-1})} \qquad (13)$$

Designers of capacitance transducers differ in their choice of Z_D. Some [*Block and Moore*, 1966] make it very large, in which case the voltage seen by the detector is

$$\frac{V(\Pi-1+q/d)}{1+\frac{C_L}{2C_0}(1-(q/d)^2)} \approx \frac{2C_0}{2C_0+C_L} V\left(\frac{q}{d}\right)$$

where to get the first expression we have assumed $\omega R_L C_L >> 1$, R_L and C_L being the resistive and capacitive parts of Z_L; the second expression assumes $\Pi = 1$ and $q << d$. In such a design, unless $C_0 >> C_L$, the sensitivity will depend on C_L, which will vary with move-

ments of the connecting cable. This design is therefore unsuitable unless the transducer is used only as a null detector or the cable to the detector is very short. To eliminate this problem, some designers [*Jones and Richards*, 1973] use a low-impedance detector, with $Z_D \ll Z_L$; the detector voltage is then as given above but with C_D (the detector capacitance) replacing C_L. This design has less gain than one with a high-impedance detector.

The noise in a capacitive transducer comes primarily from the electronics after it. Figure 12*c* includes the two main sources: Johnson noise V_L associated with the leakage resistance R_L, and voltage noise V_D in the detector (current noise I_D in the detector can also be important). The power spectral density of Johnson noise is just $4k_B TR_L$, where k_B is Boltzmann's constant and T the temperature; if we calculate the voltage noise from V_S that would produce an equivalent level at the detector, and convert to displacement using (11) with $\Pi = 1$, we find that the power spectral density of equivalent displacement is

$$\frac{4k_B TR_2}{4\omega^2 R_L^2 C_0^2} \left(\frac{d}{V}\right)^2$$

(we take Z_S to be given by (12) with $q = 0$). The contribution from the detector can be similarly converted using (13); the total displacement power spectral density is

$$\left(\frac{d}{V}\right)^2 \left\{ V_D^2 \left[\left(\frac{2C_0 + C_L + C_D}{2C_0} \right)^2 + \frac{1}{4\omega^2 R_L^2 C_L^2} \right] + \frac{4kTR_L}{4\omega^2 R_L^2 C_0^2} + \frac{I_D^2}{4\omega^2 C_0^2} \right\}$$

(taking Z_D to be capacitive only). Most published estimates of noise in such systems ignore the terms that include ω and also make the further, optimistic assumption that $C_L = C_D = 0$, in which case the noise is $(d/V)^2 V_D^2$. The leading term is limited by the allowable voltage gradient, which in air means that $d/V > 5 \times 10^{-7}$ m V^{-1}; in practical systems, d/V is usually about 10^{-4} m V^{-1}, though even larger values may be required to keep forces on the center plate small. Low-noise operational amplifiers can have voltage noise as low as 10^{-16} V^2 Hz^{-1}, which would imply a displacement noise of 10^{-24} m^2 Hz^{-1}. In real systems, nonzero shunt capacitance means that the noise level is higher; *Gladwin and Wolfe* [1975] report a 'resolution' of 10^{-10} m, which if we assume a 1-s averaging time (and therefore 1-Hz bandwidth) is equivalent to a power spectral level of 10^{-20} m^2 Hz^{-1}. The lowest noise reported is that of *Jones and Richards* [1973], who resolved 10^{-14} m with 1-s averaging, a power spectral level of 10^{-28} m^2 Hz^{-1}, though the noise at diurnal periods was about 40 dB higher.

While the AC voltage could be detected using a diode rectifier and DC amplifier, this would be sensitive to noise over a wide bandwidth. A much better method is to use a phase-sensitive detector (also called a lock-in amplifier). This generates the AC voltage with frequency ω used on the outer plates and detects only that part of the signal that is in phase with it; averaging this makes the detector sensitive to noise only over a narrow frequency band around ω (*Horowitz and Hill* [1980, chapter 14] describe the theory more fully).

The force exerted on the center plate of a three-plate capacitor can be computed by noting that (from energy considerations) the attractive force between a pair of plates is

$$\frac{V^2}{4} \frac{\partial C}{\partial d}$$

where V is an AC voltage with mean-square value $\frac{1}{2}V^2$. The formulae for the capacitance of each pair of plates then give the net force, if the voltage on each pair is V ($\Pi = 1$), as

$$\left(\frac{V}{d}\right)^2 C_0 \frac{q}{(1-(q/d)^2)^2}$$

For $q \ll d$ this is linear in q and represents a small destabilizing force on the center plate. As q approaches d, this force grows without bound; if a capacitive transducer with Π fixed is used in a 'soft' system (such as a tiltmeter), physical stops are needed to prevent this.

The discussion so far has ignored the way in which the input voltages ΠV and $(2-\Pi)V$ are generated. These voltages, and even more their ratio, must be stable with time and unaffected by the stray impedances between the output and ground (shown as Z_U in Figure 12*b*). The voltage ratio is important because if the system is run at high gain, the limited range of the output will require V_S to be kept small, which by (11) will mean that q/d is very nearly $1-\Pi$. Π is of course directly related to the voltage ratio. (In a fedback system, with V_S kept equal to 0, V affects only the loop gain; changes in voltage ratio (and hence Π) are indistinguishable from changes in q.) The input voltages are usually generated with an inductive voltage divider, also called a ratio transformer. Any circuit in which a ratio of voltages is fed to variable impedances and the output detected is a bridge, the Wheatstone bridge being the best-known example. If the voltage division is done with a transformer, the circuit is called a ratio-transformer bridge, or in British usage a Blumlein bridge; several different arrangements [*Leslie*, 1961] are possible.

In a ratio transformer the two output voltages come from two coils wound on the same core. The driving voltage may be applied to these coils directly but more often goes to a primary winding on the same core. Use of a toroidal core with high magnetic permeability assures that essentially all the flux inside each coil is also inside the other; the two coils are then closely coupled. It is this close coupling that renders the output voltage ratio insensitive to loads. The voltage from each coil is proportional to the rate of change of flux times the number of turns, and because both coils contain the same flux the voltage ratio will always be equal to the turns ratio; any load across one coil will affect, through the coupled flux, the voltage produced by the other. Because the voltage ratio depends only on geometry (turns ratio) and not material properties, it can be very stable with time.

That the ratio depends on geometry also means that a properly constructed ratio transformer can be used as a very accurate adjustable voltage divider. If we have a

100-turn coil tapped every 10 turns, we can, by moving from one tap to the next, get values of Π that are almost exactly 0.2, 0.4, ..., 1.8. By using several coils with the output of each coil feeding the next, adjustable ratio transformers [*Hill and Miller*, 1962] can be built that will give any Π to seven decimals, all of them meaningful, a dynamic range of 140 dB. Such a transformer (even with lower resolution) makes possible a sensor in which Π is set to keep V_S close to zero and q is found from $q/d = 1-\Pi$. This design combines large range with great sensitivity and also keeps the force on the center plate close to zero.

This range is useful only if the sensor is linear throughout it. Equation (11) shows the source voltage to be linear in q but neglects fringing fields; these may be reduced by use of a guard ring [*Stacey et al.*, 1969]. The source impedance (equation (12)) is nonlinear in q, but the effect of this may be corrected for, since in a sensitive system, q/d is known to high accuracy from the value of Π. *Gladwin and Wolfe* [1975] tested the linearity of a carefully designed capacitive transducer by comparing it with interferometric measurements and found that in a range of $\pm 0.2d$ the linearity was 0.0015%, and 0.2% out to $\pm 0.9d$, nearly the full range possible.

3.3.3. *Electromagnetic transducers.* Strainmeters built for seismology often use an electromagnetic velocity transducer. Benioff's first instrument [*Benioff*, 1935] used a variable reluctance transducer, in which changes in the air gap of a magnet altered the amount of flux inside a coil; with the development of stronger permanent magnets more recent instruments have used moving-coil transducers. Both of these generate a voltage $V = G\dot{q}$, where G is the generator constant and q the displacement. The minimum possible noise level is set by Johnson noise in the windings; this gives a displacement noise power spectrum $k_B TR/(\pi Gf)^2$, where R is the coil resistance. For a large moving-coil transducer [*Fix and Sherwin*, 1970] with $G = 3.2\times10^4$ N A^{-1} and $R = 165$ kΩ, the noise level was 7×10^{-26} m^2/Hz at 1 Hz, better than all but the best capacitive systems, though at longer periods the noise increases rapidly.

To be able to make measurements at very low frequency, a sensor using magnetic fields must, like a capacitive sensor, use an externally excited AC field and cause displacements to change the output amplitude. In some sensors this is done by feeding an AC input into one or two coils, so arranged that displacements, either of the coils themselves or of a passive ferromagnetic body near them, cause a change in inductance and thus of the output. These sensors take many different forms, but functionally are somewhat analogous to capacitive sensors. Most available discussions of inductive sensors [*Neubert*, 1975; *Hugill*, 1982] use simplified treatments because eddy currents and hysteresis make it difficult to model the magnetic fields fully.

The linear variable differential transformer (LVDT), which is the inductive displacement transducer most used in geophysical instruments, works somewhat differently. A sinusoidal voltage is fed to a primary solenoid with a movable ferromagnetic core inside (Figure 12*d*). Secondary coils are put on each end of the primary. The magnetization of the core by the exciting field creates fields within the secondary coils; obviously, the further within a secondary the core extends, the greater the flux linked by that coil and the voltage induced in it. A quantitative (though approximate) treatment [*Neubert*, 1975; *Herceg*, 1976] shows that the difference in induced voltage in the two coils will be

$$K_l q \left(1 - \frac{q^2}{L^2}\right)$$

where q is the displacement of the center of the core, K_l the sensitivity of the LVDT, and L a length roughly equal to the length of the primary coil. (This assumes that the core and coil housings are made from high-permeability material, that the spacing between coils is small, and that both ends of the core are inside secondary coils.) The output voltage can thus be made a reasonably linear function of displacement so long as $q << L$; the LVDT geometry lends itself to large core motions and is insensitive to transverse motion of the core. The core is completely passive, and the coils can be shielded from it (and the outside environment) inside a nonmagnetic housing; materials that get between the core and the coils will not affect the operation of an LVDT unless their permeability is much different from 1, which is not usually true. In particular, humidity, or even liquid water, has no effect.

Because they are rugged and linear over large distances, LVDT's are attractive for industrial use, and they are therefore commercially available in many sizes and sensitivities. *Herceg* [1976] discusses industrial applications and some aspects of LVDT design, though not in great detail; indeed, probably because of the commercial nature of LVDT development, little has been published about them.

Real LVDT's depart from the ideal in several ways. Because of eddy currents and hysteresis, the output voltage usually is not in phase with the input and also contains higher harmonics and a quadrature signal that do not vanish when $q = 0$. All these imperfections, and the linearity and sensitivity of the LVDT, vary with the frequency of the exciting voltage. Because the output signal depends on material properties, it will vary with temperature, though this can be minimized by operating the sensor at a frequency for which the phase lag is zero. The long-term dimensional stability of LVDT's has not been studied but is presumably not as good as that of other sensors because of the relatively complex construction. Because an LVDT cannot be modeled mathematically, it must be calibrated using an external positioner. An LVDT has a much lower output impedance than a capacitive sensor; it thus suffers less attenuation from stray capacitances in long cables. On the other hand, the lower resistances of an LVDT mean that it consumes (and dissipates) more power.

The sensitivity of commercial LVDT's is usually given in terms of output voltage per unit input voltage and displacement (volts per volt-meter); examination of equation (11) shows that the inverse of this is equivalent to the plate separation d of capacitive sensors. The most sensitive LVDT's made commercially have sensitivities around 200 m^{-1} ($d = 5$ mm), 0.2 to 0.1 of a typical capacitive system. *Wielandt and Streckeisen* [1982] have built a mini-

ature LVDT with a sensitivity of 8000 m^{-1}; this is comparable to that of the best capacitive systems, as is the noise level, which varies as f^{-1} and is 6×10^{-22} m^2 Hz^{-1} at 1 Hz. The linearity of commercial sensors is usually within 0.5% over the full range, which for the most sensitive ones is about 1 mm; the linearity over smaller ranges is not specified.

The various imperfections in the output signal (described above) mean that it is important to measure it with a phase-sensitive detector (called a synchronous demodulator in the LVDT literature) since only then can such errors be kept small. Use of such a detector is easy to assure if the electronics are separate, but sometimes they are not. One popular type of LVDT is the so-called DC-LVDT, which gets its name not because it uses DC for sensing but because it appears to, the electronics being built-in and both the supply voltages and the output being DC. Some of these use synchronous demodulators, but others use cheaper rectifier circuits which will give poorer results. DC-LVDT's are designed to have a sensitivity proportional to the supply voltage, which must therefore be carefully stabilized.

LVDT's, like other inductive sensors, apply much larger forces to the moving member than capacitive sensors do; *Hugill* [1982] shows that the ratio will usually be $O(10^5)$. One published measurement, by *Wielandt and Streckeisen* [1982], gives a 'force noise' level at 1 Hz of 3×10^{-22} N^2 Hz^{-1}, again varying as f^{-1}.

3.4. *Coupling the Instrument to the Ground*

Many designs for deformation-measuring instruments discuss only ways to improve the transducer and neglect how it is to be attached to the earth. How to make such an attachment is a difficult problem, not least because it must be done in the field rather than in a laboratory. This section first discusses some of the different places instruments may be put and the coupling problems of each, and then describes some of the particular methods adopted for coupling. We do not yet know the 'correct' method; the coupling problem remains unsolved.

What does 'properly coupled to the earth' mean? The usual notion is that a properly coupled instrument would record, without distortion, only those deformations that are really present. But, since any instrument records all tilts or strains, distinguishing some of them as real and others as not is arbitrary, and in the end comes down to what we are interested in. The usual 'real' deformations are those assumed to be present at great depths: seismic waves, earth tides, surface loads, and crustal deformation (including coseismic changes). In the first three of these, and in part in the fourth, observations show that the earth behaves very nearly as an elastic body whose moduli vary gradually with position. The success of seismometer arrays [*Davies*, 1973] shows that seismic waves are coherent over small distances, with deformations varying gradually along wave fronts. Earth tide measurements show a reasonable concordance with elastic earth models [*Berger and Beaumont*, 1976], as do crustal deformations caused by longer-period loading [*Passey*, 1981; *Peltier*, 1982; *McNutt and Menard*, 1982] (with due allowance for mantle viscosity) and coseismic deformations [*Wyatt and Agnew*, 1982]. Because we can successfully explain many observations by assuming the earth to be a nearly uniform elastic body, we naturally take this assumption to be generally valid; we thus expect a properly coupled instrument to be one that records the deformation actually present near the surface of an elastic sphere. This picture may of course break down for slow crustal deformation [*Bilham and Beavan*, 1979] and certainly does over geological time scales; it is in this area, just because our theoretical preconceptions are so weak, that it is hardest to decide whether or not an instrument is measuring 'real' deformations.

3.4.1. *Attachment near the surface.* The surface of the earth has two outstanding advantages as a place to put strainmeters and tiltmeters: it is accessible at low cost, and there is plenty of room. Many instruments have therefore been installed in 'near-surface' locations: if not on the surface, then at depths easily reached by pits and trenches.

Surface deformations might not follow 'real' deformations at all; the relatively loose and pervasively fractured material at the surface could be decoupled from deeper motions. The best evidence against this is that seismic, tidal, and geodetic measurements made at the surface clearly reflect motion at depth. Further evidence comes from borehole stress measurements in California [*McGarr et al.*, 1982*b*] which show stress changes with depth that are compatible with a purely elastic model. They also show a direction of horizontal stress similar to that found in shallower measurements [*Sbar et al.*, 1982], so that in this location at least the effects of tectonic forces are propagated to the surface.

The difficulty with surface installations is not that signals from deeper motions are absent, but that these signals are masked by other motions of the near-surface layers. Very commonly, strain or tilt measurements made near the surface show a correlation with rainfall; such meteorological noise has been observed in Japan [*Takemoto*, 1983; *Kasahara et al.*, 1983], Hawaii [*Wolfe et al.*, 1981], central and southern California [*Wood and King*, 1977; *Goulty et al.* 1979; *Wyatt*, 1982], Germany [*Herbst*, 1976], and England [*Edge et al.*, 1981]. The mechanisms causing this are not clear. At deeper sites (such as those in Germany and England) the probable cause is deformations caused by varying groundwater pressure; another possibility is the inflation of water-filled cracks [*Evans and Wyatt*, 1984]. Shallow installations are most affected by meteorological noise, which for them probably arises from local motion of the soil caused by wetting and drying. Such motions are called 'soil creep' by geomorphologists. Rates of creep near the surface can be very high on steep slopes or in clay-rich soils, but are usually less than a few millimeters per year on small slopes [*Saunders and Young*, 1983]. Creep velocity decreases with depth and may be directed downslope, transverse to it, or vertically [*Young*, 1978; *Finlayson*, 1981].

Soil motion can easily cause large signals in near-surface deformation measurements. For example, a relative motion of 0.1 mm yr^{-1} at one end of a 10-m instrument would give an apparent deformation of 3×10^{-13} s^{-1}; this is much larger than tectonic rates, but the soil creep causing it would be too slow to be measurable by geomorphological methods. The main study of these very small

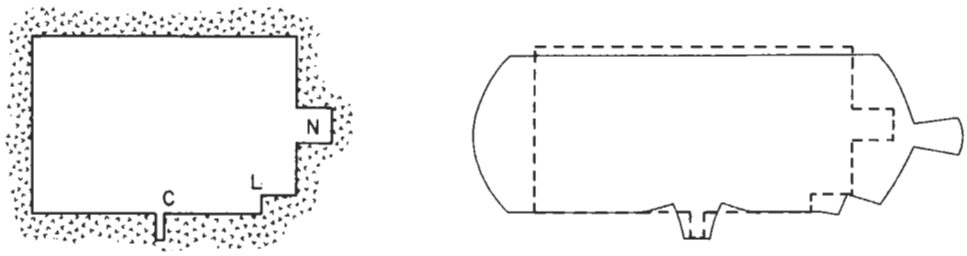

Fig. 13. Distortion of a cavity subjected to uniaxial strain, after *Harrison* [1976*a*] and *Emter and Zürn* [1985]. The outline of the cavity (a tunnel extending out of the plane of the paper) is shown on the left; the dashed line on the right shows how this outline would distort if the tunnel were not there, and the solid line shows qualitatively how it actually does, giving strain-coupled tilts near the crack C, the ledge L, and the niche N.

soil motions, done by *Wyatt* [1982] in southern California, showed that large monuments (1 m^3 or greater) at depths of 2-3 m moved .02 - 0.1 mm yr^{-1} horizontally; the horizontal displacements inferred from tiltmeters at a depth of 4.5 m were 0.002 - 0.01 mm yr^{-1}. The motion was episodic, being correlated with the infrequent rains. The material at these depths was slightly weathered granite too competent to be broken up except by drilling. Measurements at the same site of the vertical shifts of monuments 2 m deep show similar rates of motion [*Wyatt et al.*, 1984]. Very small near-surface motions are also of concern to the builders of large particle accelerators; rates of a few tenths of a millimeter per year have been observed in sandstone [*Herrmannsfeldt et al.*, 1968] and molasse [*Decae*, 1960]. It is not known how rapidly these motions diminish with increasing depth; studies of the depth of weathering [*Stierman and Healy*, 1985] suggest that it may extend to tens of meters even in 'hard-rock' locations in an arid climate.

Because near-surface noise correlates with meteorology, several attempts have been made to use linear prediction theory or other models to remove the correlated part [*Wood and King*, 1977; *Herbst*, 1976; *Goulty et al.*, 1979; *Yamauchi*, 1981]. These have had some success, but too little noise has been removed to bring the residual down to the low levels expected for tectonic motions. The mechanisms connecting rainfall to apparent deformations are very complex and unlikely to be linear, so this limited success is not surprising. The best solution is to build instruments that are insensitive to these effects. The last decade's experience has shown convincingly that surface short-base instruments are too much affected by soil motion to provide useful long-term results. If an instrument is near the surface, it must be very long, and even then may need to be coupled to depth (section 3.4.4), while short-base instruments must be installed at a depth sufficient to escape soil motion; it is not yet known how deep this is.

3.4.2. *Tunnels and caves.* Tiltmeters and strainmeters have often been installed deep in the ground, mostly to reduce thermal effects on the instrument. Until the development of borehole instruments this meant using mines, tunnels, or natural caves, usually dug for some other purpose. An obvious problem is that such cavities may not be available where measurements are needed; a less obvious but more fundamental problem is that instruments installed in an opening may not measure what is intended because the opening distorts the deformation field. The importance of such distortion for deformation measurements was first realized by *King and Bilham* [1973]. It is generally called, following *Harrison* [1976*a*], the *cavity effect*.

Figure 13 shows an example: an infinite tunnel under uniaxial stress. The tunnel outline is on the left, and the dashed line on the right shows how this outline would deform if there were no opening. The solid line shows the actual deformation. The vertical and horizontal strains are both amplified, and strains measured near any cracks (as C) will be greatly exaggerated. The floor remains flat (except near cracks), but the floors of ledges (L) and niches (N) tilt by an amount comparable to the strain.

More formally, we divide the displacement field $\mathbf{s}$ into two parts

$$\mathbf{s} = \mathbf{s}_0 + \delta\mathbf{s}$$

where $\mathbf{s}_0$ is the displacement that would occur in response to the same forces if the cavity were not present. We may then, under the same assumptions as in section 2.1, write

$$\mathbf{E} = \mathbf{E}_0 + \delta\mathbf{E} \qquad \mathbf{r} = \mathbf{r}_0 + \delta\mathbf{r} \tag{14}$$

In general, the additional deformations $\delta\mathbf{E}$ and $\delta\mathbf{r}$ will depend on the shape of the cavity and on $\mathbf{E}_0$, but not on $\mathbf{r}_0$ because it is a rigid rotation. If we suppose $\mathbf{E}_0$ to be uniform, then for a particular cavity in an elastic medium $\delta\mathbf{E}$ and $\delta\mathbf{r}$ at any position are linear functions of $\mathbf{E}_0$. We may write this as

$$\delta\mathbf{E} = \mathbf{C}_E\mathbf{E}_0 \qquad \delta\mathbf{r} = \mathbf{C}_r\mathbf{E}_0 \tag{15}$$

where $\mathbf{C}_E$ is the fourth-order strain-strain coupling tensor and $\mathbf{C}_r$ the third-order strain-rotation coupling tensor; strain-tilt coupling, by equation (3), involves both $\mathbf{C}_E$ and $\mathbf{C}_r$. In Cartesian coordinates the symmetry of $\mathbf{E}_0$ and $\mathbf{E}$ means that $\mathbf{C}_E$ has 36 independent components and $\mathbf{C}_r$ has 18. For uniform strain near the surface of the earth there are only three independent components of $\mathbf{E}_0$ (e_{11}, e_{12} and e_{22}, if the 3-axis is upward), halving the number of components in $\mathbf{C}_E$ and $\mathbf{C}_r$ [*King et al.*, 1976]. It is usually convenient to express the strain-strain coupling tensor as $\mathbf{C}_E + \mathbf{I}$; this transforms $\mathbf{E}_0$ to $\mathbf{E}$. For near-surface conditions this may be written as a 3×3 matrix; adding a fourth row gives e_{33} in terms of the independent components of $\mathbf{E}_0$.

The only analytical solution for $\mathbf{C}_E$ and $\mathbf{C}_r$ in three

dimensions is for the ellipsoidal cavity [*Eshelby*, 1957], for which the internal strains are uniform. *Harrison* [1976*a*] has described results for the case where one axis of the ellipsoid is vertical. $\mathbf{C}_r$ may then be ignored, since the only rotation caused is vertical and does not affect vertical or horizontal tiltmeters. Because shear strains and extensions are decoupled, $\mathbf{C}_E$ has only seven nonzero components. In general, the coupled strains and tilts are largest when measured in the direction along which the cavity is smallest, whether the external strain is in that direction or not. Strain measured along a long narrow cavity is not amplified very much.

A special case for which the results are very simple is an infinite horizontal circular tunnel, assuming both plane strain and the free surface condition. The standard solution for this [e.g., *Jaeger and Cook* 1976, section 10.4] gives the transformation matrix as

$$\begin{bmatrix} e_{11} \\ e_{22} \\ e_{12} \\ e_{33} \end{bmatrix} = \begin{bmatrix} 3 & 2\nu & 0 \\ 0 & 1 & 0 \\ 0 & 0 & 1 \\ -1 & -2\nu & 0 \end{bmatrix} \begin{bmatrix} e^0_{11} \\ e^0_{22} \\ e^0_{12} \end{bmatrix} \tag{16}$$

where ν is the Poisson's ratio of the material and the tunnel is along the 2 axis. Without a tunnel the transformation matrix would be

$$\begin{bmatrix} 1 & 0 & 0 \\ 0 & 1 & 0 \\ 0 & 0 & 1 \\ -\nu/(1-\nu) & -\nu/(1-\nu) & 0 \end{bmatrix} \tag{17}$$

A tunnel thus does not alter axial and shear strains, but amplifies both vertical and horizontal strains (when $\nu = 0.25$, both are multiplied by 3). Such amplification has been observed in cross-tunnel measurements of strain tides. [*Itsueli et al.*, 1975; *Beavan et al.*, 1979; *Takemoto*, 1981]. Real tunnels end, but finite-element modeling shows the distortion to be small if strain along the tunnel is measured more than one tunnel diameter away from an end.

More complicated two-dimensional problems may sometimes be treated using complex variable methods [*Khassilev*, 1979], but usually finite-element modeling is needed. Slight departures from circularity do not much alter the total strain from wall to wall, but in a square tunnel the strains concentrate near the corners [*Berger and Beaumont*, 1976]. Tiltmeters mounted on the walls, or placed on a ledge or near a crack, will be affected by strain-coupled tilts, as observed by *Baker* [1980].

Cavity effects do not add noise; they merely mean that the instrument does not measure what it is supposed to. For earth tide studies this is a major problem, as accuracies of a few percent are needed. While we can in principle build a finite-element model of any cavity, the fracturing and material variations nearby are often too poorly known to make results from such a model more than a rough guide. The measurements by *Baker* [1980] on a pier in the middle of a tunnel, which showed a 5% change in tilts measured 0.5 m apart, imply that such modeling has to be extremely detailed. Except for along-tunnel strain and tilt, deformation measurements in cavities are therefore of lessened value for some geophysical purposes, though such locations do provide an excellent place for instrument tests.

3.4.3. *Boreholes.* The more excavation needed, the higher the cost of an underground installation; if cavities are not already available, it is cheapest to put the instrument in a borehole. The small size of a borehole means that the instrument must be small and will need a high-gain transducer to get adequate sensitivity. Borehole instruments, like such transducers, are a relatively recent development, and many of the installation methods are still not fully worked out. The lack of space in a borehole creates many difficulties. All data must be telemetered to the surface. A borehole cannot be drained; if it goes below the water table, either it must be cased with a watertight pipe or the instrument must be waterproof. (To avoid motions caused by fluctuating water levels [*Herbst*, 1976; *Evans and Wyatt*, 1984], it is desirable, and usually unavoidable, to go well below the water table.) Special techniques (section 4.1.6) are also needed to find the azimuth of the instrument, or to level it.

Boreholes also cause cavity effects, but because of different geometry different distortions take place. Because there is no vertical shear strain near a horizontal free surface, there is no coupling between strain and vertical tilt (measured along the borehole), although a tiltmeter attached to the bottom of the hole will measure strain-coupled tilts. Vertical tilts are also not distorted by any casing. Strains are distorted by the borehole and by any material placed in it. If we assume that the borehole is uniform and that any inserts are axisymmetric, then the coupling tensor is isotropic for horizontal strains, and may be written as

$$\begin{bmatrix} e_{11} \\ e_{22} \\ e_{12} \\ e_{33} \end{bmatrix} = \begin{bmatrix} (H_A+H_S)/2 & (H_A-H_S)/2 & 0 & 0 \\ (H_A-H_S)/2 & (H_A+H_S)/2 & 0 & 0 \\ 0 & 0 & H_S & 0 \\ 0 & 0 & 0 & H_V \end{bmatrix} \begin{bmatrix} e^0_{11} \\ e^0_{22} \\ e^0_{12} \\ e^0_{33} \end{bmatrix}$$

H_A relates internal and external areal strain, H_S shear strain, and H_V vertical strain. All three depend on the elastic constants of the surrounding material and of the contents of the borehole. *Gladwin and Hart* [1985] compute values of H_A and H_S for realistic parameters. For an empty borehole, $H_V = 1$, $H_S = 4(1-\nu)$, and $H_A = 2/(1-\nu)$, so that instead of (17) the transformation matrix for near-surface strain is

$$\frac{1}{1-\nu} \begin{bmatrix} 3-4\nu+2\nu^2 & 4\nu-1-2\nu^2 & 0 \\ 4\nu-1-2\nu^2 & 3-4\nu+2\nu^2 & 0 \\ 0 & 0 & 4(1-\nu)^2 \\ -\nu & -\nu & 0 \end{bmatrix}$$

All horizontal strains are thus substantially magnified. For $\nu = 1/4$ the areal strain $e_{11}+e_{22}$ is amplified by 2.7 and the volume strain by 3. An insert (casing or instrument) will add stiffness to the hole and thus reduce these values; ideally, a borehole strainmeter would be designed to have the same average elastic moduli as the material around it, but in practice this condition can only be met approximately. Just as in tunnels, fractures near the

borehole can amplify the strain and should be avoided. A rough idea of the location of large fractures can be obtained by using a caliper log, which gives a record of borehole diameter. A much better method is to use a sonic televiewer [*Seeburger and Zoback*, 1982], and the best is to drill in such a way as to get cores.

3.4.4. *Coupling methods.* Just as different problems are associated with the different environments described above, so different methods of coupling are appropriate for each. In tunnels and caves a fresh rock surface is available, the question being what adhesive to use to join the instrument to it; in boreholes a more positive attachment is needed, usually provided by expanding cement; and instruments on the surface must somehow be 'anchored' to deeper levels.

The simplest mode of installation is that traditionally used for short-base tiltmeters in tunnels: the instrument is either set directly on a cleaned rock surface or on mounting posts inserted into close-fitting holes and glued in with a small amount of epoxy [*Harrison*, 1976*b*; *Melchior*, 1983]. Similarly, strainmeters in tunnels are sometimes anchored to the wall using cemented-in posts or expanding rockbolts. Tests of rockbolt mounts by *Jeffery and Sydenham* [1973] showed long-term motions of less than 10^{-13} m s^{-1} after stabilization times of a few weeks. They found similar long-term rates of motion, and faster stabilization, for a mount consisting of a heavy metal plate laid on a bed of compacted sand, a method introduced by the Cambridge strain group. This has also been used for tiltmeters, though the one installation reported [*Blair*, 1981] showed less satisfactory drift rates, from 1.4×10^{-10} rad s^{-1} initially to 8×10^{-13} rad s^{-1} after 2 months, while a nearby installation on rock had a long-term rate of 2×10^{-13} rad s^{-1}.

Sand has also become popular as a packing medium for tiltmeters in shallow boreholes, a procedure developed by *Allen* [1972] and refined by *Morrissey* [1977]. The tiltmeter most often used (the Kinemetrics TM-1) is housed in a long tube. This is centered in the borehole and sand added gradually in the gap between the tube and the hole wall, each layer of sand being tamped firmly before another is added. Even a small depth of sand forms a remarkably firm pack, and indeed if the sand pack is extended for the complete length of the tube (1 m), it appears to introduce stress in the tube, which may produce greater drift [*Morrissey and Stauder*, 1979]. S.-T. Morrissey (personal communication, 1982) advocates adding 5% quick-setting cement to produce a weakly bonded sand that stabilizes faster and is less affected by changes in water content. *Wyatt* [1982] found tiltmeters with a pure sand pack to show annual oscillations with rates of 5×10^{-13} rad s^{-1}; *Morrissey* [1983] found similar drift rates for tiltmeters packed with bonded sand in a humid environment.

The success of such a weak material as sand in these applications may appear puzzling, but can be explained by the mechanics of granular materials [*Wieghardt*, 1975], particularly the phenomenon of dilatancy. If shear stress is applied to a mass of compacted granular material, deformation can take place only if some of the grains move from being interlocked with others, which means that the volume must increase; if external constraints prevent a volume increase, no movement will take place (except for elastic deformation of the grains) until the stresses are high enough to break some grains. When sand is used for packing, the only grains that can move freely are those near the top, while the bulk are locked in place, bonding the instrument tube to the borehole wall. For small stresses the sand will deform like porous quartz; it thus produces a stiff coupling that is easily removed. The use of sand for strainmeter mounts presumably works similarly, since most of the sand is again far from a free surface. The sand used for these applications should be free from impurities such as clays; properly washed sand ('silica sand' to foundrymen) is more than 99% pure quartz. It is also desirable to use a mixture of different grain sizes chosen to give the least void space.

In deeper boreholes, bonding to the walls must be provided by concrete because it can be delivered in liquid form. (Though not by dropping it in; the impact causes the parts to separate.) Concrete is an extremely complex substance, consisting of a mix of cement (itself a combination of many materials) and aggregate; while there is a vast engineering literature (summarized by *Neville* [1981]) on its behavior, design of a concrete with specified properties is still an art. Most cements undergo shrinkage as they set, with an initial volume decrease of 1% occurring in the plastic phase. Subsequent shrinkage is governed by loss of water to the outside air; if cement is kept at 100% relative humidity, it actually swells with time, by perhaps 2×10^{-3} in 200 days for pure cement paste, but if exposed to normally dry air it shrinks, for cement paste by up to 4×10^{-3}. All such volume changes are reduced as more aggregate is included. This sensitivity to humidity makes cement piers an unreliable material for mounting in all but the wettest tunnels. For attaching borehole instruments the initial shrinkage must be offset to make a tight bond to the hole. This can be done using expanding cement; the commonest variety, ASTM Type K [*Kesler*, 1970], contains anhydrous calcium sulphoaluminate which, when water is added, becomes hydrated to ettringite, with a volume expansion that overcomes and may exceed the contraction of the other constituents (the rates of these reactions must be carefully balanced to give a good result). The long-term stability of cement under load has been tested extensively and is known to be poor; logarithmic creep can continue for 20 years. A cement specifically designed for use with a borehole strainmeter [*Moore et al.*, 1974] had an observed stability of about $10^{-12}\epsilon$ s^{-1} 200 days after setting.

Near-surface instruments need to use 'anchors' that tie their endpoints to depths away from motions of the surface layers. As this depth is usually tens of meters, anchoring has been applied only to very long base surface instruments; otherwise the anchor is longer than the instrument and it is unclear what is being measured. For tiltmeters the anchor is simply a vertical strainmeter; the types so far used include tensioned invar rods and tapes, with LVDT sensors [*Riley*, 1970; *Bilham et al.*, 1985] and a laser Michelson interferometer [*Wyatt et al.*, 1984].

Anchoring a strainmeter is more difficult. Though inverted tiltmeters using floats in a water-filled tube have been utilized for horizontal reference points [*Decae*,

1960], they have not been used in any strainmeter. The optical anchor developed by Wyatt [*Wyatt et al.*, 1982*a*] is the only strainmeter anchor so far built. This is a shear strainmeter, measuring along two equally inclined boreholes, both lying in the same vertical plane as the anchored strainmeter and intersecting at a point on the surface. If l_1 and l_2 are the distances from the point of intersection to the bottoms of the two holes, θ the angle of dip of the holes, and s the horizontal motion of the point of intersection in the plane of the holes, simple geometry gives $s = 2(l_1 - l_2)\cos\theta$. To measure $l_1 - l_2$, retroreflectors cemented at the bottom of each hole and a beamsplitter at the top form a Michelson interferometer, which having arms of nearly equal length may use an unstabilized laser. The two anchors so far built go 26 m deep, and while they were difficult and expensive to build, they have greatly reduced the apparent long-term drift on the strainmeter they are attached to.

4. TILTMETERS

So many kinds of tiltmeters have been built that classification is difficult. The most useful division is between short- and long-base instruments, the former using a pendulum or bubble as their vertical reference, the latter the free surface of a liquid. A few 'long-base' instruments have actually been smaller than some 'short-base' ones; the difference is in the length over which the system could be used.

4.1. *Short-Base Tiltmeters*

While designs for short-base tiltmeters are exceedingly diverse, they all use some form of pendulum to define the vertical. As a consequence they all satisfy the indicator equation for a damped linear vibrator; if $\boldsymbol{\Omega}$ is the tilt given by equation (3), and q the displacement of the pendulum from equilibrium, then

$$\ddot{q} + 2\zeta\omega_0\dot{q} + \omega_0^2 q = gK_p\Omega \tag{18}$$

with $\Omega = |\boldsymbol{\Omega}|$ being the amplitude of the tilt, ω_0 the natural frequency of the pendulum, ζ its damping parameter ($\zeta = 1$ for critical damping), and K_p a dimensionless constant depending on the design (and equal to 1 for an ideal simple pendulum). At long periods this gives a tilt sensitivity of

$$G_T = \frac{q}{\Omega} = \frac{gK_p}{\omega_0^2} \tag{19}$$

A fundamental limit on the noise of any such instrument is imposed by motions of the pendulum excited by thermal fluctuations in the damping system. Because the pendulum is in thermal equilibrium with its surroundings, it has mean kinetic energy $\frac{1}{2}k_B T$. The spectral level of tilt noise that would produce such energy is independent of frequency and equal to

$$\frac{8k_B T\zeta\omega_0}{g^2 M K_p^2} \tag{20}$$

where M is the mass [*Melton*, 1976]. The magnitude of this noise is such that tiltmeters with masses of a few grams or less are noisier than the ground at the frequency of the tilt noise minimum in Figure 2.

4.1.1. *Astatic mechanical pendulums.* The first design for a sensitive tiltmeter was the horizontal pendulum, originally proposed in the early nineteenth century and successfully built near its end. In this design the bob swings at the end of an arm (the boom) attached to the frame in such a way that the bob moves along a nearly horizontal circle. This is an example of an astatic system: the restoring force is kept small so that slight external forces cause large motions. The response of the horizontal pendulum to tilt is most easily found by determining its response to horizontal acceleration and then noting, from (3), that an acceleration $\ddot{x}$ is equivalent to a tilt $g\Omega$. If θ_q is the angle in the plane of rotation that the boom makes with its stable direction, and x the horizontal displacement of the frame perpendicular to that direction, the kinetic energy of the boom and bob system is, for θ_q small, $\frac{1}{2}M(\dot{x}^2 + r_g^2\dot{\theta}_q^2 + 2r_c\dot{x}\dot{\theta}_q)$, where M is the mass of the pendulum, r_c the distance from the pivot point to the center of mass, and r_g the radius of gyration. If the plane of rotation is inclined at an angle i to the horizontal, the potential energy is $-Mgr_c \sin i \cos\theta_q$. Lagrange's equation for the system is then

$$\ddot{\theta}_q + \frac{gr_c \sin i}{r_g^2}\theta_q = \frac{-r_c}{r_g^2}\ddot{x} \tag{21}$$

and comparison with (18) gives $\omega_0^2 = gr_c \sin i/r_g^2$ and $K_p = -r_c/r_g^2$. (Because θ_q is an angle rather than a displacement, we must multiply (21) by r_g to make it exactly similar to (18); thus in (20) we would put $K_p = r_c/r_g$.) The tilt sensitivity G_T is just $1/\sin i$, which may also be written as ω_0^2/ω_v^2, where $\omega_v^2 = gr_c/r_g$ is the natural frequency of the boom suspended as a vertical pendulum. For an ideal pendulum, $r_g = r_c$ and both equal the length of the boom; knowing this and the period of the horizontal pendulum we could determine the sensitivity. For a real horizontal pendulum, this calibration is more difficult.

If the angle of inclination is small, the horizontal pendulum will magnify tilts considerably. For example, if $i = 5\times10^{-5}$ the magnification would be 2×10^4; an ideal horizontal pendulum with $r_c = 0.1$ m and this angle of inclination would have a free period of 90 s. Of course, in such a pendulum the gravitational restoring force is very slight, and other forces must be kept small for it to work well. All such pendulums now use some variation of the Zöllner suspension, in which the pivots are elastic members. Figure 14 shows the classical form of this, in which the pivots are near-vertical wires; most horizontal seismometers, and some tiltmeters, instead support the boom with horizontal pivots attached to a vertical crosspiece perpendicular to it. Additional modes of vibration are possible if the classical form is used, making the full theory [*Jobert*, 1959; *Vaníček and Lennon*, 1972] very complex, though the essentials do not change.

The horizontal pendulum, most usually the quartz instruments of *Blum* [1962] and *Verbaandert and Melchior* [1961] (or VM) has been the commonest tiltmeter for earth-tide studies. These instruments are made entirely of fused silica, which provides thermal stability for the frame and boom and near-perfect elasticity for the suspension wires. The magnification and period of these

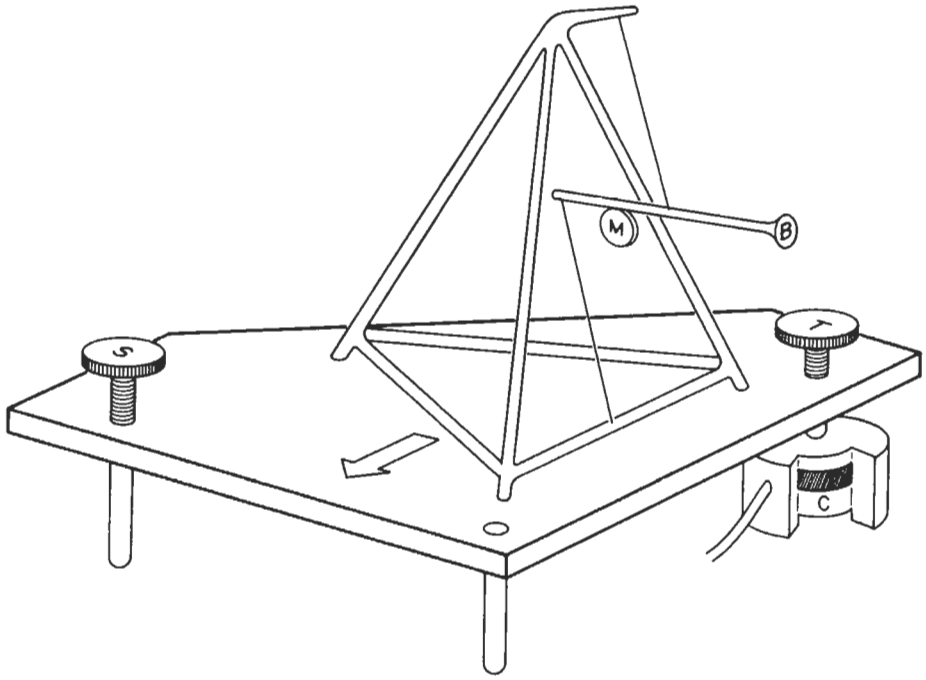

Fig. 14. Verbaandert-Melchior quartz horizontal pendulum and leveling platform. The pendulum boom B is about 10 cm long; the mirror M is used to detect motions of the boom caused by tilts in the direction of the arrow. S and T are screws that move the platform to change sensitivity and tilt. C is the distensible calibration support, shown in a cutaway view.

tiltmeters are roughly as given in the example above; the instrument baselength is 0.1 to 0.3 m. Because sin$i$ is very small, small tilts perpendicular to the direction of sensitivity can alter the sensitivity G_T significantly, so frequent calibration (section 4.1.5) is needed [*Skalsky and Picha*, 1969]. The actual recording is done with an optical lever writing directly on photographic paper, which does not allow any filtering. Some is provided if the pendulum is damped, which is done for the Blum pendulum using eddy-current damping; the VM pendulum is undamped. The space needed for the recording system and the fragility of the suspension make these instruments usable only in mines or tunnels; they are thus inevitably subject to cavity effects. The long-term drift rates observed for the Blum instrument are in the range $1-3\times10^{-14}$ rad/s, whereas the VM pendulums often have much higher rates, up to 2×10^{-13} rad/s. The likeliest source of the difference is that the VM pendulum sits on a metal base with leveling screws, whereas in the Blum pendulum the quartz frame sits directly on the rock.

Horizontal pendulums of the 'garden-gate' type have also been used for tiltmeters; an older instrument of this kind [*Ostrovsky*, 1961] has been extensively used in the Soviet Union. *Kato* [1977] describes a similar but more modern instrument, with a low mechanical magnification (sin$i$ = 0.023) and a sensitive displacement sensor (a differential transformer). Another development in the same spirit is the miniature horizontal pendulum (1 s period) manufactured by Instech (Austin, Texas), which uses a capacitive sensor; its small size (two pendulums fit in a capsule 7 cm across) makes it suitable for borehole use [*Harrison and Levine*, 1981].

Because the bob of a horizontal pendulum moves in a circular arc, a full theory of its motion must allow for cross-coupling effects from tilts and accelerations [*Skalsky and Picha*, 1969; *Rodgers*, 1968] in directions other than the one it is sensitive to. This circular motion can be avoided by a different design. The horizontal pendulum geometry makes the vertical motion of the bob small compared to the distance it moves horizontally. Put another way, the path of the bob, projected on a vertical plane in the direction of tilt sensitivity, has a large radius of curvature; this radius is the length of the equivalent simple pendulum. What is needed to avoid cross-coupling is a path of large radius lying in a vertical plane. To make the bob move in such a path it may be made part of a straight-line linkage, adjusted so that the bob follows not a straight path but one curved slightly upwards [*Lindenblad*, 1967]. *Tsubokawa et al.* [1970] have built such a tiltmeter using a suspension [*Nagasawa*, 1972] like those in geodetic levels, the motion being measured by an inductive sensor. Another design of this sort is the 'straight-line level' made by Instech (formerly Electrolevels) of Austin, Texas, which uses the spatial straight-line linkage of *LaCoste* [1983] and capacitive sensing; in early models of this instrument, hysteresis in the suspension wires caused large phase lags at low frequency (F. Wyatt, personal communication, 1982).

4.1.2. *Simple pendulums.* With improved displacement transducers, the pendulum need not itself amplify tilts very much. A simple pendulum is much easier to build than an astatic pendulum, and with capacitance transducers can achieve tidal sensitivity even for lengths of only 30 mm. *Allen* [1972] and *Jones and Richards* [1973] describe typical designs, in which the mass swings in one axis and is suspended by flexible metal strips.

The borehole tiltmeter designed by Askania [*Rosenbach and Jacoby*, 1969] and now sold by Bodenseewerke (Fig-

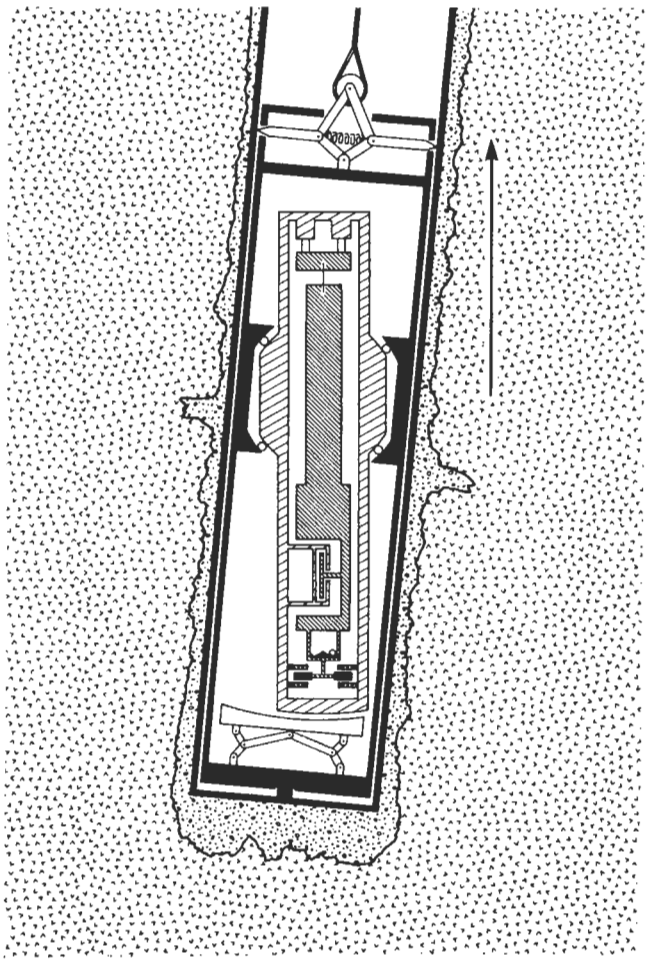

Fig. 15. Simplified cross section of an Askania borehole tiltmeter, shown inside a cemented-in casing. The borehole is not vertical, but the pendulum holder (light hatching) and pendulum (heavy hatching) are. The capacitive sensor, ball calibration, and feedback magnets are shown schematically at the bottom of the pendulum. For clarity, the locking plunger on the bottom of the pendulum holder has been omitted and the clamping plate shown as movable instead.

ure 15) also uses this design. A single pendulum 0.6 m long measures tilt in both axes, the suspension strips being arranged to allow movements in any direction. Capacitive transducers measure the displacements; these sensors have high sensitivity (10^5 V m^{-1}), and because they are affected by motion in one direction only, two orthogonal sensors can be used on one pendulum. The linearity is better than 10^{-3} for tilts less than 1.5 μrad. In the original version of this tiltmeter the pendulum was only lightly damped, and it could not be used in seismically noisy areas. Feedback, applied through Helmholtz coils near the bottom of the pendulum to magnets within it, was later added to provide active damping. This not only improves the frequency response but also raises the linear range to 50 μrad [*Bodenseewerke Geosystem*, 1978]. This instrument is especially designed for borehole operation; its leveling and calibration devices are discussed in sections 4.1.5 and 4.1.6.

A smaller instrument (total length 0.43 m) designed on similar principles (a two-axis simple pendulum with capacitive sensing and electromagnetic feedback) is now being widely deployed in Japan [*Sato et al.*, 1980]. It is designed, like the Askania, specifically for borehole installations.

4.1.3. *Diamagnetic tiltmeter.* In order to make a tiltmeter with a truly frictionless suspension, *Simon et al.* [1968], working at Arthur D. Little (ADL) floated the sensing mass in a magnetic field. Such flotation can be done with a superconducting mass and magnetic coils or by active servo control of an electromagnetically suspended ferromagnetic mass, both of which are awkward in a field instrument. Passive flotation at room temperature is possible if the mass is made from a material, such as graphite, with a negative magnetic susceptibility.

The ADL tiltmeter (Figure 16) suspends a cylindrical graphite mass in the field from a permanent magnet. Shaped pole pieces make the field strongly nonuniform perpendicular to the axis of the cylinder but only slightly nonuniform along it, so that the mass is sensitive to tilt along the second axis. The free period of the mass can be as much as 10 s. Eddy currents in an aluminum sleeve around the graphite damp the motion. This motion is sensed optically, using the shading of a split photodiode by a vane attached to one end of the mass; while simple, this makes the stability (except at null) depend on having a lamp of stable brightness. (Earlier versions used two photodiodes looking at opposite ends of the mass and wired as a bridge.) Most tests of this instrument have been tidal measurements using a borehole version which has given good results [*Wyatt et al.*, 1982*b*; *Cabaniss*, 1978]. The diamagnetic suspension should be excellent for long term measurements because of its freedom from stickiness and creep; it is also relatively robust.

4.1.4. *Bubble tiltmeters.* Yet another way to get a long

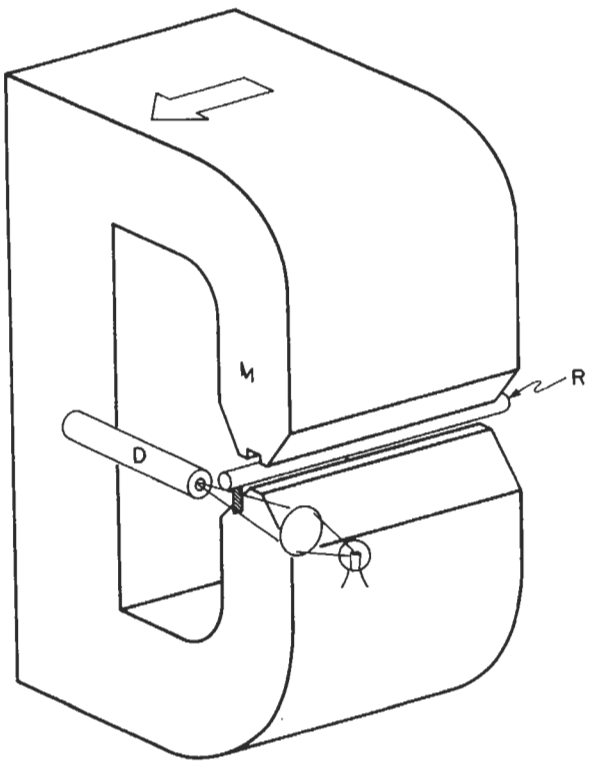

Fig. 16. A. D. Little diamagnetic tiltmeter. A graphite rod R (~5 cm long) floats in the field from the magnet M. The direction of tilt sensitivity is shown by the broad arrow. D is the detector.

TABLE 4. Properties of Tiltmeter Liquids

Liquid	β K^{-1} (10^{-4})	ρ kg m^{-3} (10^3)	η N s m^{-2} (10^{-3})	c_p J $kg^{-1}K^{-1}$ (10^3)	K W m^{-2} K^{-1} (1)	S_0 N m^{-1} (10^{-2})
MFL 18	13.1	1.82	4.2	1.2	0.075	1.8
Methyl ethyl ketone	12.7	0.81	0.44	2.23	0.15	2.6
Ethanol	10.7	0.79	1.3	2.34	0.18	2.2
N-butyl alcohol	8.6	0.81	2.9	2.47	0.17	2.5
Ethylene glycol	6.2	1.13	24.	2.34	0.29	4.8
Water	2.1	0.998	1.0	4.18	0.59	7.3
Mercury	1.82	13.55	1.6	0.14	8.36	45.

Quantities are density (ρ), thermal coefficient of volume expansion (β), dynamic viscosity (η), specific heat (c_p), thermal conductivity (K), and surface tension (S_0). All values are for 20°C, or as near to it as possible; to get them in the units specified, the numbers must be multiplied by the scaling factor at the head of each column. Under field conditions the actual surface tension will usually be less than the values given here.

apparent pendulum length is to sense the motion of a bubble trapped beneath a curved surface; as in a spirit level, if the curvature is slight, small tilts will cause large bubble displacements. Tiltmeters based on this principle have been widely used, but the only detailed descriptions are in unpublished technical reports [*Cooper*, 1970; *Cooper and Schmars*, 1973], and a relatively full discussion therefore seems warranted.

A bubble trapped beneath a surface experiences several forces. To begin with we consider only three:

1. Buoyancy. If the surface is locally tilted at an angle θ_S to the vertical, the bubble experiences a force

$$g\rho v_B \sin\theta_S$$

where ρ is the density of the surrounding liquid and v_B is the bubble volume. θ_S includes not only ground tilts Ω, but also any 'built-in' tilt of the surface θ_I; if all these are small the buoyancy force is

$$g\rho v_B (\theta_I + \Omega)$$

2. Viscous drag. The Reynolds number for an object of diameter b moving through a liquid of dynamic viscosity η at velocity $\dot{q}$ is $\mathrm{Re} = \rho b\dot{q}/\eta$. In most bubble systems, $\dot{q}$ is so small that $\mathrm{Re} \ll 1$: the flow is purely viscous. The force on a body is then given by Stokes' law [*Batchelor*, 1967] and is

$$D_B\dot{q}$$

where D_B is a damping constant which must be determined empirically.

3. Inertial forces. Motion of the bubble causes the surrounding liquid to move, and the inertia of this liquid gives the bubble a resistance to acceleration, or apparent mass [*Lamb*, 1932, Chapter 6]. The flow is purely laminar inside the boundary layer; at low Reynolds number this includes the whole body of liquid. The flow therefore changes intensity, but not form, as the bubble velocity changes, and the bubble therefore experiences a resistance to its acceleration relative to the liquid of

$$I_B\rho v_B\ddot{q}$$

where I_B depends on details of the flow and again must be empirically determined.

We now suppose that the bubble rests below a surface with radius of curvature r_P. The local tilt of this surface at a distance q from its highest point is $\theta_I = -q/r_P$. Combining terms, we then find that the equation of motion of the bubble is

$$\ddot{q} + \frac{D_B}{I_B\rho v_B}\dot{q} + \frac{g}{I_B r_P}q = \frac{g}{I_B}\Omega \qquad (22)$$

and comparison with (18) and (19) gives the natural frequency ω_0 as $(g/r_P I_B)^{1/2}$, and the tilt sensitivity G_T as r_P. Since in practice $I_B \approx 1$, we may take r_P as the length of the equivalent simple pendulum for calculating both frequency response and tilt sensitivity.

In the preceding discussion the bubble has been treated as a rigid body sliding along the surface above it. This is only an approximation; it is valid because of a force not yet discussed, namely surface tension. The importance of this relative to gravity is expressed by the Bond number $Bo = \rho g b^2/4S_0$ (which also applies to any other acceleration), and relative to viscosity by the capillary number $Ca = \dot{q}\eta/\rho S_0$ where b is the bubble diameter, $\dot{q}$ a typical velocity, and S_0 the surface tension. For the Rockwell tiltmeter described below $b = 8$ mm and ρ, η, and S_0 are those for ethanol (Table 4); $\dot{q} \leqslant 10^{-4}$ m s^{-1} and $\ddot{q} \leqslant 10^{-4}$ m s^{-2} except during large nearby earthquakes. This gives $Bo < 10^{-6}$ and $Ca < 10^{-5}$: the bubble is therefore not significantly deformed by its own motion. On the other hand, an acceleration of g gives $Bo = 5.6$, so that the bubble would deform substantially during strong ground motion. Another and potentially very troublesome effect of surface tension exists along the contact line, where the bubble wall meets the surface it rests below. The angle the bubble wall makes with this surface, called the contact angle, partly determines the shape of the bubble. If this angle does not remain the same as the bubble moves, then the bubble shape will depend on its velocity, and in particular, if a range of contact angles is possible for a bubble at rest, it will tend to stick in one position before moving to another [*Dussan V. and Chow*, 1983]. This last situation, termed contact-angle hysteresis, is unfortunately very common [*Dussan V.*, 1979] but can be eliminated. Though many discussions suggest that the surface must be very smooth, most bubble tiltmeters use one that is slightly roughened so that all of it is wet by the liquid and there is no contact line. The need

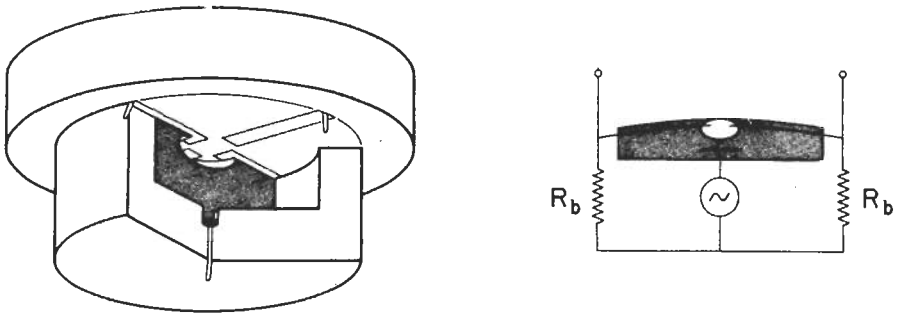

Fig. 17. (Left) A cutaway view of the Autonetics two-axis bubble sensor. Four sensing strips give sensitivity to tilt in two axes. The upper cylinder is 5 cm in diameter. (Right) A schematic of the circuit used; R_b is the reference resistance of the bridge. The output voltage is sensed across the two terminals at the top.

to reduce bubble stickiness makes the construction of bubble levels an art; they are much better bought from an established manufacturer than built for oneself.

The bubble position is usually sensed with a resistance bridge, arranged as shown in Figure 17. Three electrodes are inserted into the liquid container, two being arranged so that as the bubble uncovers one it covers the other. When the bubble is centered, the resistances between each of these and the common electrode is the same (R_L), and the bridge is balanced. Any movement of the bubble produces an imbalance, the output being

$$2V \frac{R_L R_b}{(R_L+R_b)^2} \frac{1}{R_L} \frac{\partial R_L}{\partial q} q$$

where V is the applied voltage and R_b the resistance of the external resistor.

For conduction to be possible the liquid used must be an electrolyte, and to avoid electrolysis the bridge must be operated at AC. This also reduces electronic noise, but it has created problems in some commercial bubble tiltmeters. If square wave excitation is used, small inductive and capacitive effects cause distortion of the output signal; this distortion will usually change with temperature, and simple integration of the output signal will therefore give poor results. Two remedies are possible: sine wave excitation [*Morrissey*, 1977], and square wave excitation, chopping out the initial part of each output transition where most of the distortion occurs (box-car averaging) [*Westphal et al.*, 1983].

Because the dielectric constant of the gas in the bubble is much less than that of the liquid, the bubble position may be sensed using a capacitive bridge, which has the advantage that no electrodes need penetrate the container. A recent example of this technique [*Xie*, 1983] had an overall response of 3.8×10^5 V rad^{-1}.

The bubble tiltmeter most extensively deployed in geophysics has been the system formerly marketed as the Kinemetrics model TM-1. This uses a bubble sensor developed by the Autonetics division of Rockwell Corporation, originally for inertial guidance systems in Minuteman missiles [*Cooper*, 1970; *Cooper and Schmars*, 1973]. In this sensor (Figure 17), the bubble is in an ethanol-based liquid and trapped beneath a spherical glass surface with $r_P = 0.305$ m, to give a period of 1 s and roughly critical damping. The detection electrodes are platinum strips plated on the glass; with 1 V excitation, $R_L = 4$ kΩ, and $R_b = 7$ kΩ, the output sensitivity is 42 V rad^{-1}. The sensor is affected by temperature in two ways: the bubble diameter changes with temperature at a rate of 0.1% K^{-1}, causing an apparent signal except at null, and there is a direct dependence of tilt on temperature gradient at the rate of 3.3 μrad m K^{-1}. The linearity is fair, though not adequate for precise tidal measurements (J. C. Harrison, personal communication, 1981). Care in construction, especially avoidance of all contamination, is needed to assure good sensor performance. The small size of the bubble gives this sensor a relatively high Brownian noise; using equation (20) with $M = \rho v_B$ and $I_B = 1$ gives a limit of −170 dB (rad^2 Hz^{-1}). Slightly higher levels observed in actual tests [*Wyatt and Berger*, 1980] presumably reflect additional electronics noise or bubble stick-slip.

The Autonetics sensor, while relatively sensitive and fairly robust, is also very expensive. *Westphal et al.* [1983] have used a less expensive bubble sensor (manufactured by the Fredericks Corporation) to make a cheap (and therefore expendable) tiltmeter for use near volcanoes. This sensor has $r_P = 0.356$ m and is overdamped; both the sensor resistance (1 kΩ) and the nominal gain (28 V rad^{-1}) are less than for the Autonetics sensor, and published tests indicate a somewhat higher noise level.

The use of feedback makes possible a different design of tiltmeter. If we measure the bubble position using a transducer with a response of K_a V m^{-1}, and put its output through a forcer that tilts the confining surface by K_t rad V^{-1}, the equation of motion for the bubble changes from (22) to

$$\ddot{q} + \frac{D_B}{I_B v_B} \dot{q} + \frac{g}{I_B} \left[\frac{1}{r_P} + K_a K_t \right] q = \frac{g}{I_B} \Omega$$

Feedback thus shortens the period and decreases the sensitivity; while this may seem undesirable, it can be useful. If r_P is infinite (a bubble trapped beneath a flat surface), application of feedback stabilizes this otherwise unstable system. The natural frequency is then $(gK_a K_t / I_B)^{0.5}$, and the tilt sensitivity of the output $K_a q$ is K_t^{-1}, which is independent of the bubble and its detector and hence can be made very stable and linear. Another advantage is that with the feedback off a constant tilt causes a constant bubble velocity rather than a displacement, so that drift in the position sensor cannot masquerade as tilt.

Several tiltmeters of this design [*Harrison*, 1976*b*] were

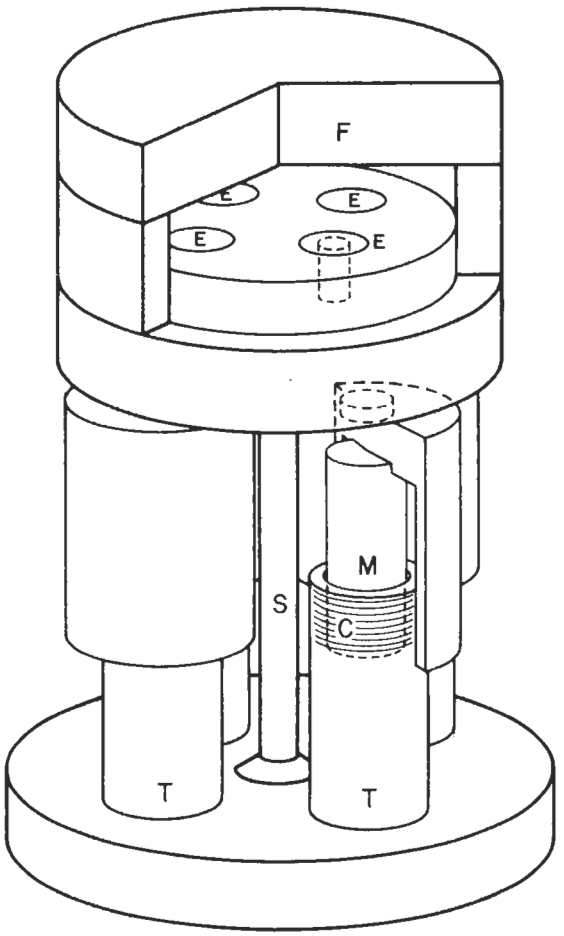

Fig. 18. Partial cutaway view of the Hughes tiltmeter. F is the flat plate below which the bubble moves; E are the terminals used to detect changes in resistance from its motion. C is a coil wound on tube T; current through this coil acts on magnet M to cause the stalk S to bend and the plate to tilt. For clarity, S has been drawn thinner than it actually is.

built by Hughes Research, all using a liquid container supported on a long stalk (Figure 18). Feedback was applied through coils acting on permanent magnets attached to the container; forces on these would bend the stalk and tilt the confining surface, which was a quartz optical flat 7.5 cm in diameter. Four electrodes in the bottom of the container formed two resistance bridges, orthogonal pairs being used for both input and output. The stalk was (except in early models) beryllium copper, which has good elastic behavior but relatively rapid creep. Results published by *Harrison* [1976*b*] for an installation in the Poorman Mine show that this tiltmeter design is linear over a wide range; the noise level at tidal frequencies was only 10 dB above the minimum shown in Figure 2, even though the baselength of the Hughes tiltmeter was only 0.1 m and the minimum spectral level was obtained with a 535-m-long tiltmeter.

4.1.5. *Calibrating small tiltmeters.* Calibrating any short-base tiltmeter is difficult, especially if it is to be used for accurate tidal measurements. Tilting the instrument base by well-known small amounts requires the precise control and accurate measurement of small displacements: to calibrate to 1% of the tides (10^{-9} rad) would mean moving one end of a 1-m tilt platform accurately to 1 nm. Piezoelectric materials can generate displacements of the right size, but they are not well calibrated and have considerable hysteresis [*Basedow and Cocks*, 1980; *Mills and Hurst*, 1981]. A mechanical system using a fine screw can produce more accurate but much larger displacements; conventional commercial micrometers read to 2×10^{-6} m. (Differential micrometers have higher resolution but no greater accuracy.) Smaller displacements may be obtained through reduction systems, either a reduction gear (though this is prone to backlash) or a lever system such as the one in the LaCoste-Romberg gravity meter. The tilt table made by Radian (now by Instech) used such a lever system. This table had a nominal resolution of 1 nrad and a total range of 100 μrad; a check of the linearity over the full range in 10-μrad steps showed no departures at the 0.5% level [*Harrison*, 1976*b*]. In any screw-driven system, the accuracy of interpolation to smaller intervals depends on the size of periodic or other screw errors, which are not usually known.

A different approach to making small displacements is to rely on the motion of an elastic system subjected to known forces; if the forces can be accurately subdivided, Hooke's law means that the displacements will be also. This has been applied to tiltmeter calibration in the distensible support (usually called a 'crapaudine') of *Verbaandert* [1962]. This is a short, wide, thick-walled hollow cylinder filled with liquid (Figure 14). Changes in the internal pressure cause the ends to bulge slightly; since mercury is the liquid used, changes in the height of a reservoir connected to the support can produce significant pressure variations. These distensible supports are installed permanently beneath each tiltmeter after being calibrated in a test fixture which both simulates the load on the support and measures its displacement response interferometrically. The support is calibrated over a range of displacements corresponding to 8 μrad in steps of 1 μrad; the large step size, which comes from the coarseness of interferometry, means that tidal calibrations must again rely on accurate interpolation. There is some evidence [*Baker and Lennon*, 1976] that the effective calibration of a particular support may vary by 5% with time, though recently constructed ones appear to be more stable [*Melchior*, 1983].

A completely different method of calibration is the 'ball-calibrator' in the Askania tiltmeter (Figure 15). This consists of a small chamber within the pendulum, in the floor of which are two parallel notches. A current pulse through a nearby electromagnet makes a small steel ball hop back and forth from one notch to the other; this changes the center of mass of the pendulum and causes a small apparent tilt. Many repetitions allow the relative instrument gain to be determined to 0.2% precision; the calculated effect of moving the ball, and thus the absolute calibration, is claimed to be accurate to 0.1% [*Flach et al.*, 1971].

4.1.6. *Borehole techniques.* Because of the limited dynamic range of most tiltmeters (usually less than 10 μrad) some mechanical method of leveling them is needed; this must be capable of adjustment over a wide range and also needs to be stable, once adjusted, to 0.1 μrad or better. For tiltmeters placed in large cavities the mounting studs can sometimes be set accurately level; if

not, the tiltmeter can be mounted on a platform with three leveling screws arranged in a right triangle (Figure 14). In a borehole the problem is much more difficult, since without special precautions the hole can be tilted as much as 0.1 rad. For compact tiltmeters the simplest solution is to build a motor-driven version of the platform with leveling screws, often in an upside-down version, with the screws attached to the outer case and the platform resting on them. This has been used in borehole versions of the Hughes and ADL tiltmeters, and also in the borehole instruments developed by *Harrison and Levine* [1981].

The Askania tiltmeter uses a somewhat different system (Figure 15), partly because of its length. The sensing pendulum is inside a suspension case whose midpoint is attached to the outer case through bearings that allow the suspension case to swing freely. At the bottom of the suspension case is a plunger which can be forced against a bearing surface attached to the outer casing. For leveling the plunger is retracted; once the suspension case has settled to a nearly vertical position, releasing the plunger locks it into position, final adjustments being made by moving the bearing surface by a small amount. Locking by the plunger stresses the lower part of the suspension case but not the upper part, to which the pendulum is connected. (For simplicity, in Figure 15 the bearing surface has been shown as movable and the plunger omitted.) The total range of this system is 3°.

Another problem in borehole measurements is determining the azimuth of the tiltmeter (in a mine or tunnel this can be done using conventional survey methods). If the hole is straight and dry, the best method is to sight down on a mark on top of the tiltmeter case. Alignment rods can be used to transfer the tiltmeter orientation mechanically: a rod is attached to the tiltmeter, sections are added as the instrument is lowered, and the orientation of the rod is found when the tiltmeter is in place, after which the rods are pulled out. This can give an accuracy of 1°−2° to depths of 30 m. In deeper holes an alignment fixture ('muleshoe') can be cemented in and its orientation determined before the tiltmeter is installed; this service is available commercially. If the instrument itself is to be cemented in, a telemetering orientation device must be built into it. Magnetic compasses are relatively inexpensive but may be affected by local rock magnetism; gyrocompasses avoid this problem but cost much more.

4.2. *Long-Base Tiltmeters*

Because a short-base tiltmeter is small, it and its coupling must be very stable: for example, a tilt rate of 10^{-14} rad s^{-1} corresponds, over a 10-cm baseline, to a differential movement of $0.03\,\mu m\ yr^{-1}$, a displacement only 60 times the size of the unit cell in a quartz crystal. This problem is reduced for a bigger instrument, and many long-base tiltmeters have been built for this reason. They all use the surface of a liquid to define the horizontal, and most measure tilts by monitoring the motion of this surface.

Unfortunately, influences other than tilts can make the liquid surface move. Elementary hydrostatics assumes a liquid of uniform density, but real liquids, even if homogeneous, never satisfy this condition because of density variations caused by temperature differences. Tables 4 and 3 show that the least temperature-sensitive liquid (mercury) has a volume coefficient of thermal expansion (β) greater than that of most solids. Liquid tiltmeters must either be operated where the temperature is stable or be designed to be insensitive to temperature changes. The effect of temperature for particular designs will be discussed in the following sections, but some general principles that apply to all will be introduced here. We concentrate on the case of a liquid at rest, both for simplicity and because static effects persist at arbitrarily long periods. If the liquid is subject to a body force derived from a potential, then no motion implies that equipotentials, isobars, and isopycnals (surfaces of constant density) coincide, and the relation between pressure p and potential U is

$$\frac{\partial p}{\partial U} = -\rho(U) \tag{23}$$

where ρ is the local density [*Batchelor*, 1967, section 1.4]. For a homogeneous liquid, isotherms and isopycnals coincide, and the surface (the zero isobar) will therefore be horizontal so long as the temperature is horizontally uniform. In general, horizontally varying temperatures cause static instability and convection, a complicated fluid-dynamical problem discussed briefly in section 4.2.4. For certain shapes of the liquid container (described in sections 4.2.1 through 4.2.3) it is also possible to have static apparent tilts for horizontally varying temperatures.

The surface of the liquid also departs from the horizontal because of surface tension acting on the walls of its container. Most tiltmeters measure the position of the liquid surface in a cylindrical container, for which the distortion produced by surface tension is well known [*Concus*, 1968]. The amount of distortion depends on two parameters: the Bond number $Bo = \rho g r_C^2 / S_0$, where r_C is the radius of the cylinder and S_0 and ρ are the surface tension and density of the liquid; and the liquid-solid contact angle, which for a worst-case analysis may be set to zero (the liquid drawn upward). If $Bo > 100$ (true except in small containers) and we are not near the edge, the height of the surface above equilibrium at a distance r from the center is

$$h(r) = 2.4 r_C \exp(-Bo^{0.5})\, Bo^{0.25} I_0\left(Bo^{.5}\frac{r}{r_C}\right)$$

where I_0 is a modified Bessel function. The mean elevation out to r is $(r/r_C)^3 h(r)$. Even if $h(r)$ is small, contact-angle hysteresis (section 4.1.4) can make the liquid surface move irregularly. *Bilham et al.* [1979] suggested using a porous lining to avoid this problem, but this may not be necessary in practice since the problem has not been widely reported.

Most liquid tiltmeters determine tilt by taking the difference between liquid levels measured at each end. While the symmetry of this technique can render the instrument insensitive to certain errors (such as leaks), for it to work the transducers used must be well-matched and linear.

One other general principle for long-base liquid tiltmeters is that they must be sealed from the atmosphere,

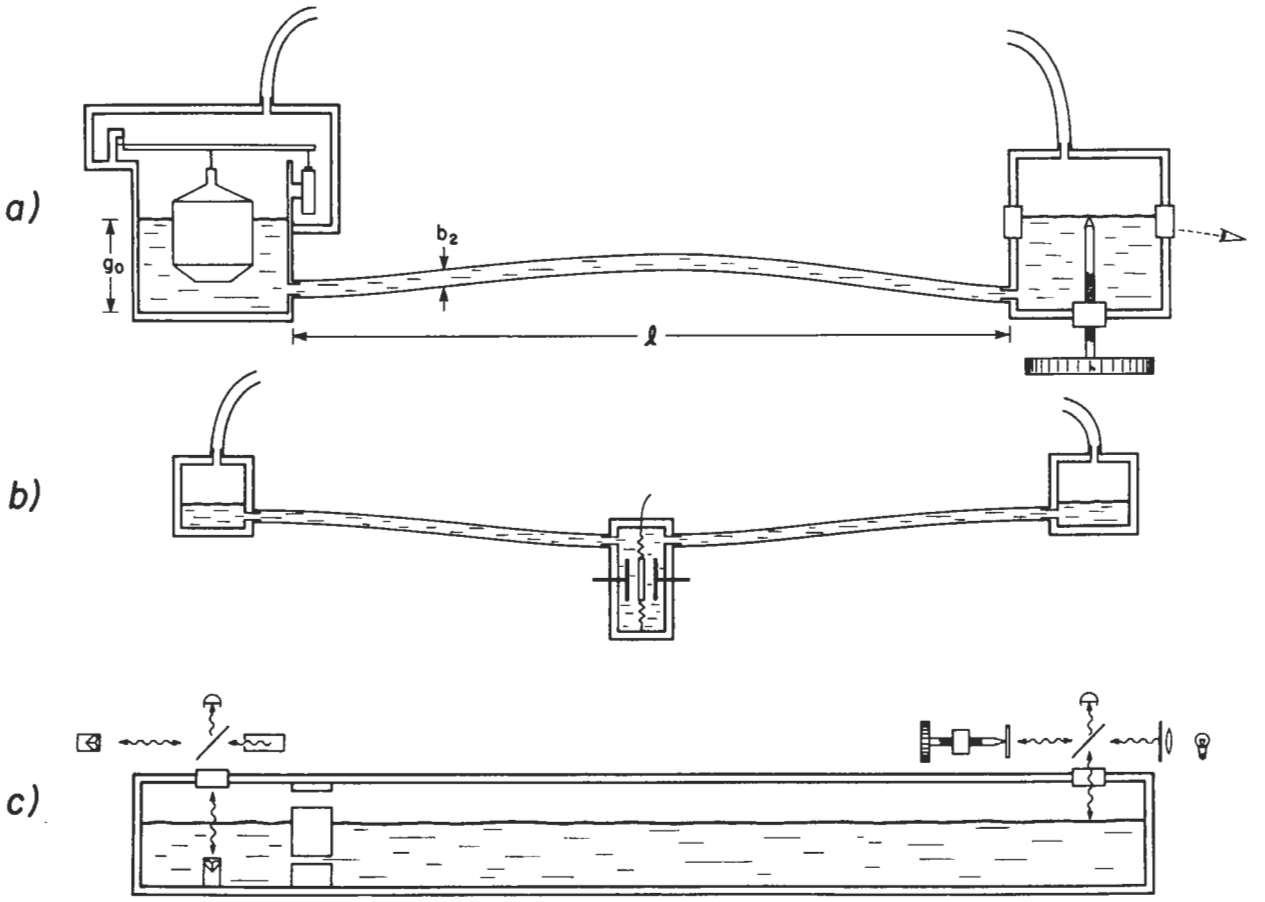

Fig. 19. Different designs of long-base tiltmeters. For greater completeness, different sensors are shown at each end, though in reality such instruments are symmetric. (*a*) Pot-and-tube tiltmeter with (left) a typical design of float sensor and (right) a visually read micrometer. (*b*) Center-pressure tiltmeter. (*c*) Michelson-Gale tiltmeter, with (left) a laser interferometer and (right) a white-light interferometer used to measure the liquid level.

since otherwise differences in air pressure between the two ends can cause large apparent tilts. While these differences should average out over long times, they increase the dynamic range needed in the sensors. Tiltmeters in tunnels, along which large pressure differences do not usually exist, can sometimes be operated unsealed.

4.2.1. *Pot-and-tube tiltmeters.* The most popular design for long-base tiltmeters is two end pots connected by a tube completely filled with liquid. Many variations of this have been built, but before describing them I will give some general theory that applies to all.

The equation of motion of this system can be most easily derived by finding its Lagrangian [*Shepard*, 1971]. If we let q be the departure of the liquid level from an equilibrium depth q_0 in the pot with area A_0, and x the horizontal displacement of the container, the kinetic energy of the liquid is

$$\tfrac{1}{2}\rho\,[A_0 q_0(\dot{q}^2+\dot{x}^2) + A_1 q_0(B_1^2\dot{q}^2+\dot{x}^2) + A_2 l\,(\dot{x}^2+2\dot{x}\dot{q}B_2+(4\dot{q}^2B_2^2/3))]$$

where A_1 is the area of the other pot and A_2 that of the tube, l is the tube length, $B_2 = A_0/A_2$, $B_1 = A_0/A_1$, and the equilibrium depth is the same in both pots (see Figure 19*a*). This expression also assumes only vertical flow in the pots; in the tube the profile of flow is taken to be parabolic, as is appropriate for steady laminar flow. Friction in the tube provides most of the damping; the dissipation function is

$$4\pi\eta l B_2^2\dot{q}^2$$

where η is the dynamic viscosity of the liquid. The potential energy is that needed to move a slab of liquid with volume $A_0 q$ from $-B_1 q/2$ to $q/2$:

$$\tfrac{1}{2}\rho g A_0(1+B_1)q^2$$

Lagrange's equation then gives for the equation of motion

$$\ddot{q}\left[q_0(1+B_1)+\frac{4lB_2}{3}\right]+\dot{q}\left[\frac{8\pi\eta lB_2^2}{\rho A_0}\right]+q\,[g\,(1+B_1)] = -lg\Omega$$

which has the same form as (18). In practice, $3q_0(1+B_1) \ll 4lB_2$, and then $\omega_0^2 = 3g\,(1+B_1)/4lB_2$, $K_p = 3/4B_2$, and $\zeta = 12\eta/\rho b_2^2\omega_0$, where b_2 is the diameter of the tube. The long-period tilt sensitivity of q is $G_T = l/(1+B_1)$. In the designs of *Thomson* [1876], *Bonchovsky and Skur'yat* [1961], and *Eto* [1966], the level is sensed in only one pot, which is made much smaller ($B_1 \approx 0$) so that all the motion will be in it. Usually the

level is measured at both ends and then differenced; the tilt sensitivity G_T is then l, and the tiltmeter can be made symmetric ($B_1 = 1$). If l is very large (to maximize G_T) the free period can become very long; the tube must then be large enough that the tiltmeter will not be overdamped. For example, a water-filled instrument with a length of 10 m, a pot diameter of 10 cm and a tube diameter of 1 cm will have a period of 52 s and be critically damped; if it were lengthened to 30 m, the period would be 90 s and the damping 1.7 times critical.

This design is very sensitive to changes in liquid temperature [*Beavan and Bilham*, 1977]. If the liquid in one pot is denser than that in the other, the surface of the less dense liquid will be higher but the system will still be in equilibrium. While isopycnals must be horizontal in a container, the density in one part of the container need not be the same in another part at the same level so long as the container is connected only at a lower level. However, in static equilibrium equation (23) holds at each point in the liquid. If we consider a line element dm at an angle ψ to the local vertical, then we may use (23) to write

$$\frac{dp}{dm} = \frac{dp}{dU} \cdot \frac{dU}{dm} = -\rho(m) g \sin\psi$$

If we choose two points in the liquid and integrate along a line to find the pressure difference, and then change the liquid temperature by T, the density changes from ρ_0 to $\rho_0(1 - \beta T)$, and the resulting change in pressure is

$$\Delta p = -g \int \Delta\rho(m) \sin\psi(m) dm$$
$$= \rho_0 g \beta \int T(m) \sin\psi(m) dm$$

To apply this to the pot-and-tube tiltmeter, suppose it is initially in equilibrium and we integrate from one free surface to the other, the integral thus being zero. Then a temperature change will result in a pressure change, which must be balanced (to first order) by a change in level of

$$\frac{\Delta p}{\rho_0 g} = \beta \int T(m) \sin\psi(m) dm \qquad (24)$$

Note that, as would be expected from the previous discussion, vertical stratification of temperature will not cause any effect: only horizontal variations matter. If the path of integration is vertical in the end pots, we may rewrite (24) as

$$\delta h = \beta \int_{\text{tube}} T(m) \sin\psi(m) dm + \beta \int_0^{q_0} \Delta T(z) dz \qquad (25)$$

where ΔT is the temperature difference between pots.

The pot-and-tube tiltmeter was first proposed by *Thomson* [1876] but was not much used for precise measurements before the work of *Hagiwara* [1947], who was dissatisfied with the instabilities of short-base tiltmeters. His design used a 20-m tube connecting two pots, the levels of which were read manually by moving a submerged micrometer point upward until it coincided with its totally reflected image (Figure 19*a*). (This method, a variation on the hook gauge used with atmometers, gives a much more precise measurement than lowering a point from above; precisions of 2 μm have been reported.) This design has been extensively used in the Japanese network of crustal deformation observatories; as these are all in tunnels, temperature is not a problem. *Bonchovsky and Skur'yat* [1961] describe a similar device, with several small pots connected to a larger reservoir. A pot-and-tube tiltmeter can be set up relatively rapidly, though care must be taken to keep bubbles out of the connecting tube; this ease of deployment led *Eaton* [1959] to design a portable instrument for repeat tilt measurements on surface baselines.

While manual reading is perfectly adequate for monitoring tectonic changes, continuous measurement is clearly desirable. Several techniques have been developed for this, primarily in Japan and China. *Tsumura* [1960] and *Eto* [1966] used floats whose motion was magnified by an optical lever. Later systems (Figure 19*a*) have usually continued to use floats, but measure their displacements with inductive sensors [*Riley*, 1970; *Kato*, 1977; *Shichi et al.*, 1980; *Liu and Zhong*, 1984]. Using floats complicates the dynamics of the instrument, since forces on them must be taken into account [*Ishii et al.*, 1977*a*, *b*]; thermal expansion of the float must also be considered. Another sensor used in Japanese instruments [*Okada et al.*, 1975] is an acoustic monitor, or 'sing-around,' in which acoustic pulses are generated at the bottom of the pot, reflected (from below) off the liquid surface, and received back at the transducer, changes in their travel time indicating changes in level.

A number of tiltmeters have also been built with this geometry but using capacitive level sensing and mercury as the liquid. If the mercury is treated as the 'center plate' of a three-plate system, each of the other two plates being mounted in one of the end pots, the methods described in section 3.3.2 will produce an output proportional to tilt. The first instrument of this type was designed by Benioff [*Gile*, 1974] apparently to serve as a long-period horizontal seismometer; it used matched resonant circuits to measure capacitance changes. A revision of the design by *Buck et al.* [1971] used phase-sensitive detection in an instrument 90 m long. A much shorter version ($l = 1$ m), developed independently by the Ideal Aerosmith Company (East Grand Forks, Minnesota), is available commercially. Another mercury tiltmeter was developed by *Stacey et al.* [1969], who used a ratio transformer capacitance bridge to obtain high dynamic range (up to 10 mrad) and sensitivity (1 nrad) in a small instrument ($l = 0.4$ m). A larger system ($l = 11$ m), also using a capacitance bridge, was built by *Peters* [1978] for studies of earth tides.

One difficulty with capacitance-measuring systems is their sensitivity to common-mode effects: a rise in the level of the mercury at both ends changes the gap between plates and hence the gain. Unless the bridge is nulled, this will produce an apparent signal. One source of level changes is the thermal expansion of the mercury. In the Benioff instrument this problem was reduced by using plastic tubes and pots, which had nearly the same expansion coefficient as mercury, and also by putting another pot halfway along the tube, a plunger in this pot being moved to keep the average level constant. *Stacey et al.* [1969] used steel pots and tubes to get better long-

term stability, and mounted the pot and sensing plate on spacers whose sizes and thermal coefficients provided compensation for the changing level of the mercury. Another and less controllable source of common-mode changes is variation of the height of the mercury surface as contamination lowers its surface tension [*Rogers et al.*, 1980].

Because many long-base tiltmeters measure displacement with sensors whose gains cannot be determined a priori (micrometers are an exception), they must be calibrated in place. The commonest technique adds and removes a known volume (usually a solid plunger) from a central pot. Reported accuracies have been 0.25% [*Peters* 1978; *Kato* 1977].

4.2.2. *Two-liquid tiltmeters.* The thermal effects discussed in the previous section are most serious when the system is exposed to large temperature variations, as it must be if hydrostatic methods are used in leveling. One solution, apparently first proposed in the 1950's and recently revived [*Sneddon*, 1974, 1979], is to use two liquids with different thermal expansion coefficients; *Huggett et al.* [1976] independently suggested this for tiltmeters. The principle is clear from equation (24): if the integral

$$\int T(m)\,\sin\psi(m)\,dm$$

is the same for both liquids, and the recorded height changes are Δh_1 and Δh_2, the quantity

$$\Delta h_1 - \frac{\beta_1}{\beta_1-\beta_2}\,(\Delta h_1-\Delta h_2)$$

will be zero in the absence of any true tilt. *Slater* [1983] constructed a prototype instrument about 200 m long, using methyl ethyl ketone and N-butyl alcohol as liquids; as Table 4 shows, these have very different expansion coefficients but similar specific heats, so they should change temperature at about the same rate. However, measurements showed that the compensation was not effective against rapid temperature changes, suggesting that dynamic effects are important.

4.2.3. *Center-pressure tiltmeters.* Another method for reducing the effect of temperature, as well as broadening the frequency response, is the center-pressure system developed by *Horsfall* [1977] and *Horsfall and King* [1978]. This uses a pot-and-tube geometry, but instead of measuring the level at each end, the differential pressure is measured at the center (Figure 19*b*). *Beavan and Bilham* [1977] show that the thermal effects are more complex for this design than for a level-sensing instrument, partly because the pressure transducer eliminates flow. There are three different effects: the thermal expansion of the liquid in the tube (offset by the expansion of the tube itself) expels liquid into the end pot, causing a rise in level and change in pressure

$$\frac{\rho g\,(\beta-3\alpha_T)}{B_2}\int_{\text{tube}} T(m)\,dm$$

where α_T is the coefficient of linear expansion of the tube; the area of the end pot changes, also altering the liquid level and changing the pressure by

$$-2\alpha_P\int_0^{q_0} T(z)\,dz$$

where α_P is the linear thermal expansion coefficient of the pot material; and the pressure change caused by density variations of the liquid in the tube is

$$\rho g\beta\int_{\text{tube}} T(m)\,\sin\psi(m)\,dm$$

We may ignore density changes in the liquid in the pots, since these cause compensating level changes. Differencing the pressure signals across opposite sides of the central transducer, we find that the thermal effect, in terms of head of liquid, is in terms of head of liquid, is

$$\frac{(\beta-3\alpha_T)}{B_2}\left[\int_0^{Sl} T(m)\,dm - \int_{Sl}^{l} T(m)\,dm\right]$$

$$-\beta\int_{\text{tube}} T(m)\,\sin\psi(m)\,dm + 2\alpha_P\int_0^{q_0}\Delta T(z)\,dz$$

Unless the slope of the tube, ψ, is kept very small (e.g, for Horsfall's prototype instrument 0.001°), the second term is much larger than the first; neglecting the first term gives an expression similar to (25), except that the coefficient for the term involving differential pot temperature has become $2\alpha_P$ instead of β. With suitable materials the temperature of the end pots is less important in this design than in a level-sensing instrument.

The central pressure transducer also broadens the frequency response by providing a stiffer restoring force than gravity. The kinetic energy and dissipation of the system are the same as in the conventional pot-and-tube system, but the potential energy is augmented by the stored elastic strain of the diaphragm in the pressure transducer. Using the expressions for the deformation of a clamped circular plate [*Timoshenko*, 1940] this additional potential energy is

$$\frac{q^2}{2}\left[\frac{3A_0^2}{k_D A_D}\right]$$

where k_D is the 'spring rate' of the diaphragm (the displacement of its center in response to a pressure p being $w = k_D p$) and A_D its area. If we add this term to the others in section 4.2.1 and solve for the equation of motion, we get (for $B_1 = 1$)

$$\ddot{q}\left[2q_0 + \frac{4lB_2}{3}\right] + \dot{q}\left[\frac{8\pi\eta lB_2^2}{\rho A_0}\right] + q\left[2g + \frac{3B_D}{\rho k_D}\right] = -l\ddot{x}$$

where $B_D = A_0/A_D$. In general, $(\rho k_D)^{-1} >> g$; if we ignore the term in g and solve for the tilt sensitivity in terms of the diaphragm deflection $w = 3qB_D$, we obtain $G_T = gl\rho k_D$, which can be thought of as the equivalent pendulum length of the instrument; its natural frequency is given by $\omega_0^2 = 9B_D/4l\rho k_D B_2$. There is thus a tradeoff between giving the instrument a broad frequency response and having to measure small displacements of the diaphragm. Use of a capacitance system makes the

latter task relatively simple, though it requires the liquid to be an insulator.

This instrument was designed to be easy to deploy, and small-bore copper tubes are therefore used to connect the end pots. This makes removal of bubbles difficult, a problem reduced by using a special fluorocarbon liquid (formerly made by ICI with the tradename MFL 18) that dissolves air easily and is a good electrical insulator. The end pots are Pyrex flasks with diameter 0.3 m, and the connecting tube has a diameter of 4 mm; the diameter of the diaphragm is 0.1 m, and its spring constant is 2.5×10^{-7} m Pa^{-1}. For the prototype instrument, l was 100 m, making the free period 22 s and the equivalent pendulum length 0.44 m, but damping 6.2 times critical. For a later instrument installed in California, l is 535 m, giving 52 s, 2.4 m, and 14 times critical damping. Experimental tests suggest that the time constant is longer than given by the theory above, perhaps because of liquid compressibility. From an operational standpoint the passive nature of the end pots can be an advantage, though it is not if the ends of the instrument must be anchored (section 3.4.4).

4.2.4. *Michelson-Gale tiltmeters.* The simplest way of making an equipotential liquid surface is to leave it uninterrupted, forming a miniature lake whose changes in level indicate tilts. This design is usually called a Michelson-Gale tiltmeter, after the builders of the first one [*Michelson*, 1914; *Michelson and Gale*, 1919] which, though constructed 70 years ago, produced records of a quality comparable to the best modern tiltmeters. This design uses a level tube half filled with liquid (water in the first instrument). Michelson and Gale measured the level at each end with an interferometer that had one arm penetrating the surface of the liquid and reflecting from a submerged mirror, so that a change in water level h caused a change in optical path of $2h(n_L - 1)$, where n_L was the index of refraction of the liquid. Interference fringes were recorded on moving film, and their shifts measured to 0.1 fringe, which for this instrument corresponded to about 4 nrad. The original Michelson-Gale instrument was 153 m long; a more recent version built by *Kääriänen* [1979] uses a similar measurement system and is 177 m long.

Perhaps because of the difficulty of laying out a straight and level tube, near-surface Michelson-Gale tiltmeters were not made for almost 65 years after Michelson's installation (with one unsuccessful exception by *Takahasi* [1930]). The great merit of this design — its long-term stability — has led to a recent revival of it for measuring tectonic tilt. One version (Figure 19*c*) has been built by *Bilham et al.* [1979, 1985]. The only example presently in use is an instrument in California which is 535 m long and buried 1.5 m deep. The half-filled pipe is 8 cm in diameter and is connected at intervals to an air-return pipe of the same size. While these tubes are of course level, they are not straight, but follow a curving contour line. The liquid surface is broken only at the ends: the measurement pots are connected to the pipe through submerged capillary tubes, which filter out any motion set up in the connecting pipe. This breakage of the free surface is allowable because there are no large thermal gradients over such a small distance. The position of the surface is measured at each end with a laser Michelson interferometer, one arm of which goes to an underwater corner cube. This gives the same response as Michelson's arrangement but is less affected by sloshing in the end pots. Fringe counting gives a tilt resolution of about 2 nrad. Suitable dimensioning of the supports for the laser and corner cube compensates for temperature changes in the optical path length, including the effect of temperature on n_L. This interferometer has operated fairly reliably, but since it is not an absolute position sensor, separate micrometers are read occasionally to give absolute tilts.

Another version of the Michelson-Gale tiltmeter (Figure 19*c*) has been developed by F. Wyatt of the University of California, San Diego (Frank Wyatt, personal communication, 1980). It is also 535 m long but uses a single connecting pipe 15 cm in diameter, an arrangement less sensitive to settling (which always occurs after the pipe has first been laid). The pipe is buried 1.5 m deep and is half filled with distilled water, ethylene glycol being added to reduce surface tension and prevent fouling. The end pots are connected directly to the pipe. The level in each pot is measured using a white-light interferometer, with one arm reflecting off the liquid surface and the other off a mirror attached to a micrometer. A stepper motor drives this micrometer (through reduction gearing) to make the two interferometer paths equal and produce a null at the detector (cf. section 3.3.1). A piezoceramic crystal attached to the micrometer head varies the mirror displacement at 1 Hz; this modulates the fringe so that it can be observed with a phase-sensitive detector. Surface ripples or a power failure cause the fringe to disappear; when this happens, the mirror hunts back and forth by increasing amounts until the fringe is recovered. This system is much more complex than the laser interferometer, but its use of a unique fringe gives an absolute reference, which is useful in editing across gaps in the data. Its main defect is dependence on a mechanical translator, which introduces such errors as hysteresis gear train backlash. This can be remedied by putting a displacement transducer on the micrometer head.

No work has been done on the dynamics of Michelson-Gale tiltmeters. For a depth of 0.1 m and length of 500 m the free period of the gravest mode of oscillation is 1000 s. For motions of this period the viscous boundary layer (in water) would be about 0.02 m thick, a significant fraction of the depth, and ordinary wave theory (which assumes the liquid to be inviscid) may not be applicable. Certainly at tidal periods and longer the motion of the liquid is completely governed by a balance between viscous and buoyancy forces; if these instruments are to produce useful tidal measurements, the resulting phase lags need to be estimated.

There is also little work available on possible temperature effects. Temperature variations along the pipe will cause convection cells, but it is unclear how much these will reduce the free surface distortion from the 'isostatic' profile that it would have in the absence of flow. Most work on convection has considered the effects of vertical rather than horizontal temperature gradients; experimental evidence [*Imberger*, 1974] suggests that, in shallow

layers of liquid, flows driven by horizontal temperature gradients can be greatly affected by surface tension [*Scriven and Sternling*, 1964].

5. STRAINMETERS

For engineering design stresses and strains have long been of great importance [*Bell*, 1973], and most of the literature on strain measurement is in this field. Most engineering 'strain gauges' are small devices in which the resistance of a metal wire or semiconductive film varies with strain [*Neubert*, 1975]. These have seen geophysical use in rock stress measurements [*McGarr and Gay*, 1978], but they are generally too small and too insensitive to measure temporal strain variations in the earth.

Most geophysical strainmeters are extensometers, measuring the displacement between two separated points. Much of the work on these instruments has been devoted to improving the displacement measurement, a subject discussed in section 3.3. Extensometers may usefully be divided into three classes according to what they use to span the distance between endpoints: rod strainmeters (some used in boreholes), wire strainmeters, and optical strainmeters. A final class of strainmeters uses hydraulic amplification to make borehole measurements; the best-known example is the Sacks-Evertson dilatometer.

Where there is fault creep, the strain can locally be large. Several extensometers have been designed to measure it; they usually resolve strains down to 1 $\mu\epsilon$ [*Schulz et al.*, 1982, 1983].

5.1. *Rod Strainmeters*

Experiments in geophysical strain measurement were made in 1882 [*Dewey and Byerly*, 1969], but the first useful strainmeter was built 50 years later by *Benioff* [1935] for seismometry. This consisted of a 20-m iron pipe attached at one end to a pier and at the other to a variable reluctance transducer, which drove a recording galvanometer. Using a solid rod to transfer the relative displacement of one point to another has the merit of extreme simplicity: for all but the highest frequencies the rod may be treated as a rigid body, and the frequency response is flat. Because Benioff used a velocity transducer, his instrument actually measured strain rate, which is desirable for seismic recording because it reduces the noise from temperature fluctuations and tides. Many later instruments have also used solid rods as the reference length against which the separation between piers is compared, the only major variations being what the rod is made of and how the displacements between it and the piers are measured.

Significant changes in both were made by *Benioff* [1959] to get useful signals at longer periods. The length standard was made from 3-m sections of fused-quartz tubing cemented together to a length (in the first instrument) of 24 m and suspended by wire slings inside a concrete trough. To record low-frequency strains, displacements were measured with an optical lever, and later with a capacitance transducer using resonant circuits. Instruments of this design, installed in California, New Jersey, and Peru, produced free oscillation data after the 1960 Chilean earthquake.

Later designs have followed several different lines of development. One has emphasized the use of strainmeters as seismometers, combining records from strain and inertial instruments to reduce the noise level from microseisms while enhancing body waves. An elaborate installation for this purpose was built by *Shopland* [1966] at the Wichita Mountain seismic array with four 20-m strainmeters in shallow (2-4 m deep) trenches. These had quartz rods and both moving-coil and capacitance transducers. *Shopland* [1970] put similar, though shorter (6 m), instruments around the Nevada Test Site to measure strain release from nuclear explosions. Because a combination of vertical strain and vertical displacement should reduce noise from surface waves, a vertical strainmeter was built and operated in several boreholes. This instrument [*Shopland and Kirklin*, 1970] had a 19-m steel rod as a length standard, using powered clamps at both ends to grip the wall of the borehole, and both moving-coil and capacitance sensors to measure displacements. As part of a program to build the most sensitive seismic system possible, *Fix and Sherwin* [1970, 1972] installed strainmeters with 40-m Invar rods in an abandoned mine at Queen Creek, Arizona. To take advantage of the low noise level of this location, these strainmeters used moving-coil transducers with a very high generator constant. This allowed detection of small teleseismic events [*Fix*, 1973].

Most strainmeter designers have concentrated on measuring tidal and secular strains. Several quartz-rod systems were built in the United States after Benioff's design, which required installation underground [*Major et al.*, 1964; *Blayney and Gilman*, 1965]. *Major* [1966] attempted to build instruments with temperature compensation (using a reentrant aluminum coupling) so that they could be run in shallow trenches. These were not very successful, probably because of soil instability (section 3.4.1) and possibly because varying humidity causes fused-quartz rods to change length [*Smith*, 1974].

The largest number of rod strainmeters have been installed in Japan as part of the national network of crustal deformation observatories, which are almost all in tunnels driven specifically for this purpose (see, for example, *Okada et al.* [1975]). A number have also been built in China. The length standards used are either quartz or 'superinvar' (an Invar-like alloy for which *Berthold and Jacobs* [1976] measured a thermal expansion coefficient of -3×10^{-7} K^{-1}). Many of the earlier instruments used optical sensors, for example, letting the end of the rod tilt a horizontal pendulum [*Ozawa*, 1965]. A less sensitive system, also used in strainmeters in the Soviet Union [*Latynina et al.*, 1968; *Boulatsen*, 1974], is to rest the end of the rod on a small roller, motions of the rod causing the roller (and an attached mirror) to turn. Comparative tests by *Takemoto* [1979] show that this technique can suffer badly from friction. More recent Japanese designs have used capacitive or inductive sensors [*Tanaka*, 1966; *Sato et al.*, 1983].

Though a rod strainmeter is conceptually very simple, several design details are important. One is how to sup-

port the rod so that it is free to move along its own axis but not sideways (both to keep the displacement transducer aligned and to eliminate spurious modes of vibration). The method used in the Benioff quartz-rod instruments and many in Japan and China is to suspend the rod in wire slings every few meters; this provides only a loose constraint and is tedious to set up. *Blayney and Gilman* [1965] used supports that acted like a nearly unstable inverted pendulum; *Benioff* [1935] and *Fix and Sherwin* [1970] used tension rods to provide a stiff sideways constraint. How to join pieces of whatever material is used (usually available in lengths up to 3 m) to form a long rod is another problem. Suitable couplings can be machined in metal rods; fused-quartz rods are usually joined by welding or by special cements.

Accurate calibration of mechanical strainmeters is difficult because the associated displacements are small. *Benioff* [1959] applied a force to the free end of the strainmeter rod and used its known elasticity to convert this to a displacement, a method followed in many later designs. Another method is to mount the 'fixed' part of the sensor on a motion reducer driven by a micrometer [e.g., *Shopland*, 1970]. Interferometers have also been used for calibration; *Blayney and Gilman* [1965] utilized a multicolor system not only for calibration but also for a long-term record of rod displacement. Laser Michelson interferometers have been applied to calibrate rod strainmeters and to record their long-term motion [*Hade et al.*, 1968; *Takemoto*, 1979].

5.1.1. *Borehole extensometers.* Because of the advantages of a borehole instrument, both in flexibility of deployment and possible long-term stability, several miniature rod extensometers have been built for borehole installation. In all of these the ends of the extensometer are attached to a thin canister that is cemented to the borehole wall. Because the baselength is short, the displacements to be detected are small, and they are usually measured with capacitance sensors. *Moore et al.* [1974] designed a borehole strainmeter that used a 0.14-m quartz-rod length standard. At high frequencies the nominal noise was -230 dB relative to $1\ \epsilon^2\ \mathrm{Hz}^{-1}$. The only installation reported was made in a 1.5-m-deep borehole drilled in a mine tunnel; the strainmeter recorded tides adequately and showed an exponentially decreasing drift (about $10^{-13}\ \mathrm{s}^{-1}$ after 200 days) presumably from cement expansion.

A much simpler instrument of similar design has been built in China by *Chi* [1982]. The length standards, 0.11 m long, are quartz. Details of the electronics are not given, but the capacitance transducers are said to allow detection of displacements of 3×10^{-12} m. Differential operation of appropriately oriented pairs of extensometers gives outputs equal to areal strain or shear strain, the latter being preferred because it is least affected by temperature changes in the instrument or air pressure loading of the surface. Instruments were installed in soil at depths of 20 to 40 m, and coupled to the earth by packing soil around them. After about one month's stabilization the instrument recorded tides and small local earthquakes. More recent installations have been cemented in at depths of tens of meters (Chi Shunliang, personal communication, 1985). A third instrument in this style has been developed by *Gladwin* [1984], and is designed to be cemented into boreholes at depths of 100-200 m. The baselength is 0.125 m, and the resolution of the transducer 30 pm, or 0.3 nϵ. Taking advantage of the stable temperature in deep boreholes, the length standards are stainless steel. A differential capacitor measures the displacements, a high dynamic range (100 $\mu\epsilon$) being obtained using an adjustable ratio transformer (section 3.3.2), automatically reset to keep the output near zero. This resetting, along with numerous tests and calibrations, is done under microprocessor control, making the instrument suitable for remote operation. Each extensometer is in a separate module, and three of these (at an angular spacing of 60°) plus a fourth reference module (in which the length standard does not contact the canister wall) make up a complete instrument. Recent installations of this strainmeter in California have shown good tidal records; measured shear strains are largely free of the long-term trends introduced by the setting of the bonding cement.

Another Chinese borehole strainmeter, developed by *Wang et al.* [1983], is not strictly a rod strainmeter, since it uses a stretched vibrating wire to measure strain changes. The frequency of vibration is measured by 'plucking' the wire with an electromagnet and counting the number of vibrations in a fixed time. This frequency depends on the tension in the wire and thus on its elongation. The resolution is said to be about 3 nϵ. This strainmeter also uses three identical sensors plus a null. The one installation described (in a shallow hole in a mine) shows tides and an annual cycle of amplitude 2 $\mu\epsilon$.

5.2. *Wire Strainmeters*

Although several rigid-rod strainmeters have been designed to be 'portable,' this has never been practical because the length standard is so cumbersome. As a more convenient alternative, several designs have instead used a flexible wire. Because a wire must be supported by keeping it in tension, which increases creep, this might seem unwise, but in fact wire strainmeters have been very successful, especially for tidal measurements. The earliest design (developed by Sassa around 1950) hung an Invar wire between two points in a shallow catenary; changes in the distance between the ends caused the bottom of the catenary to rise and fall. This motion was recorded with an optical lever. More recent instruments stem from the design by *Sydenham* [1969] of a strainmeter in which the wire is fixed at one end and at the other is free to move but kept under constant tension.

The design of such an instrument is governed by the theory of a flexible line suspended in a catenary. The usual development [*Bomford*, 1962] gives the relation between baselength l, wire length w, and central sag y as

$$w = L_c \sinh(l/L_c) \tag{26}$$

$$y = \tfrac{1}{2}L_c\,[\cosh(l/L_c) - 1]$$

where the catenary scaling length L_c is $2F_0/\rho g A_w$, ρ being the density of the wire and A_w its cross-sectional area. F_0 is the tension at the lowest point; for a shallow catenary this is very nearly the tension at the end. This tension will stretch the wire elastically to an extension e_w; expressing F_0 in terms of e_w, we find

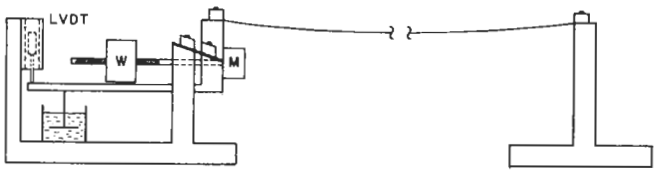

Fig. 20. Simplified drawing of a wire strainmeter. The sensing element pivots on flexure strips and includes a movable weight W that is driven by the motor M to extend the dynamic range. The position is measured with the LVDT.

$$L_c = 2e_w \frac{E}{\rho g} \equiv e_w L_w$$

where E is the Young's modulus of the material and we have defined a wire scaling length $L_w = 2E/\rho g$. For a given material, L_w is fixed, and while it is desirable to make L_c large to keep the catenary flat, this entails increasing e_w, which should be kept small to minimize creep.

Any change in the tension will both stretch the wire elastically and, by (26), alter w by changing L_c; the resulting movement of the free end of the wire will appear as a strain signal. For a fractional change in tension $\delta = \Delta F/F_0$ the resulting apparent strain is

$$-\delta e_w \left[1 + \frac{1}{3e_w}\left(\frac{l}{L_c}\right)^2\right] \equiv -\delta e_w W \qquad (27)$$

The first term inside square brackets is the contribution from elastic deformation, and the second that caused by change in the shape of the catenary; their sum W is the overall stiffness of the wire. To minimize the apparent strain for a given δ, we must set e_w equal to $(2l^2/3L_w^2)^{1/3}$, in which case (27) becomes $-1.5\,\delta e_w$. For most materials and reasonable lengths the optimal e_w is of order 10^{-4}. This is small enough that creep of the stretched wire will be small.

Because the length standard is flexible, wire strainmeters have many spurious resonances at relatively low frequencies [*Bilham and King*, 1971]. One mode is longitudinal oscillation of the wire and tensioning system. Tension is usually applied by a weight on a lever; in a longitudinal oscillation this acts as a mass and the wire as a spring. The frequency of oscillation f_l depends on the moment of inertia of the tensioning system (I_p), the distance from the pivot point to the attachment point of the wire (r_a), and the effective spring constant of the wire (which by (27) acts as though it had a Young's modulus of E/W). The result is

$$f_l = \frac{r_a}{2\pi}\left(\frac{A_w E}{I_p W}\right)^{1/2}$$

The wire can also oscillate transversely, with the restoring force being some combination of tension and gravity. The gravest purely tensional mode has a frequency of

$$f_t = \frac{1}{l}\left(\frac{gL_w e_w}{8}\right)^{1/2}$$

It is relatively easy to make these frequencies a few hertz (above the microseism band), but difficult to make them much larger; wire strainmeters are poor seismometers.

An obvious material for the wire is Invar ($L_w = 3.8\times10^6$ m), and most wire strainmeters have used it. It is readily available, easy to clamp, and has a low temperature coefficient and good long-term stability. Its main disadvantages are that it rusts and that its high density (reflected in the low value of L_w) makes it unsuitable for spans of more than 10 to 20 m. Carbon fiber has been used extensively by Bilham. It has a much larger L_w (3×10^7 m) and so can be used over longer spans than Invar; over short spans the spurious modes have frequencies well above the maximum seismic noise. Carbon fiber is resistant to corrosion but does adsorb water; the resulting change in weight can cause spurious initial drifts (R. Bilham, personal communication, 1985). It has a temperature coefficient similar to that of Invar (Table 2) and may not be as stable, though this depends on the type used [*Hauksson et al.*, 1979]. Fused quartz (in the form of 2-m rods hooked together) was used by *Sydenham* [1974*b*]; it has a slightly larger L_w than Invar (6.8×10^6 m) but is much more fragile and introduces many more contact surfaces.

Several groups have designed constant-tension wire strainmeters, all tensioning the wire with weights mounted on flexure pivots, movements of the wire and pivoted section being measured with an inductive displacement transducer, usually an LVDT [*Bilham and King*, 1971; *Gerard*, 1971; *Sydenham*, 1972]. The most widely used design (Figure 20) was developed at Cambridge University by *King and Bilham* [1976]; it includes a motor to reset the distance of the weight from the pivot, stretching the wire to keep the instrument on scale for strains up to 10^{-4}. An oil dashpot attached to the pivoted section damps the longitudinal mode of vibration. The Cambridge group also developed methods for getting relative calibrations to 0.1%. For installations in shallow trenches, the instrument may be completely immersed in an inert liquid such as kerosene or silicone oil. This protects it from insects, corrosion, and groundwater, increases the value of L_w, and damps out transverse oscillations.

5.3. *Laser Strainmeters*

Because the wavelength of light, unlike any material object, is an invariant standard, interferometry has obvious attractions for strain measurement. The development of the laser, with its very long coherence length, made it possible to build extensometers using interferometers with very unequal arms. Though several groups have built laser strainmeters, only three designs have produced significant results: one from the University of California, San Diego (UCSD) [*Berger and Lovberg*, 1970], one from Cambridge University [*Goulty et al.*, 1974], and one from the U.S. National Bureau of Standards (NBS) [*Levine and Hall*, 1972]. Though for simplicity of exposition I will describe many features in each instrument in terms of those in another, in fact they were nearly independent developments, each aiming to satisfy somewhat different goals.

The UCSD strainmeter uses the most straightforward optical design: an unequal-arm Michelson interferometer (section 3.3.1), in which changes in the length of the long arm cause fringe shifts at the detector. Counting fringes gives the strain change, with the frequency response and

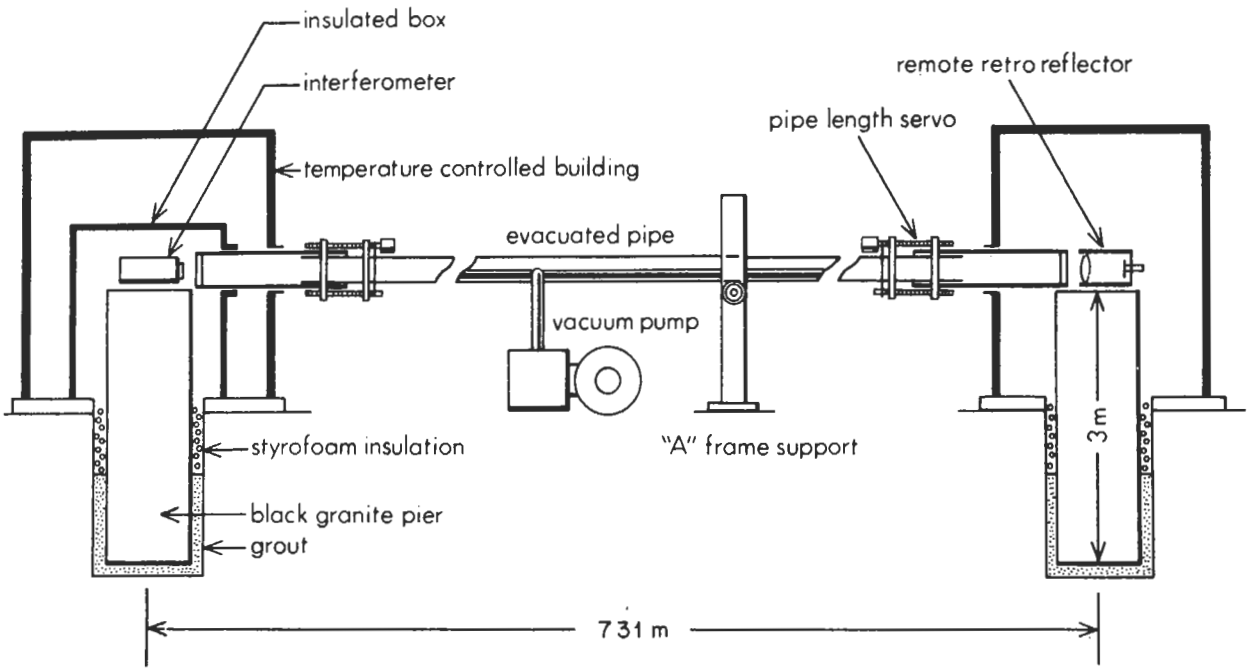

Fig. 21. Mechanical design of the UCSD laser strainmeter. The two endpoints are tall piers of dimension stone sunk in the ground. These, and the optics they carry, are inside temperature-controlled enclosures in air-conditioned buildings. The measurement path is inside a vacuum pipe except at the very ends; telescopic joints keep the length of the air paths constant.

dynamic range being limited by the counting electronics. Using suitable optics, a change of $\lambda/4$ can be detected in the path length difference Λ; since the path length is twice the instrument baselength l, this corresponds to a strain of $\lambda/8l$. While the optics are relatively simple, l must be fairly large to get adequate resolution. For the UCSD instrument, l is 731 m, giving a least count of 0.108 nε. This length means that the instrument has to be located above ground; in fact, building an instrument that could be so installed was a goal of this design, since such a surface installation allows a wider choice of sites than one in mines and tunnels.

On the other hand, a surface installation complicates the mechanical design of the strainmeter (Figure 21). Almost all of the optical path along the long arm runs through a pipe evacuated to 1 Pa, so that temperature and pressure changes do not matter. For ease of adjustment the interferometer optics and remote retroreflector are not in the vacuum. Because of this, any motion of the end of the evacuated pipe changes the proportion of the path in air and in vacuum, and therefore the optical path length, with 1 mm of motion causing an apparent strain of 0.4 nε. Temperature changes cause the aluminum pipe to expand and contract up to 0.6 m. To eliminate this problem, the vacuum pipe is anchored in the middle, and telescopic joints are put at each end; these joints are servo-controlled to keep the end of the evacuated path a constant distance from the optics. A prism at the midpoint of the pipe allows a break in the optical path, so that the pipe need not be in a single straight section. The optics at each end are inside heavily-insulated boxes in small air-conditioned buildings. In the three instruments first built the endpoints were long columns (up to 4 m) of dimension stone sunk into the ground. Because these tilted (causing spurious strains), the endpoints for the fourth instrument were short piers in vaults just below the surface. Displacements of these piers proved to be large enough [*Wyatt*, 1982] that optical anchors (section 3.4.4) were needed to correct for them.

The optical system followed the basic principles described in section 3.3.1, with several refinements. One was isolation of the laser from the light returning through the beamsplitter, using a polarizer and quarter-wave plate. This is needed to keep the laser from 'seeing' the modes of the optical cavity formed by the long interferometer arm, and having its frequency pulled towards them. Because of the length of the instrument, the laser beam must be expanded before being sent into the vacuum pipe, to reduce diffractive spreading. The retroreflector is a 'cats-eye' (lens and mirror) which minimizes beam distortion.

The interferometer is illuminated by a single-frequency laser whose wavelength is stabilized by locking it to a reference cavity; since all three designs of laser strainmeter lock lasers to a cavity either for stabilization or for measurement, this is worth describing in some detail. In the UCSD instrument (Figure 22) the cavity is two mirrors separated by a 30-cm quartz spacer and kept in a tightly controlled environment. The mirrors form a Fabry-Perot interferometer [*Born and Wolf*, 1980] in which there is multiple interference of the light that bounces back and forth between the two ends. If the mirrors transmit slightly so that light can be sent in one end, the ratio of intensity coming out the other to that sent in is

$$\frac{I_T}{I_I} = \left[1 + \frac{4F_n^2}{\pi^2} \sin^2\left(\frac{4\pi\Lambda_c}{\lambda}\right)\right]^{-1}$$

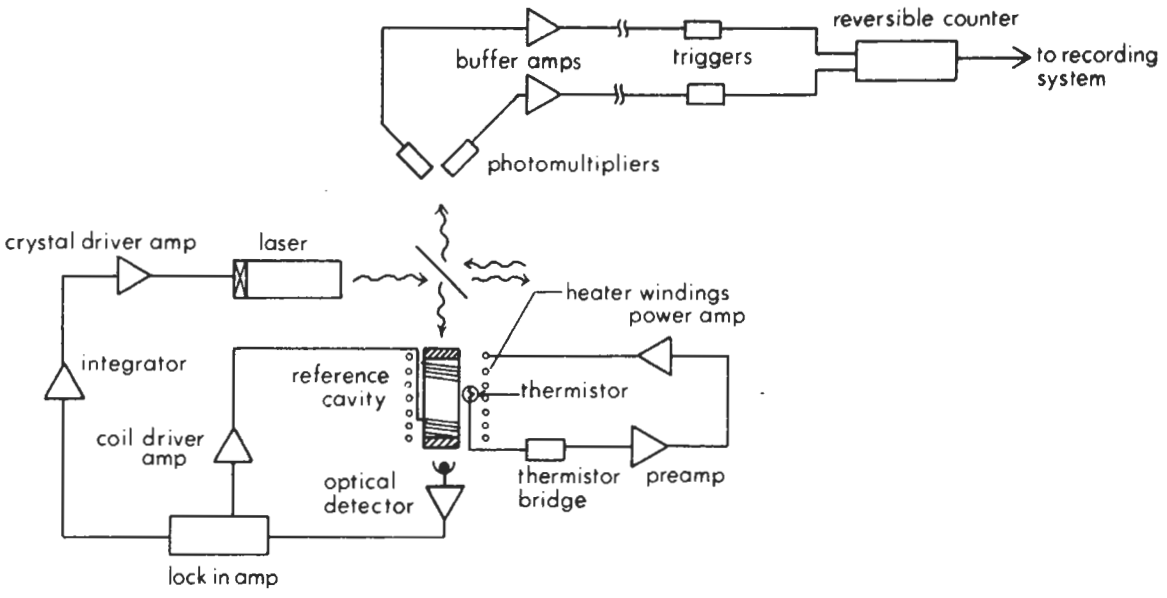

Fig. 22. Electronics used in the UCSD laser strainmeter. The feedback loop that stabilizes the laser frequency is on the lower right. The lock-in amplifier modulates the length of the Fabry-Perot reference cavity to improve detection. Light from the laser shines through this cavity; the detector and integrator then give a signal that locks the laser frequency to a resonant mode of this cavity. The cavity temperature controller and the fringe-counter are also shown.

where λ is the wavelength of the light, Λ_c the optical path length between the ends (including phase shifts at the mirrors), and F_n the finesse (optical Q) of the system, which depends on the reflectivity and alignment of the mirrors. Even for highly reflective mirrors, the system is transparent for $\Lambda_c = N\lambda/2$ (N an integer) and transmits less well for other values of λ; for F_n large the transmittance falls rapidly as λ shifts away from one of the resonant values. In the UCSD instrument, Λ_c is fixed (aside from a slight modulation added to allow phase-sensitive detection), and the laser light transmitted through it is measured by a photodetector. (Modulation by varying the length of the passive cavity avoids having to impose a frequency modulation on the laser output, which would make fringe counting more difficult [*Berger*, 1973].) Because F_n is about 100, small shifts in λ cause a large change in the intensity received. The signal from the photodetector changes the size of the laser cavity to maximize this intensity.

In this application the Fabry-Perot cavity can be thought of as a wavelength-to-intensity transducer in the feedback loop that controls the laser wavelength. Of course, the control depends on Λ_c being fixed; any change in Λ_c will cause λ to change, which will in turn cause an apparent strain. This laser strainmeter thus remains dependent on a material standard, but one that is small enough that its environment can be well controlled. Data from three of these instruments at Piñon Flat Observatory (F. Wyatt, personal communication, 1984) have shown that, compared to monument instability, drifts of the Fabry-Perot cavities are not a major source of noise. The addition of optical anchors (section 3.3.4) has made cavity instability the leading source of drift at very long periods.

The Cambridge laser strainmeter, in some ways a more sophisticated design than the UCSD instrument, aimed to be a relatively simple instrument that could be used to make precise and stable measurements of earth tides and secular strain. The Cambridge strainmeter was 54 m long and avoided complex mechanical design by putting all the interferometer optics in the vacuum and by being in the benign thermal environment of a tunnel. Bellows were adequate to allow the length of the vacuum pipe to change by several centimeters without displacing the end piers, which were girders bolted to the tunnel floor and wall. The shortness of the instrument also allowed a simple solution to the optical isolation problem: the retroreflector was a corner cube, so that the outgoing and returning beams did not overlap.

The interferometer was an unequal-arm Michelson, and in its final form used a beat-frequency system to detect strain changes, a technique that allows precise comparison with a separate stabilized laser. The interferometer laser was locked to the changing length of the measurement arm; a feedback loop varied the wavelength of the laser light so as to fix the fringe pattern. Equation (10) shows that this means that Λ/λ is constant, just as in the Fabry-Perot: if the measurement arm strains by ϵ, λ will change to $\lambda(1+\epsilon)$. Changes in the wavelength of the locked laser were detected by shining the light from this laser and from a stabilized laser on a photodetector. If we assume that λ is the wavelength of the stabilized laser light and that the intensities are equal, the electric field in the combined light beam is

$$\Sigma_C = e^{2\pi ict/\lambda} + e^{2\pi ict/\lambda(1+\epsilon)}$$

The photodetector responds to the intensity $\frac{1}{2}\Sigma_C \Sigma_C^*$,

which for the expression above contains terms with frequencies twice that of the light (too fast for the detector to respond) and one with the beat frequency

$$\frac{c}{\lambda}\left(\frac{\epsilon}{1+\epsilon}\right)$$

Since $\epsilon \ll 1$, the beat frequency is nearly linear in strain. Furthermore, it can be measured very accurately, giving much higher resolution than fringe counting could even with a very long instrument. The nominal resolution for the Cambridge system was 0.2 pε, though the overall system noise was higher.

The locked laser used in the Cambridge strainmeter was a relatively inexpensive multifrequency laser; while this is not usually acceptable in an unequal-arm interferometer, it can be if the path length difference is nearly a multiple of the laser cavity length. The stabilized laser used an iodine absorption cell (section 3.3.1), which gives excellent long-term stability but is less good at short periods (e.g., 8 pε instability over 100 s). The dynamic range and frequency response were limited by the range over which the locked laser could be driven and by the loop bandwidth.

The NBS instrument was a relatively short (30 m) system installed in a mine, built with the goal of making the quietest and most stable instrument possible. The optics were in the vacuum system, and care was taken to balance atmospheric forces on the piers. Like the Cambridge instrument it used a beat-frequency measuring system, with one laser stabilized to an atomic feature in the infrared and the other locked to the measuring arm. In this instrument the measuring arm was a Fabry-Perot interferometer with a finesse of 80. This gave larger changes in intensity for a given strain change than did the Michelson interferometer used in the Cambridge strainmeter; despite the shorter baselength and longer wavelength, the NBS design produced 40 dB more response (in terms of intensity change for a given strain). The increased total gain of the feedback loop meant that the laser was locked more tightly to the measurement arm, resulting in a very low noise level (−254 dB relative to 1 $\epsilon^2 Hz^{-1}$). Use of a Fabry-Perot cavity for the measurement arm is not without difficulties: components must be selected carefully to keep spurious modes from occurring in such a long resonator, and the laser must be isolated.

The stabilized laser in the NBS system used a methane absorption cell. This has excellent noise properties (Figure 11) but because it operates in the infrared, beam alignment is more difficult. The locked laser was a specially-built single-frequency system. As in the Cambridge instrument, frequency response and dynamic range were limited by the servo loop bandwidth and laser adjustment.

Perhaps the most important characteristic of all laser strainmeters is their great complexity; while the foregoing descriptions may seem detailed, they have in fact been rather superficial. Their complexity has undoubtedly kept laser strainmeters from being widely used, even though the few that have been built have had stability and linearity unmatchable by a mechanical system. Their complexity also means that they have a short mean time between failure; because all laser systems measure relative changes in strain, sections of data separated by any system failure can be offset by arbitrary multiples of a wavelength. For short instruments the corresponding strain may be so large that over a brief gap the offset can be unambiguous. Frequent or lengthy failures greatly complicate interpretation.

5.4. *Borehole Hydraulic Strainmeters*

In his first strainmeter paper, *Benioff* [1935] suggested that dilatational strains might be measured by burying a large container of liquid with a small opening. Strains in the ground would change the volume of the container and force liquid to flow in and out; for a sufficiently small opening the flow could be detected. (Hydraulic amplification had been tried, unsuccessfully, in 1900 by Oddone [*Dewey and Byerly*, 1969].) Benioff's idea does not seem to have been tried until 30 years later, when it was revived by Sacks and Evertson. Their design has seen wide use, especially in Japan [*Suyehiro*, 1982]; the most complete description of it is in the thesis written by *Evertson* [1977]. The basic principle is the same as that suggested by Benioff, with the sensing volume (Figure 23) cylindrical so that it fits in a borehole. The outer case is divided into two parts: the actual sensing volume, completely filled with liquid, and a smaller backing volume, partly filled with inert gas. Changes in the size of the sensing volume force liquid in and out of the backing volume, which offers little resistance because of the high compressibility of the gas. The liquid actually flows into and out of a bellows inside the backing volume, connected to the sensing volume though a narrow tube, and the bellows motion is measured. The two volumes are also connected by a valve; if the sensing volume changes so much that the bellows would be pushed past its limits, opening this valve equalizes the pressure in the two volumes and rezeroes the bellows. The tube connecting the sensing volume to the bellows attenuates high-frequency motions, protecting the bellows from large, rapid changes, such as those expected near an earthquake.

The response of the hydraulic system depends not only on the relative sizes of the volumes but also on the compressibility of the liquid in the sensing volume and on the stiffness of the bellows. If the bellows is much smaller than the sensing volume, we may assume the liquid in the bellows to be incompressible. The sensing volume is

$$v_s = v_s^0(1+D)$$

where D is the dilatation of the instrument. The bellows volume is

$$v_b = v_b^0 + A_b q$$

where A_b is the effective area of the bellows and q the displacement of its end; this linear approximation is very accurate for well-made bellows [*Scaife et al.*, 1977]. By conservation of mass we find

$$\left(\frac{\rho}{1+p_s/\kappa_s}\right) v_s^0\,(1+D) + \rho\,(v_b^0+A_b\,q) = \rho\,(v_s^0+v_b^0)$$

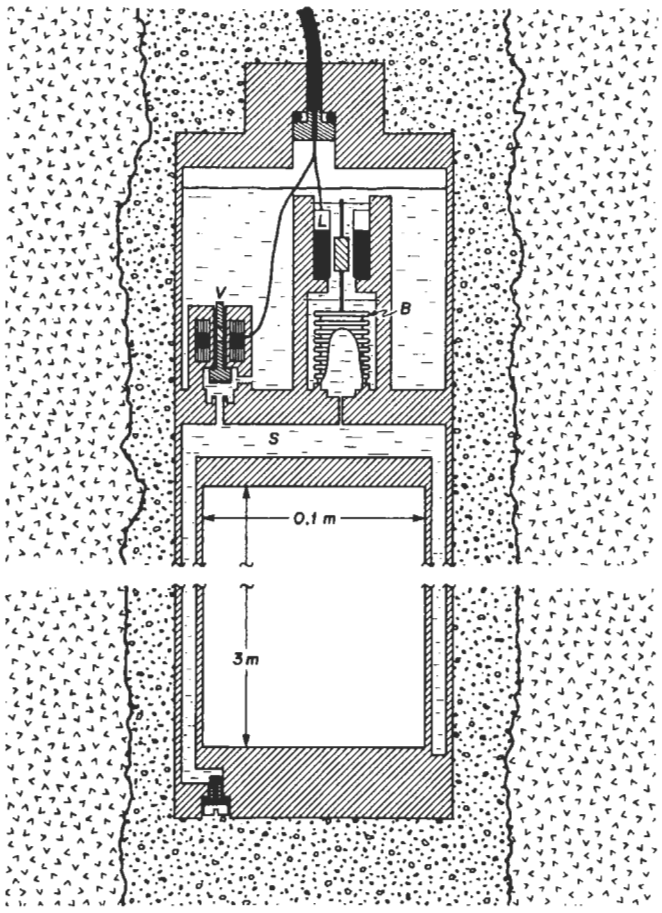

Fig. 23. Simplified cross section through a Sacks-Evertson dilatometer, shown cemented in a borehole. The sensing volume S is largely filled by a hollow insert and has a filling port at the bottom. The only openings between the sensing volume (lower) and backing volume (upper) are the rezero valve V (shown open) and the capillary to the bellows B. A DC-LVDT L (section 3.3.3) above the bellows measures the bellows motion.

where ρ is the density of the liquid, κ_s its bulk modulus, and p_s the pressure in the sensing volume, which is given by

$$p_s = \frac{k_b q}{A_b} + \frac{128\eta L_t A_b}{\pi b_t^4}\dot{q}$$

where the first term comes from the pressure produced by the bellows, which has a spring rate k_b, and the second term comes from the pressure drop along the connecting tube, assuming laminar flow. L_t is the tube length, b_t its diameter, and η the dynamic viscosity of the liquid. Making the approximation that $p_s \ll \kappa_s$, these two equations can be combined to give

$$q\left(1+\frac{k_b v_s^0}{A_b^2\kappa_s}\right)+\dot{q}\left(\frac{128\eta L_t v_s^0}{\pi b_t^4\kappa_s}\right)=\frac{-v_s^0}{A_b}D$$

At long periods the effect of liquid compressibility is thus to reduce the instrument response from the 'ideal' $(-v_s^0/A_b)$ by a factor

$$K_H = \left(1+\frac{k_b v_s^0}{A_b^2\kappa_s}\right)^{-1}$$

At high frequencies the connecting tube attenuates the response, acting as a single-pole low-pass filter with a corner frequency of

$$f_c = \frac{b_t^4\kappa_s}{256K_H\eta L_t v_s^0}$$

In the instruments put in Japan, v_s^0 was 0.033 m^3 and A_b 2 cm^2, giving an ideal response of $q = 170D$, so that the displacements to be measured were roughly the same as for a 170-m extensometer. However, the liquid used (silicone oil) was relatively compressible ($\kappa_s = 9\times10^8$ Pa), and the bellows relatively stiff (k_b = 970 N m^{-1}, though in fact 85% of this came from the stiffness of a piezoelectric displacement transducer), so that K_H was 0.51, reducing the effective 'length' to 85 m. Because the liquid had a relatively high viscosity (0.019 N s m^{-2}), it was not difficult to make b_t small enough for f_c to be about 1 Hz.

In the early instruments [*Sacks et al.*, 1971] an inductive sensor measured the long-term bellows motion; in more recent versions, an LVDT is used for this, and the piezoelectric transducer has been eliminated. Another change has been to reduce the volume of liquid by filling most of the sensing volume with a solid insert, usually a sealed hollow tube. This changes the apparent bulk modulus κ_s from that of the liquid, κ_L, to $\kappa_L(\chi_L+(1-\chi_L)\kappa_L/\kappa_I)^{-1}$, where κ_I is the bulk modulus of the insert and χ_L the fraction of v_s^0 occupied by liquid. Instruments recently installed in California have had v_s^0 = 0.028 m^3, A_b = 0.43 cm^2, and k_b = 230 N m^{-1}; given the increased effective rigidity of the liquid, the effective length was 325 m. The size of the connecting tube has been enlarged to raise f_c into a range near 10 Hz (A. Linde, personal communication, 1985).

The response of the instrument depends not only on the relation between q and Δ but also on that between instrument deformation and earth strain. If the instrument were perfectly flexible, the equations for an empty borehole (section 3.4.3) show that

$$D = \left(\frac{2-\nu}{1-\nu}\right)\Delta$$

where Δ is the volumetric strain in the absence of a hole and ν the Poisson's ratio of the material. An approximate solution [*Evertson*, 1977] to the problem of an elastic tube cemented into a hole shows that the vertical strain is not altered and that for the tube used in the Sacks-Evertson instrument, the areal strain is 90% of what it would be in an empty hole, the above equation remaining about right (see also *Gladwin and Hart* [1985]).

The success of this strainmeter depends on careful attention to details. For example, any gas bubbles in the sensing volume would greatly decrease κ_s and reduce the response. To avoid this, the volume is filled under vacuum, the silicone oil being distilled into it to remove volatile components. The installation must also be done carefully. Sacks's group places a slow-setting expansive cement of relatively low viscosity in the hole; the instrument is then lowered into this material, which sets around it, forming a tight prestressed bond.

While the Sacks-Evertson design is simple and robust, it cannot provide directional information. The borehole extensometers described in section 5.1.1 are one solution to this; another is a three-component hydraulic instrument recently developed by *Sakata et al.* [1982]. In this

the sensing volume is almost completely filled by a solid cylinder, and the remaining annulus of liquid is divided into three sectors. The volume change of each sector is measured separately by a bellows and inductive displacement sensor, and the complete horizontal strain tensor is reconstructed from these three outputs.

6. SUMMARY AND CONCLUSIONS

This paper began by pointing out how little progress has been made in measuring tilt and strain reliably. This has certainly not been for lack of work on instruments, but despite an abundance of good ideas, the geophysical harvest has been small.

Why is this? Partly it is because this is a hard problem: one thing that has been learned is that strain rates in the earth are very low, often not much above those in material length standards. To be successful, a tiltmeter or strainmeter must operate near the limits of what is feasible, and will therefore not be cheap. Many designs have emphasized simplicity and low cost so that many instruments could be used. However advisable this may be after instruments have proven useful, it is not a good idea before then. A bigger problem has been the difficulty of deciding whether an instrument is making useful measurements or not, and more particularly how to compare the results from one instrument with those from another. Without this information, it cannot be determined if a new design, or a change to an old one, is an improvement or not. Investigators rarely express their results in a useful way (section 2.4), but the fundamental difficulty is that the outputs of instruments at different locations need not be comparable. One example is earth tide measurements made in tunnels: because of strain-tilt coupling, the tilt on one side of the tunnel may differ from that on the other. For measurements of tectonic deformation the situation is even worse; we know so little about these motions that if two instruments even a few kilometers apart differ, we cannot say if the differences are in the earth or are merely instrument noise. This problem has been exacerbated by the natural tendency of different investigators to make measurements in different places, so as to increase the probability of seeing a unique event and avoid the wastefulness of redundant observations.

However, in measuring poorly known phenomena with instruments whose noise may exceed the signal, redundancy is necessary, not wasteful. The only way in which tiltmeters and strainmeters can be compared to decide which ones work better is to put them so close together that all geophysical prejudice would say that for the signals of interest they ought to observe the same thing; this was pointed out long ago by *Milne* [1896]. Physical arguments and geodetic data show that tectonic motions, even if partly in block form [*Bilham and Beavan*, 1979], have a sufficiently large scale that instruments up to a few hundred meters apart should certainly agree. (If they did not, there would be no point in trying to measure tectonic motions at all.)

6.1. *Comparison Tests*

In a comparison, all parts of the instrument must be tested, including its coupling to the ground. A good example was the experiment of *Latynina et al.* [1968] in which two quartz-bar strainmeters were set up on separate piers in a tunnel. There is little point in testing transducers alone, for example by attaching two different displacement sensors to the same reference; not only does this test only a small part of the system, but it can be done better and more conveniently on a test fixture in the laboratory. (Running transducers in the field does, however, check reliability.)

In a field test the outputs cannot be compared with a known input (except for the tides), but only with each other. Some care is needed in doing this. The least satisfactory, and commonest, method is visual comparison. Because the tides are the largest signal except at very long periods, two records may appear identical even though only the tides agree, but just because the tides are so large this is not very exciting. Visual comparisons are more useful at periods of weeks to years, and are probably the best that can be done for a relatively short record. Elementary regression analysis (such as the correlation coefficient) must be used with care because a high degree of serial correlation is present in deformation records. The best comparison technique is cross-spectral analysis, which gives the correlation between series (coherence) as a function of frequency The coherence sets limits on instrument noise, though because of statistical uncertainty these are usually not very strong [*Wyatt and Berger*, 1980].

At the longest periods, an even more stringent test is to compare a continuous deformation record with nearby geodetic measurements. Errors in geodetic techniques are so large that this is only meaningful at periods of a year or more; this also is precisely the range in which tiltmeter and strainmeter stability is hardest to attain. Such a comparison tests not only stability but also whether a measurement made over a small baseline (tenths to hundreds of meters) agrees with larger-scale deformations.

Most useful instrument comparisons have been made only in the last 10-15 years; earlier tests (mostly in Japan [*Shichi and Okada*, 1979]) concentrated on comparing transducers and on the consistency of tidal results. An early test of secular stability was a comparison by *Sacks et al.* [1975] between quartz-rod extensometers and two Sacks-Evertson dilatometers; this showed very similar trends over a 16-month period, though the agreement at annual frequencies and above appeared to be poor. Unfortunately no thorough analysis was made of these records, and no similar comparison has been made since. Another important result was a comparison by *Beavan and Goulty* [1977] between the Cambridge laser strainmeter and earlier wire strainmeter measurements at the same site, which showed the wire instruments to be 10 dB noiser than the laser system at frequencies up to 5×10^{-5} Hz. *Wyatt and Berger* [1980] examined coherence over a wide range of frequencies for data from bubble tiltmeters installed in shallow (3.5 m) boreholes. They showed that, except at the frequencies of tides and microseisms, two instruments installed 10 m apart were incoherent. In the long-period seismic band this disagreement was caused by the high noise level of the bubble sensor (section 4.1.3), but at lower frequencies it appears to have been caused by soil motion (section 3.4.1). A later test by *Wyatt et al.*

[1982] extended this comparison to include a diamagnetic tiltmeter in a 26-m borehole and a 535-m Michelson-Gale tiltmeter near the surface. Again, no coherence was observed, but the deeper instrument, though indifferently installed, showed a lower noise level (by 15 dB) than the shallow instruments, though it was still 5 dB noisier than the long-base instruments. Even if installed within a tunnel, however, borehole tiltmeters can sometimes perform much worse than a nearby long-base instrument [*Okada and Watanabe*, 1976]. *Wyatt et al.* [1984] have compared three long-base tiltmeters (two Michelson-Gale and one center-pressure) over a one-year period; this showed possible coherence between the Michelson-Gale instruments at periods of several days.

Though most of the comparisons between geodetic and continuous deformation measurements have been done in Japan, a test in California by *Savage et al.* [1979] should be mentioned; it showed that shallow borehole tiltmeters were much less stable than geodetic leveling over short (40 to 400 m) baselines. The Japanese tests have yielded equally discouraging results. A comparison between leveling and a pot-and-tube tiltmeter at Aburatsubo [*Yamada*, 1971] showed some times of agreement but also long intervals without any, and the tilt rates and directions found by the two techniques did not agree [*Kasahara*, 1973]. The experience of *Sato et al.* [1979] is perhaps typical of results not just in Japan but in other areas as well: while long-base tiltmeters ($l = 30$ m) showed one-tenth the fluctuations observed with horizontal pendulums ($l = 1$ m), leveling ($l = 10$ km) showed changes ten times smaller still.

6.2. *Lessons and Future Directions*

To begin with, a theme stated several times above bears repetition: existing displacement or tilt transducers are adequate for use in deformation-monitoring instruments. Further work should concentrate not on them, welcome though improvements always are, but on the messier, harder, and unsolved problem of stably coupling the instrument to the ground. One result now generally accepted is that such stable attachment is impossible in near-surface material, so that an instrument must either be made very long (and even then anchored to depth (section 3.4.4)) or, if small, must go in a deep borehole. Either technique requires expensive preparation, so that the idea of being able to make useful measurements of tectonic motion with cheap, simple instruments is untenable.

A borehole instrument can of course be installed in a wider variety of places than a long-base instrument, though only certain rock types may be suitable. This is one of many things not yet fully understood, since the use of borehole instruments has only just begun. Another question is how deep an installation should be, but beyond this there are the issues of how the hole should be drilled, what types of logs are most useful, what special installation techniques (such as centralizers) should be used, and what method of attachment works best. (As an example of the sort of work needed, *Sato et al.* [1980] have developed an elaborate procedure for installing borehole tiltmeters in a carefully drilled and cased hole.) There is much room for work on better borehole instruments, both tiltmeters and strainmeters, whose cost would at least be low enough to allow them to be cemented in, a mode of installation which the Sacks-Evertson strainmeter has shown to be relatively sound. (This instrument also shows that in a deep borehole some of the usual design rules, such as a low temperature coefficient, can be relaxed.) It is not yet clear that even good borehole instruments can match the low noise levels of the best long-base instruments; given this, it also makes sense for further work to be done on engineering long-base tiltmeters and strainmeters to make them more reliable and easy to operate and thus more suitable for field operation.

It is unlikely that any particular instrument will 'solve' the problem of measuring crustal deformation. A more reasonable development would be a variety of tiltmeters and strainmeters in which quality (however defined) is traded off against cost. To some extent, this has already begun: instruments exist that are relatively inexpensive and give good results in areas of rapid deformation. The bubble tiltmeter of *Westphal et al.* [1983] and the wire strainmeter of *King and Bilham* [1976] both fall into this class. For tidal measurements, 'high quality' means low noise and accurate calibration. Because of cavity effects, only borehole and surface instruments can satisfy this; the Askania borehole tiltmeter (section 4.1.2) is an excellent (albeit expensive) instrument for this purpose, and the work of *Harrison and Levine* [1981] shows that a cheaper instrument may do as well. Future work should concentrate on exploring these trade-offs further, so that the geophysicist who wants to make deformation measurements can select an instrument suitable for his needs. The cost of obtaining high-quality secular measurements may turn out to be prohibitive, but this negative result would still be of positive value, for it would save investigators from continuing the measurements with inadequate tools that have plagued this field in the past.

Acknowledgments. My understanding of this subject has been deepened and the number of my mistakes reduced by those who read over drafts of all or part of this paper. I especially thank Frank Wyatt for his very careful critique; both he and Mark Zumberge were very helpful in explaining the finer points of laserology. I have also benefited from comments and advice by John Beavan, Roger Bilham, Larry Burris, Chi Shunliang, Mike Gladwin, Judah Levine, Alan Linde, Chuck Meertens, and Sean-Thomas Morrissey. I thank Jean Filloux and Jim Fix for providing me with unpublished material from their files, and Wang Lingnan for translations from the Chinese. Preparation of this paper was supported by NASA under the Crustal Dynamics Program.

REFERENCES

Agnew, D. C., Strain tides at Piñon Flat: Analysis and interpretation, *Ph. D. Thesis*, University of California, San Diego, La Jolla, 1979.

Aki, K., and P. Richards, *Quantitative Seismology: Theory and Methods*, 932 pp., W. H. Freeman, San Francisco, California, 1980.

Allen, R. V., A borehole tiltmeter for measurements at tidal sensitivity, *Bull. Seismol. Soc. Am.*, *62*, 815–821, 1972.

Baer, T., F. V. Kowalski, and J. L. Hall, Frequency stabilization of a 633 nm He-Ne longitudinal Zeeman laser, *Appl. Opt.*, *19*, 3173–3177, 1980.

Baird, K. M., and G. R. Hanes, Stabilization of wavelengths from gas lasers, *Rep. Prog. Phys.*, *37*, 927–950, 1974.

Baker, T. F., What can earth tide measurements tell us about ocean tides or earth structure?, in *Applications of Geodesy to Geodynamics: Proceedings of the Ninth GEOP Conference*, edited by I. I. Mueller, pp. 299–307, Ohio State University Department of Geodetic Science, Columbus, Ohio, 1978.

Baker, T. F., Tidal tilt at Llanrwst, north Wales: Tidal loading and earth structure, *Geophys. J. R. Astron. Soc.*, *62*, 269–290, 1980.

Baker, T. F., and G. W. Lennon, Calibration: Confidence in the performance of tiltmeters and gravimeters, in *Proceedings of the 7th International Symposium on Earth Tides*, edited by G. Szadeczky-Kardoss, pp. 223–230, E. Schweizerbart'sche, Stuttgart, 1976.

Barton, D. B., *The Cornish Beam Engine,* D. Bradford Barton, Truro, Cornwall, England, 1966.

Basedow, R. W., and T. D. Cocks, Piezoelectric ceramic displacement characteristics at low frequencies and their consequences in Fabry-Perot interferometry, *J. Phys. E*, *13*, 840–844, 1980.

Batchelor, G. K., *An Introduction to Fluid Dynamics,* 614 pp., Cambridge University Press, New York, 1967.

Beavan, J., and R. Bilham, Thermally induced errors in fluid tube tiltmeters, *J. Geophys. Res.*, *82*, 5699–5704, 1977.

Beavan, J., and N. Goulty, Earth-strain observations made with the Cambridge laser strainmeter, *Geophys. J. R. Astron. Soc.*, *48*, 293–305, 1977.

Beavan, J., R. Bilham, D. Emter, and G. King, Observations of strain enhancement across a fissure, *Veroeff. Deutsch. Geodaet. Komm., Reihe B*, *231*, 47–58, 1979.

Bell, J. F., The Experimental Foundations of Solid Mechanics, in *Handb. Phys.*, vol. 6a/1, pp. 1–778, Springer-Verlag, New York, 1973.

Benioff, H., A linear strain seismograph, *Bull. Seismol. Soc. Am.*, *25*, 283–309, 1935.

Benioff, H., Fused-quartz extensometer for secular, tidal, and seismic strains, *Geol. Soc. Am. Bull.*, *70*, 1019–1032, 1959.

Berger, J., Application of laser techniques to geodesy and geophysics, *Adv. Geophys.*, *16*, 1–56, 1973.

Berger, J., A note on thermoelastic strains and tilts, *J. Geophys. Res.*, *80*, 274–277, 1975.

Berger, J., and C. Beaumont, An analysis of tidal strains from the United States of America, II, The inhomogeneous tide, *Bull. Seismol. Soc. Am.*, *66*, 1821–1846, 1976.

Berger, J., and J. Levine, The spectrum of earth strain from 10^{-8} to 10^{2} Hz, *J. Geophys. Res.*, *79*, 1210–1214, 1974.

Berger, J., and R. Lovberg, Earth strain measurements with a laser interferometer, *Science*, *170*, 296–303, 1970.

Berthold, J. W., and S. F. Jacobs, Ultraprecise thermal expansion measurements of seven low expansion materials, *Appl. Opt.*, *15*, 2344–2347, 1976.

Berthold, J. W., S. F. Jacobs, and M. A. Norton, Dimensional stability of fused silica, invar, and several ultra-low thermal expansion materials, *Metrologia*, *13*, 9–16, 1977.

Bilham, R. G., and R. J. Beavan, Strains and tilts on crustal blocks, *Tectonophysics*, *52*, 121–138, 1979.

Bilham, R. G., R. J. Beavan, K. Evans, and K. Hurst, Crustal deformation metrology at Lamont-Doherty Geological Observatory, *Earthq. Pred. Res.*, *3*, 391–411, 1985.

Bilham, R. G., and G. King, Strain-gauges for geophysics, *Commun. Obs. R. Belg., Ser A*, *13*, 258–278, 1971.

Bilham, R. G., R. Plumb, and J. Beavan, Design considerations in an ultra-stable, long baseline tiltmeter – Results from a laser tiltmeter, in *Terrestrial and Space Techniques in Earthquake Prediction Research*, edited by A. Vogel, pp. 235–254, Friedrich Vieweg, Wiesbaden, Federal Republic of Germany, 1979.

Blair, D. P., Solid tidal tilting observed in the West Australian goldfields, *Geophys. J. R. Astron. Soc.*, *67*, 293–304, 1981.

Blayney, J. L., and R. Gilman, A portable strain meter with continuous interferometric calibration, *Bull. Seismol. Soc. Am.*, *55*, 955–970, 1965.

Block, B., and J. Dratler, A review of tidal, earth normal mode and seismic data obtained with quartz torsion accelerometers, *Geophys. J. R. Astron. Soc.*, *31*, 239–269, 1972.

Block, B., and R. D. Moore, Measurements in the earth mode frequency range by an electrostatic sensing and feedback gravimeter, *J. Geophys. Res.*, *71*, 4361–4375, 1966.

Blum, P. A., Contribution a l'étude des variations de la verticale en un lieu, *Ann. Geophys.*, *19*, 215–243, 1962.

Bodenseewerk Geosystem, Borehole tiltmeter Gpb 10, *Tech. Bull. 19*, Überlingen, Federal Republic of Germany, 1978.

Bomford, G., *Geodesy,* 2nd ed., Clarendon, Oxford, England, 1962.

Bonchovsky, V. F., and A. N. Skur'yat, The level variometer, *Izv. Acad. Sci. USSR Phys. Solid Earth,* Engl. Trans., 47–54, 1961.

Born, M., and E. Wolf, *Principles of Optics,* 6th ed., 808 pp., Pergamon, New York, 1980.

Boulatsen, V., Etalonnage et sensibilité des extensomètres à tige en quartz avec transformateur du type à torsion, *Bull. Inf. Marees Terr.*, no. 72, 4123–4142, 1974.

Bracewell, R., *The Fourier Transform and Its Applications,* 378 pp., McGraw-Hill, New York, 1965.

Brown, N., Frequency stabilized lasers: Optical feedback effects, *Appl. Opt.*, *20*, 3711–3714, 1981.

Buck, S. W., F. Press, D. Shepard, M. Toksöz, and H. Trantham, Development of a mercury tiltmeter for seismic recording, *Rep. CSDL-R-655 (NTIS AD-726-521)*, Draper Laboratories, Cambridge, Mass., 1971.

Cabaniss, G. H., The measurement of long-period and secular deformation with deep borehole tiltmeters, in *Applications of Geodesy to Geodynamics: Proceedings of the Ninth GEOP Conference*, edited by I. I. Mueller, pp. 165–169, Ohio State University Department of Geodetic Science, Columbus, Ohio, 1978.

Chartier, J.-M., Results of international comparisons using methane-stabilized He-Ne lasers at 3.39 μm and iodine-stabilized He-Ne lasers at 633 nm, *IEEE Trans. Instrum. Meas.*, *32*, 81–83, 1983.

Chi Shunliang, Preliminary experimental result of a capacitance-type borehole earth strain meter (in Chinese), *Te Chen Hsueh Pao*, *4*, 98–103, 1982.

Concus, P., Static menisci in a vertical right circular cylinder, *J. Fluid Mech.*, *34*, 481–495, 1968.

Cooper, G. L., Development and use of a two-axis electrolytic bubble level as a precision vertical reference and tilt indicator, in *Conf. on Guidance, Control, and Flight Mechanics*, Am. Inst. of Aeronaut. and Astronautic., Anaheim, Calif., 1970.

Cooper, G. L., and W. T. Schmars, Selected applications of a biaxial tiltmeter in the ground motion environment, in *Conf. on Guidance, Control, and Flight Mechanics*, Am. Inst. of Aeronaut. and Astronautic., Key Biscayne, Fla., 1973.

Darwin, G. H., On an instrument for detecting small changes in the direction of the force of gravity, *Br. Assoc. Adv. Sci. Annu. Rep.*, 93–126, 1881.

Darwin, G. H., The lunar disturbance of gravity; variations in the vertical due to elasticity of the earth's surface, *Br. Assoc. Adv. Sci. Annu. Rep.*, 95–119, 1882.

Davies, D., Seismology with large arrays, *Rep. Prog. Phys.*, *36*, 1233–1283, 1973.

Decae, A., On some movements of the ground in Geneva, *Geophys. J. R. Astron. Soc.*, *3*, 112–120, 1960.

Dewey, J., and P. Byerly, The early history of seismology (to 1900), *Bull. Seismol. Soc. Am.*, *59*, 183–227, 1969.

Duffield, W. A., R. L. Christiansen, R. Y. Koyanagi, and D. W. Peterson, Storage, migration, and eruption of magma at Kilauea Volcano, Hawaii, 1971-1972, *J. Volcanol. and Geotherm. Res.*, *13*, 273–307, 1982.

Dussan V., E. B., On the spreading of liquids on solid surfaces: Static and dynamic contact lines, *Annu. Rev. Fluid Mech.*, *11*, 371–400, 1979.

Dussan V., E. B., and R. T. Chow, On the ability of drops or bubbles to stick to non-horizontal surfaces of solids, *J. Fluid Mech.*, *137*, 1–29, 1983.

Eastman, F. S., Flexure pivots to replace knife edges and ball bearings: An adaptation of beam-column analysis, *Univ. Wash. Eng. Exp. Stn. Bull.*, no. 86, 5–47, 1933.

Eaton, J. P., A portable water-tube tiltmeter, *Bull. Seismol. Soc. Am.*, *49*, 301–316, 1959.

Edge, R., T. Baker, and G. Jeffries, Borehole tilt measurements: Aperiodic crustal tilt in an aseismic area, *Tectonophysics*, *71*, 97–109, 1981.

Emter, D., and W. Zürn, Observations of local elastic effects on earth tide tilts and strains, in *Earth Tides*, edited by J. C. Harrison, pp. 309–327, Van Nostrand Reinhold, New York, 1985.

Eshelby, J. D., The determination of the elastic field of an ellip-

soidal inclusion and related problems, *Proc. R. Soc. London, Ser. A*, *241*, 376–396, 1957.
Estler, W. T., High-accuracy displacement interferometry in air, *Appl. Opt.*, *24*, 808–815, 1985.
Eto, T., A recording water-tube tiltmeter, *Bull. Disaster Prev. Res. Inst. Kyoto Univ.*, *15*, 21–33, 1966.
Evans, K., and F. Wyatt, Water table effects on the measurement of earth strain, *Tectonophysics*, *108*, 323–337, 1984.
Evertson, D. W., Borehole strainmeters for seismology, *Rep. ARL-TR-77-62*, Applied Research Laboratories, University of Texas, Austin, Texas, 1977.
Farrell, W. E., A gyroscopic seismometer: Measurements during the Borrego earthquake, *Bull. Seismol. Soc. Am.*, *59*, 1239–1245, 1969.
Farrell, W. E., Deformation of the earth by surface loads, *Rev. Geophys.*, *10*, 761–797, 1972.
Ferguson, E. S., The mind's eye: Nonverbal thought in technology, *Science*, *197*, 827–836, 1977.
Filloux, J. H., An ocean-bottom, D component magnetometer, *Geophysics*, *23*, 978–987, 1967.
Filloux, J. H., Optical lever and detecting system, and plate assembly for use therewith, *U. S. Patent 3,535,538*, 1970.
Finlayson, B., Field measurements of soil creep, *Earth Surf. Processes Landforms*, *6*, 35–48, 1981.
Fix, J. E., Ambient earth motion in the period range from 0.1 to 2560 sec., *Bull. Seismol. Soc. Am.*, *62*, 1753–1760, 1972.
Fix, J. E., Strain-inertial seismograph complexes, *Rep. TR-73-16 (NTIS AD-A005 708/3GI)*, Teledyne-Geotech, Garland, Texas, 1973.
Fix, J. E., and J. R. Sherwin, A high-sensitivity strain-inertial seismograph installation, *Bull. Seismol. Soc. Am.*, *60*, 1803–1822, 1970.
Fix, J. E., and J. R. Sherwin, Development of LP wave discrimination capability using LP strain instruments, *Rep. TR-72-3 (NTIS AD-748-232)*, Teledyne-Geotech, Garland, Texas, 1972.
Flach, D., G. Jentzsch, O. Rosenbach, and H. Wilhelm, Ball-calibration of the Askania borehole tiltmeter (earth tide pendulum), *Z. Geophys.*, *37*, 1005–1011, 1971.
Garratt, J. D., Survey of displacement transducers below 50 mm, *J. Phys. E*, *12*, 563–573, 1979.
Gerard, V. B., An invar wire earth strain meter, *J. Phys. E*, *4*, 689–692, 1971.
Gervaise, J., High-precision survey and alignment techniques in accelerator construction, *CERN Rep. 74-9*, pp. 47–66, European Organization for Nuclear Research, Geneva, 1974.
Gilbert, F., An introduction to low-frequency seismology, in *Physics of the Earth's Interior — Proceedings of the International School of Physics 'Enrico Fermi'*, edited by A. M. Dzeiwonski, pp. 41–81, North-Holland, Amsterdam, 1980.
Gile, W. W., A mercury pendulum seismometer, *Geophys. J. R. Astron. Soc.*, *36*, 153–165, 1974.
Gill, R. M., *Carbon Fibres in Composite Materials*, Iliffe, London, 1972.
Gladwin, M. T., High precision multi-component borehole deformation monitoring, *Rev. Sci. Instrum.*, *55*, 2011–2016, 1984.
Gladwin, M. T., and R. Hart, Design parameters for borehole strain instrumentation, *Pure Appl. Geophys.*, *123*, 59–80, 1985.
Gladwin, M. T., and J. Wolfe, Linearity of capacitance displacement transducers, *Rev. Sci. Instrum.*, *46*, 1099–1100, 1975.
Goulty, N. R., Strainmeters and tiltmeters in geophysics, *Tectonophysics*, *34*, 245–256, 1976.
Goulty, N. R., G. C. P. King, and A. J. Wallard, Iodine stabilized laser strainmeter, *Geophys. J. R. Astron. Soc.*, *39*, 269–282, 1974.
Goulty, N. R., P. M. Davis, R. Gilman, and N. Motta, Meteorological noise in wire strainmeter data from Parkfield, California, *Bull. Seismol. Soc. Am.*, *69*, 1983–1988, 1979.
Hade, G., M. Connor, and J. Kuo, Laser interferometer calibration system for extensometers, *Bull. Seismol. Soc. Am.*, *58*, 1379–1383, 1968.
Hagiwara, T., Observation of changes in the inclination of the earth's surface at Mt. Tsukuba, *Tokyo Daigaku Jishin Kenkyusho Iho*, *25*, 27–31, 1947.
Hall, J. L., Saturated absorption spectroscopy with applications to the 3.39 μm methane transition, in *Atomic Physics, 3: Proceedings of the 3rd International Conference in Atomic Physics*, edited by S. J. Smith and G. K. Walters, pp. 615–646, Plenum, New York, 1973.
Hanna, T. H., *Field Instrumentation in Geotechnical Engineering*, Trans Tech, Clausthal-Zellerfeld, Federal Republic of Germany, 1985.
Harrison, J. C., Cavity and topographic effects in tilt and strain measurement, *J. Geophys. Res.*, *81*, 319–328, 1976*a*.
Harrison, J. C., Tilt observations in the Poorman Mine near Boulder, Colorado, *J. Geophys. Res.*, *81*, 329–336, 1976*b*.
Harrison, J. C., and K. Herbst, Thermoelastic strains and tilts revisited, *Geophys. Res. Lett.*, *4*, 535–537, 1977.
Harrison, J. C., and L. J. B. LaCoste, The measurement of surface gravity, *Applications of Geodesy to Geodynamics: Proceedings of the Ninth GEOP Conference*, 239–243, Ohio State University Department of Geodetic Science, Columbus, Ohio, 1978.
Harrison, J. C., and J. Levine, A measurement of long-term tilt in Colorado and Wyoming, *Rep. AFGL-TR-81-0304 (NTIS AD108-865-17)*, Air Force Geophysics Laboratory, Bedford, Mass., 1981.
Hart, K. H., and K. M. Baird, On the relation between the old and new definition of the international metre, *Can. J. Phys.*, *39*, 781–787, 1961.
Haubrich, R. A., and H. M. Iyer, A digital seismograph system for measuring earth noise, *Bull. Seismol. Soc. Am.*, *52*, 87–93, 1962.
Haubrich, R. A., and K. McCamy, Microseisms: Coastal and pelagic sources, *Rev. Geophys.*, *7*, 539–571, 1969.
Hauksson, E., J. Beavan, and R. Bilham, Improved carbon-fiber extensometers (abstract), *Eos Trans. AGU*, *60*, 936, 1979.
Helstrom, C. W., *Statistical Theory of Signal Detection*, Pergamon, New York, 1968.
Herbst, K., Interpretation of tilt measurements in the period range above that of the tides, *Rep. AFGL-TR-79-0093 (NTIS AD-A074 525/7)*, Air Force Geophysics Laboratory, Bedford, Mass., 1976 (published 1979).
Herceg, E. E., *Handbook of Measurement and Control*, Schaevitz Engineering, Pennsauken, N. J., 1976.
Herrmannsfeldt, W., M. Lee, J. Spranza, and K. Trigger, Precision alignment using a system of large rectangular Fresnel lenses, *Appl. Opt.*, *7*, 995–1005, 1968.
Hill, J. J., and A. P. Miller, A seven-decade adjustable-ratio inductively-coupled voltage divider with 0.1 part per million accuracy, *Proc. IEE (London)*, *109B*, 157–162, 1962.
Horowitz, P., and W. Hill, *The Art of Electronics*, 716 pp., Cambridge University Press, New York, 1980.
Horsfall, J. A. C., A new geophysical tiltmeter, *Ph.D. Thesis*, University of Cambridge, Cambridge, England, 1977.
Horsfall, J. A. C., and G. C. P. King, A new geophysical tiltmeter, *Nature*, *274*, 675–676, 1978.
Huggett, G. R., L. E. Slater, and G. Pavlis, Precision leveling with a two-fluid tiltmeter, *Geophys. Res. Lett.*, *3*, 754–756, 1976.
Hugill, A. L., Displacement transducers based on reactive sensors in transformer ratio bridge circuits, *J. Phys. E*, *15*, 597–606, 1982.
Imberger, J., Natural convection in a shallow cavity with differentially heated end walls, 3, Experimental results, *J. Fluid Mech.*, *65*, 247–260, 1974.
Ishii, H., T. Sato, and K. Tachibana, On the characteristics of water-tube tiltmeter, 1, static characteristics (in Japanese), *J. Geod. Soc. Jpn.*, *23*, 88–98, 1977*a*.
Ishii, H., T. Sato, and K. Tachibana, On the characteristics of water-tube tiltmeter, 2, dynamic characteristics (in Japanese), *J. Geod. Soc. Jpn.*, *23*, 99–109, 1977*b*.
Itsueli, U. J., R. G. Bilham, N. R. Goulty, and G. C. P. King, Tidal strain enhancement observed across a tunnel, *Geophys. J. R. Astron. Soc.*, *42*, 555–564, 1975.
Jaeger, J. C., and N. G. W. Cook, *Fundamentals of Rock Mechanics*, Halsted, New York, 1976.
Jeffery, G. J., and P. H. Sydenham, Stability of strain-meter mounts, *Geophys. J. R. Astron. Soc.*, *33*, 185–193, 1973.
Jobert, G., Théorie du pendule de Zöllner et du pendule de Lettau, *Geofis. Pura Appl.*, *44*, 25–73, 1959.
Jones, R. V., Some developments and applications of the optical lever, *J. Sci. Instrum.*, *38*, 37–45, 1961.
Jones, R. V., Some uses of elasticity in instrument design, *J. Sci. Instrum.*, *39*, 193–203, 1962.

Jones, R. V., and S. T. Forbes, A microbarograph, *J. Sci. Instrum.*, *39*, 420–427, 1962.
Jones, R. V., and J. C. S. Richards, The design and some applications of sensitive capacitance micrometers, *J. Phys. E*, *6*, 589–600, 1973.
Kääriäinen, J., Observing the earth tides with a long water-tube tiltmeter, *Suom. Geod. Laitoksen Julkaisuja*, no. 88, 1979.
Kasahara, K., Tiltmeter observation in complement with precise levelings (in Japanese), *J. Geod. Soc. Jpn.*, *19*, 93–99, 1973.
Kasahara, M., R. Shichi, and Y. Okada, On the cause of long-period crustal movement, *Tectonophysics*, *97*, 327–336, 1983.
Kato, M., Observations of crustal movements by newly-designed horizontal pendulum and water-tube tiltmeters with electromagnetic transducers, *Bull. Disaster Prev. Res. Inst. Kyoto Univ.*, *27*, 155–171, 1977.
Kesler, C. E., Expansive cement concretes – Present state of knowledge, in *ACI Manual of Concrete Practice*, edited by ACI Committee on Concrete Practice, pp. 223/1–223/28, American Concrete Institute, Detroit, Mich., 1970.
Khassilev, L. E., Le calcul de l'effet de cavitée dans les marées terrestres, *Bull. Inf. Marees Terr.*, no. 80, 4851–4863, 1979.
Kimball, B. A., and E. R. Lemon, Spectra of air pressure fluctuations at the soil surface, *J. Geophys. Res.*, *75*, 6771–6777, 1970.
King, G. C. P., and R. Bilham, Tidal tilt measurement in Europe, *Nature*, *243*, 74–75, 1973.
King, G. C. P., and R. Bilham, A geophysical wire strainmeter, *Bull. Seismol. Soc. Am.*, *66*, 2039–2047, 1976.
King, G. C. P., R. J. Beavan, and J. R. Evans, Strainmeter technology, *Nature*, *257*, 513–514, 1975.
King, G. C. P., W. Zürn, R. Evans, and D. Emter, Site correction for long-period seismometers, tiltmeters, and strainmeters, *Geophys. J. R. Astron. Soc.*, *44*, 405–411, 1976.
Kümpel, H.-J., and G. Lohr, In-situ permeability from non-dilatational soil deformation caused by groundwater pumping – A case study, *J. Geophys.*, *57*, 184–190, 1985.
LaCoste, L., LaCoste and Romberg straight-line gravity meter, *Geophysics*, *48*, 606–610, 1983.
Lamb, H., *Hydrodynamics,* 738 pp., Cambridge University Press, Cambridge, 1932.
Latynina, L., E. Starkova, B. Podgornykh, and R. Karmalyeva, Deformations of the earth's crust at the Kondara station of the Tadzhik Socialist Soviet Republic, *Izv. Acad. Sci. USSR Phys. Solid Earth,* Engl. Trans., 184–189, 1968.
Layer, H. P., A portable iodine-stabilized helium-neon laser, *IEEE Trans. Instrum. Meas.*, *IM-29*, 358–361, 1980.
Leslie, W. H. P., Choosing transformer ratio-arm bridges, *Proc. IEE (London)*, *108*, 539–545, 1961.
Levine, J., Strainmeter technology, *Nature*, *257*, 513, 1975.
Levine, J., and J. L. Hall, Design and operation of a methane absorption stabilized laser strainmeter, *J. Geophys. Res.*, *77*, 2595–2609, 1972.
Lindenblad, N. E., Little pendulums that oscillate like big ones, *Sci. Am.*, *216* (4), 124–126, 1967.
Liu Changen, and Zhong Julin, Development of the WSQ-1 eddy current type automatic recording water-tube tiltmeter (in Chinese), *Te Chen Hsueh Pao*, *6*, 111–120, 1984.
Major, M., Strainmeters, in *ESSA Symposium on Earthquake Prediction*, pp. 69–71, U.S. Government Printing Office, Washington, D.C., 1966.
Major, M., G. Sutton, J. Oliver, and R. Metsger, On elastic strain in the earth in the period range 5 seconds to 100 hours, *Bull. Seismol. Soc. Am.*, *54*, 295–346, 1964.
Malk, E. G., and I. A. Ramsay, Reliability factors in gas lasers, *Proc. Soc. Photo Opt. Instrum. Eng.*, *328*, 7–14, 1982.
Malvern, L. E., *Introduction to the Mechanics of a Continuous Medium,* 713 pp., Prentice-Hall, Englewood Cliffs, N.J., 1969.
Mark, R. K., J. C. Tinsley, E. B. Newman, T. D. Gilmore, and R. O. Castle, An assessment of the accuracy of the geodetic measurements that define the Southern California uplift, *J. Geophys. Res.*, *86*, 2783–2808, 1981.
Mavko, G., Mechanics of motion on major faults, *Annu. Rev. Earth Planet. Sci.*, *9*, 81–111, 1981.
McDonald, J. A., and E. Herrin, Properties of pressure fluctuations in an atmospheric boundary layer, *Boundary Layer Meteorol.*, *8*, 419–436, 1974.
McGarr, A., and N. C. Gay, State of stress in the earth's crust, *Annu. Rev. Earth Planet. Sci.*, *6*, 405–436, 1978.
McGarr, A., I. S. Sacks, A. T. Linde, S. M. Spottiswoode, and R. W. Green, Coseismic and other short-term strain changes recorded with Sacks-Evertson strainmeters in a deep mine, South Africa, *Geophys. J. R. Astron. Soc.*, *70*, 717–740, 1982*a*.
McGarr, A., M. D. Zoback, and T. C. Hanks, Implications of an elastic analysis of in situ stress measurements near the San Andreas fault, *J. Geophys. Res.*, *87*, 7797–7806, 1982*b*.
McNutt, M. K., and H. W. Menard, Constraints on yield strength derived from observations of flexure, *Geophys. J. R. Astron. Soc.*, *71*, 363–394, 1982.
Melchior, P., *The Tides of the Planet Earth,* Pergamon, New York, 1983.
Melton, B., The sensitivity and dynamic range of inertial seismographs, *Rev. Geophys.*, *14*, 93–116, 1976.
Michelson, A. A., Preliminary results of measurements of the rigidity of the earth, *Astrophys. J.*, *39*, 105–138, 1914.
Michelson, A. A., and H. G. Gale, The rigidity of the earth, *Astrophys. J.*, *50*, 330–345, 1919.
Mills, A., and A. Hurst, A piezoceramic fine-movement control, *J. Phys. E*, *14*, 295–296, 1981.
Milne, J., Movements of the earth's crust (bradyseisms, earthquakes, diurnal waves, tremors), *Geograph. J.*, *7*, 229–247, 1896.
Moore, T. C., L. H. Rorden, R. L. Kovach, and S. W. Smith, Deep borehole strainmeter to measure earth strain, *Final Rep. AFOSR-TR-75-0021 (NTIS AD/A-003710)*, Develco, Inc., Palo Alto, Calif., 1974.
Morrissey, S.-T., A study on the adaptation of a commercial tiltmeter for monitoring earth tilts in unfavorable environments, *Special technical report, contract 14-08-0001-15848*, U.S. Geological Survey, Menlo Park, Calif., 1977.
Morrissey, S.-T., Tiltmeter and earthquake prediction program in Southern California and at Adak, Alaska, *Semi-annual technical report, contract 14-08-0001-21244*, U.S. Geological Survey, Menlo Park, Calif., 1983.
Morrissey, S.-T., and W. Stauder, Tiltmeter research at New Madrid and at Adak: the stability and reliability of shallow borehole tiltmeters, *Open File Rep. 79-730*, pp. 348–363, U.S. Geological Survey, Menlo Park, Calif., 1979.
Murphy, A. J., and J. R. Savino, A comprehensive study of long-period (20-200 sec) earth noise at the high-gain worldwide seismograph stations, *Bull. Seismol. Soc. Am.*, *65*, 1827–1862, 1975.
Nagasawa, K., The cross-suspension pendulum (in Japanese), *J. Geod. Soc. Jpn.*, *18*, 141–148, 1972.
Neubert, H. K. P., *Instrument Transducers,* 2nd ed., Clarendon, Oxford, 1975.
Neville, A. M., *Properties of Concrete,* 3rd ed., Pitman, London, 1981.
Okada, Y., Surface deformation due to shear and tensile faults in a half-space, *Bull. Seismol. Soc. Am.*, *75*, 1135–1154, 1985.
Okada, Y., and S. Watanabe, Observation of crustal deformation at the Fujigawa observatory, central Honshu, Japan, 2 (in Japanese), *J. Geod. Soc. Jpn.*, *22*, 77–93, 1976.
Okada, Y., S. Watanabe, and K. Kasahara, Observation of crustal deformation at the Fujigawa observatory, central Honshu, Japan (in Japanese), *J. Geod. Soc. Jpn.*, *21*, 179–190, 1975.
Ostrovsky, A. E., Le clinometre à enregistrement photoelectrique, *Bull. Inf. Marees Terr.*, no. 25-26, 500–553, 1961.
Owens, J. C., Optical refractive index of air: Dependence on pressure, temperature, and composition, *Appl. Opt.*, *6*, 51–58, 1967.
Ozawa, I., On the extensometer whose magnifier is a Zöllner suspension type tiltmeter, and the observations of the earth's strains by means of the instruments, *Ann. Geofis.*, *18*, 263–278, 1965.
Palmer, C. H., and B. Z. Hollmann, Transmission of incoherent light between Ronchi grids, *Appl. Opt.*, *11*, 780–785, 1972.
Passey, Q. R., Upper mantle viscosity derived from the difference in rebound of the Provo and Bonneville shorelines: Lake Bonneville Basin, Utah, *J. Geophys. Res.*, *86*, 11701–11708, 1981.

Peltier, R., Dynamics of the Ice Age earth, *Adv. Geophys.*, *24*, 1–146, 1982.

Peters, J., Tidal measurements using a new long baselength tiltmeter, *Ph.D. Thesis*, University of Liverpool, Liverpool, England, 1978.

Peterson, J., H. M. Butler, L. G. Holcomb, and C. R. Hutt, The Seismic Research Observatory, *Bull. Seismol. Soc. Am.*, *76*, 2049–2068, 1976.

Poland, J. F., and G. H. Davis, Land subsidence due to withdrawal of fluids, *Rev. Eng. Geol.*, *2*, 187–269, 1969.

Press, W. H., Flicker noises in astronomy and elsewhere, *Comments Astrophys.*, *7*, 103–119, 1978.

Priestley, M. B., *Spectral Analysis and Time Series,* 890 pp., Academic, Orlando, Fla., 1981.

Rawlings, A., *The Science of Clocks and Watches,* Pitman, New York, 1944.

Reilinger, R., M. Bevis, and G. Jurkowski, Tilt from releveling: An overview of the U.S. database, *Tectonophysics*, *107*, 315–330, 1984.

Riley, F. S., Land-surface tilting near Wheeler Ridge, southern San Joaquin Valley, California, *U.S. Geol. Surv. Prof. Pap.*, *497-G*, 1970.

Robertson, N. A., R. W. Drever, I. Kerr, and J. Hough, Passive and active seismic isolation for gravitational radiation detectors and other instruments, *J. Phys. E*, *15*, 1101–1105, 1982.

Rodgers, P. W., The response of the horizontal pendulum seismometer to Rayleigh and Love waves, tilt, and free oscillations of the earth, *Bull. Seismol. Soc. Am.*, *58*, 1384–1406, 1968.

Rogers, J. S., C. U. Park, and F. W. Jones, Test cell results for a mercury level tiltmeter, *J. Phys. E*, *13*, 161–162, 1980.

Rosenbach, O., and H. Jacoby, First experience with the Askania borehole tiltmeter (earth tide pendulum), in *Problems of Recent Crustal Movements – Third International Symposium*, edited by Yu. D. Bulanzhe, pp. 467–478, U.S.S.R. Academy of Science, Moscow, 1969.

Roughton, J. E., and W. S. Jones, Electromechanical transducers in hostile environments, *IEE Rev.*, *126*, 1029–1052, 1979.

Rutman, J., Characterization of phase and frequency instabilities in precision frequency sources: Fifteen years of progress, *Proc. IEEE*, *66*, 1048–1075, 1978.

Sacks, I. S., S. Suyehiro, D. W. Evertson, and Y. Yamagishi, Sacks-Evertson strainmeter, its installation in Japan and some preliminary results concerning strain steps, *Pap. Meteor. Geophys.*, *22*, 195–207, 1971.

Sacks, I. S., J. Snoke, Y. Yamagishi, and S. Suyehiro, Borehole strainmeters: Long-term stability and sensitivity to dilatancy, *Year Book Carnegie Inst. Washington*, *74*, 287–291, 1975.

Sacks, I. S., A. T. Linde, J. A. Snoke, and S. Suyehiro, A slow earthquake sequence following the Izu-Oshima earthquake of 1978, *Year Book Carnegie Inst. Washington*, *80*, 499–511, 1981.

Sakata, S., S. Shimada, and S. Noguchi, Development of new-type three-component borehole strainmeters, in *Proceedings of the Third Joint Panel Meeting of the U.N.J.R. Panel on Earthquake Prediction Technology*, 1982.

Sato, H., H. Takahasi, E. Yamamoto, N. Fukuo, M. Uehara, and Y. Terasawa, Development of the crustal tilt observation method using borehole-type tiltmeters (in Japanese), *Jishin*, *33*, 343–368, 1980.

Sato, T., K. Tachibana, and H. Ishii, Observation of crustal movements at the Akita geophysical observatory, 5 (in Japanese), *J. Geod. Soc. Jpn.*, *25*, 277–288, 1979.

Sato, T., M. Ooe, and N. Sato, Tidal tilt and strain measurements and analyses at the Esashi earth tide station, in *Proceedings of the Ninth International Symposium on Earth Tides*, pp. 223–237, E. Schweizerbart'sche, Stuttgart, Federal Republic of Germany, 1983.

Saunders, I., and A. Young, Rates of surface processes on slopes, slope retreat and denudation, *Earth Surf. Processes Landforms*, *8*, 473–501, 1983.

Savage, J. C., Strain accumulation in western United States, *Annu. Rev. Earth Planet. Sci.*, *11*, 11–43, 1983.

Savage, J. C., W. H. Prescott, J. Chamberlain, M. Lisowski, and C. Mortensen, Geodetic tilt measurements along the San Andreas fault in central California, *Bull. Seismol. Soc. Am.*, *69*, 1965–1981, 1979.

Sbar, M. L., R. Richardson, C. Flaccus, and T. Engelder, Strain-relief stress measurements along the San Andreas fault, *Open File Rep. 82-1075*, pp. 353–393, U.S. Geological Survey, Menlo Park, Calif., 1982.

Scaife, W. G., C. Lyons, J. Vij, and S. Ruttle, Calibration of a metallic bellows dilatometer, *J. Phys. E*, *10*, 874–876, 1977.

Schulz, S., G. Mavko, R. Burford, and W. Stuart, Long-term fault creep observations in central California, *J. Geophys. Res.*, *87*, 6977–6982, 1982.

Schulz, S., R. Burford, and B. Mavko, Influence of seismicity and rainfall on episodic creep on the San Andreas fault system in central California, *J. Geophys. Res.*, *88*, 7475–7484, 1983.

Schwiderski, E. W., Global ocean tides, II, the semidiurnal principal lunar tide (M_2), *Rep. TR 79-414 (NTIS AD-A084 694/9)*, Naval Surface Weapons Center, Dahlgren, Va., 1979.

Scriven, L. E., and C. V. Sternling, On cellular convection driven by surface-tension gradients: Effects of mean surface tension and surface viscosity, *J. Fluid Mech.*, *19*, 321–340, 1964.

Seeburger, D. A., and M. D. Zoback, The distribution of natural fractures and joints at depth in crystalline rock, *J. Geophys. Res.*, *87*, 5517–5534, 1982.

Shepard, D., Dynamic analysis of a mercury tiltmeter, *Rep. E-2598*, Draper Laboratories, Cambridge, Mass., 1971.

Shichi, R., and Y. Okada, Strain measurement in the vault (in Japanese), *J. Geod. Soc. Jpn.*, *25*, 101–134, 1979.

Shichi, R., T. Okuda, and S. Yoshioka, A new design of moving float type water-tube tiltmeter (in Japanese), *J. Geod. Soc. Jpn.*, *26*, 1–16, 1980.

Shopland, R. C., Shallow strain seismograph installation at the Wichita Mountains seismological observatory, *Bull. Seismol. Soc. Am.*, *56*, 337–360, 1966.

Shopland, R. C., Portable 30-day unattended system for recording earth strain in a 66-dB range, *IEEE Trans. Geosci. Electron.*, *GE-8*, 295–305, 1970.

Shopland, R. C., and R. H. Kirklin, Application of a vertical strain seismograph to the enhancement of *P* waves, *Bull. Seismol. Soc. Am.*, *60*, 105–124, 1970.

Simon, I., A. G. Emslie, P. Strong, and R. K. McConnell, Sensitive tiltmeter utilizing a diamagnetic suspension, *Rev. Sci. Instrum.*, *39*, 1666–1671, 1968.

Sinclair, D. C., and W. E. Bell, *Gas Laser Technology*, Holt, Rinehart & Winston, New York, 1969.

Skalsky, L., and J. Picha, On some problems of tidal observations with tiltmeters and their accuracy, *Studia Geophys. et Geodet.*, *13*, 138–172, 1969.

Slater, L. E., A long-baseline two-fluid tiltmeter (abstract), *Eos Trans. AGU*, *64*, 208, 1983.

Smith, S., Engineering evaluation of strainmeters (abstract), *Eos Trans. AGU*, *55*, 839, 1974.

Sneddon, J., Temperature effects in hydrostatic levelling, *Surv. Rev.*, *22*, 361–374, 1974.

Sneddon, J., The wider application of hydrostatic levelling, *Surv. Rev.*, *25*, 23–27, 1979.

Sorrells, G. G., and E. J. Douze, A preliminary report on infrasonic waves as a source of long-period seismic noise, *J. Geophys. Res.*, *79*, 4908–4917, 1974.

Sporton, T. M., The design of a general purpose air thermostat, *J. Phys. E*, *5*, 317–321, 1972.

Stacey, F. D., J. M. W. Rynn, E. C. Little, and C. Croskell, Displacement and tilt transducers of 140 dB range, *J. Phys. E*, *2*, 945–949, 1969.

Stierman, D. J., and J. H. Healy, A study of the depth of weathering and its relationship to the mechanical properties of near-surface rocks in the Mojave Desert, *Pure Appl. Geophys.*, *122*, 425–439, 1985.

Strange, W. E., The impact of refraction correction on leveling interpretations in southern California, *J. Geophys. Res.*, *86*, 2809–2824, 1981.

Strong, J., *Procedures in Experimental Physics,* Prentice-Hall, Englewood Cliffs, N.J., 1938.

Suyehiro, S., Continuous observation of crustal movement, in *Earthquake Prediction Techniques: Their Application in Japan*,

edited by T. Asada, pp. 133–174, University of Tokyo Press, Tokyo, 1982.
Sydenham, P. H., A tensioned-wire strain seismometer, *J. Phys. E, 2*, 1095–1097, 1969.
Sydenham, P. H., Progress in the design of tensioned-wire earth strainmeters, *Geophys. J. R. Astron. Soc., 29*, 319–327, 1972.
Sydenham, P. H., Where is experimental research on earth strain?, *Nature, 252*, 278–280, 1974*a*.
Sydenham, P. H., 2000 hr comparison of 10 m quartz-tube and quartz-catenary tidal strainmeters, *Geophys. J. R. Astron. Soc., 38*, 377–387, 1974*b*.
Sydenham, P. H., Strainmeter technology, *Nature, 257*, 514, 1975.
Takahasi, R., Preliminary report on the observation of the tilting of the earth's crust with a pair of water pipes, *Tokyo Daigaku Jishin Kenkyusho Iho, 8*, 143–152, 1930.
Takemoto, S., Laser interferometer systems for precise measurement of ground strains, *Bull. Disaster Prev. Res. Inst. Kyoto Univ., 29*, 65–81, 1979.
Takemoto, S., Effects of local inhomogeneities on tidal strain measurements, *Bull. Disaster Prev. Res. Inst. Kyoto Univ., 31*, 211–237, 1981.
Takemoto, S., Effects of meteorological and hydrological changes on ground strain measurements, *Bull. Disaster Prev. Res. Inst. Kyoto Univ., 33*, 15–46, 1983.
Tanaka, T., On an extensometer of variable capacitor type, *Bull. Disaster Prev. Res. Inst. Kyoto Univ., 15*, 49–59, 1966.
Thatcher, W., and T. Matsuda, Quaternary and geodetically measured crustal movements in the Tokai district, central Honshu, Japan, *J. Geophys. Res., 86*, 9237–9247, 1981.
Thomson, W., Review of evidence regarding the physical condition of the earth, *Br. Assoc. Adv. Sci. Annu. Rep.*, 1–12, 1876.
Timoshenko, S. P., *Theory of Plates and Shells,* 492 pp., McGraw-Hill, New York, 1940.
Tsubokawa, I., K. Nagasawa, M. Yanagisawa, I. Murata, H. Tajima, and T. Sato, New electromagnetic tiltmeter (in Japanese), *J. Geod. Soc. Jpn., 16*, 209–231, 1970.
Tsumura, K., On a high sensitive water tube tiltmeter and its application to the earth tides, *J. Geod. Soc. Jpn., 6*, 85–88, 1960.
Vaníček, P., and G. W. Lennon, The theory of motion of the horizontal pendulum with a Zöllner suspension and some indications for the instrument design, *Stud. Geophys. Geodet., 16*, 30–50, 1972.
Verbaandert, J., L'étalonnage des pendules horizontaux, *Boll. Geofis. Teor. Appl., 4*, 419–446, 1962.
Verbaandert, J., and P. Melchior, Les stations geophysiques souterraines et les pendules horizontaux de l'Observatoire Royal de Belgique, *Monogr. Obs. R. Belg., 7*, 1–147, 1961.
Verdeyan, J., *Laser Electronics,* 444 pp., Prentice-Hall, Englewood Cliffs, N.J., 1981.
Wang Quimin, Feng Xianshui, and Ma Hongjun, A string-frequency bore-hole strain meter (in Chinese), *Te Chen Hsueh Pao, 5*, 370–376, 1983.
Weinstein, W. D., Flexure-pivot bearings, 1, Spring rate, bearing types, single-strip design, *Mach. Des., 37*, no. 13, 150–157, 1967*a*.
Weinstein, W. D., Flexure-pivot bearings, 2, Two-strip design, three-strip design, materials, hysteresis, fatigue, *Mach. Des., 37*, no. 16, 136–145, 1967*b*.
Wenschof, E. D., Low-expansion alloys, in *Metals Handbook, vol. 3*, pp. 792–798, American Society for Metals, Metals Park, Pa., 1980.
Westphal, J. A., M. A. Carr, and W. F. Miller, Expendable bubble tiltmeter for geophysical monitoring, *Rev. Sci. Instrum., 54*, 415–418, 1983.
Widrow, B., Statistical analysis of amplitude-quantized sampled-data systems, *Trans. Am. Inst. Electr. Eng., 79* (2), 555–568, 1961.
Wieghardt, K., Experiments in granular flow, *Annu. Rev. Fluid Mech., 7*, 89–114, 1975.
Wielandt, E., and G. Streckeisen, The leaf-spring seismometer: Design and performance, *Bull. Seismol. Soc. Am., 72*, 2349–2367, 1982.
Wilding, B. R., Heat treatment and dimensional stability, in *Heat Treatment of Engineering Components*, pp. 20–25, Iron & Steel Institute, London, 1970.
Wolfe, J. E., E. Berg, and G. H. Sutton, 'The change in strain comes mainly from the rain': Kipapa, Oahu, *Bull. Seismol. Soc. Am., 71*, 1625–1635, 1981.
Wood, M. D., and N. E. King, Relation between earthquakes, weather, and soil tilt, *Science, 197*, 154–156, 1977.
Wyatt, F., Displacement of surface monuments: Horizontal motion, *J. Geophys. Res., 87*, 979–989, 1982.
Wyatt, F., and D. Agnew, Strain and tilt offsets from an earthquake in southern California (abstract), *Eos Trans. AGU, 63*, 375, 1982.
Wyatt, F., and J. Berger, Investigations of tilt measurements using shallow borehole tiltmeters, *J. Geophys. Res., 85*, 4351–4362, 1980.
Wyatt, F., K. Beckstrom, and J. Berger, The optical anchor – a geophysical strainmeter, *Bull. Seismol. Soc. Am., 72*, 1707–1715, 1982*a*.
Wyatt, F., G. Cabaniss, and D. Agnew, A comparison of tiltmeters at tidal frequencies, *Geophys. Res. Lett., 9*, 743–746, 1982*b*.
Wyatt, F., R. Bilham, J. Beavan, A. G. Sylvester, T. Owen, A. Harvey, C. Macdonald, D. D. Jackson, and D. C. Agnew, Comparing tiltmeters for crustal deformation measurements: A preliminary report, *Geophys. Res. Lett., 11*, 963–966, 1984.
Xie Liangyun, A capacitive bubble level and its application to the transit instrument, *Chin. Astron. Astrophys., 7*, 150–153, 1983.
Yamada, J., Water-tube tiltmeter observations at Aburatsubo as compared with precise levellings along the Miura peninsula, *J. Geod. Soc. Jpn., 17*, 170–177, 1971.
Yamauchi, T., A simulation of strain responses to rainfall (in Japanese), *J. Geod. Soc. Jpn., 27*, 40–49, 1981.
Young, A., A twelve-year record of soil movement on a slope, *Z. Geomorph. Suppl., 29*, 104–110, 1978.
Zürn, W., Detectability of small harmonic signals in digitized records, *J. Geophys. Res., 79*, 4433–4438, 1974.

D. C. Agnew, IGPP A-025, University of California at San Diego, La Jolla, CA 92093.

(Received December 24, 1984;
accepted February 10, 1986)